Protein Engineering of Targeted Cancer Therapies

Michael Keith San Diego Santos
B. S., Chemical Engineering, Stanford University (2010)

Submitted to the Department of Chemical Engineering
in partial fulfillment of the requirements for the degree of

DOCTOR OF PHILOSOPHY IN CHEMICAL ENGINEERING
at the
MASSACHUSETTS INSTITUTE OF TECHNOLOGY

June 2017

Signature of Author: Signature redacted
Department of Chemical Engineering
January 13, 2017

Certified by: Signature redacted
Bradley L. Pentelute
Pfizer-Laubach Career Development Associate Professor of Chemistry
Thesis Supervisor

Certified by: Signature redacted
K. Dane Wittrup
Carbon P. Dubbs Professor of Chemical Engineering and Biological Engineering
Thesis Supervisor

Accepted by: Signature redacted
Daniel Blankschtein
Herman P. Meissner (1929) Professor of Chemical Engineering
Chairman, Committee for Graduate Students

Protein Engineering of Targeted Cancer Therapies

Michael Keith San Diego Santos
B. S., Chemical Engineering, Stanford University (2010)

Submitted to the Department of Chemical Engineering on January 13, 2017 in partial fulfillment of the requirements for the degree of Doctor of Philosophy in Chemical Engineering

Abstract

Protective antigen (PA), the pore-forming component of anthrax toxin, has emerged as a platform for the development of cancer therapies because of its versatility and robust ability to translocate proteins into a cell's cytosol. More recently, development of new techniques for modifying PA is enabling it to be retargeted to receptors of interest via fusion with existing protein binders. There is a vast library of potential binders for PA based on natural or novel protein scaffolds generated by the field of protein engineering. This has allowed new approaches for tumor cells to be targeted for cytosolic delivery of toxins as a therapeutic strategy.

In our work, we sought to leverage the anti-tumor properties of an antibody, E1v3, to retarget PA to epidermal growth factor receptor (EGFR). This PA construct was shown to be capable of translocating a recently discovered protease, Ras and Rap1 Specific Protease (RRSP), which cleaves and inactivates the signal effector, Ras, found in the cytosol. We demonstrated that when Ras is inhibited in this manner, downstream growth signaling through pERK is ablated and health of a pancreatic cancer cell line (AsPC-1) is affected. Our results suggest that this retargeted PA, mPA-E1v3, efficiently translocates cytotoxic material into EGFR-positive tumor cells and thus presents a possible avenue for development of a potent therapeutic.

Using the same approach, we also took another previously engineered antibody, sm3e, and expressed it as a fusion to PA to confer specificity to carcinoembryonic antigen (CEA). Though CEA is not typically internalized, we demonstrated that this retargeted PA (mPA-sm3e) retained the property of endocytosis and translocation and was able to deliver toxins to inhibit proliferation of AsPC-1 tumor cells.

Finally, the retargeted PA variants, mPA-E1v3 and mPA-sm3e, were further characterized for tumor growth inhibition using mouse models. Nude mice were treated with the engineered PA variants against EGFR and CEA to test delivery of toxins into the cells of subcutaneous tumors. Initial results were promising, and future work should be aimed at additional studies confirming this work in mouse models.

Our work has demonstrated that protein engineering can be used to retarget PA against tumor cells with positive results. We believe that the modularity and versatility of this retargeting strategy holds great potential in the design of anti-cancer therapeutics.

Thesis Advisor: Bradley L. Pentelute
Title: Pfizer-Laubach Career Development Associate Professor of Chemistry

Thesis Advisor: K. Dane Wittrup
Title: Carbon P. Dubbs Professor of Chemical Engineering and Biological Engineering

Acknowledgements

Unsurprisingly, grad school is tough. No one does it alone, and I am lucky enough to have had an incredible support network to help me through to the end. My advisor, Prof. Brad Pentelute, has gone above and beyond in guiding me throughout my time in his lab, and I want to thank him for taking me on and truly being a mentor. I also want to thank my committee members, Prof. Kris Prather and Prof. Angela Koehler, for helping me understand both the science and the rigors of traversing academic life at MIT.

I'm fortunate that my time at MIT has overlapped with so many brilliant and wonderful people. In particular, I want to thank Amy Rabideau for her kindness and patience as I learned about the anthrax toxin project and lab in general, and Alex Loftis for being a helpful and always entertaining collaborator. I'm also grateful for all of the help and input from the other members of Team Translocation: Mike Lu, Xiaoli Liao, and Mette Ishoey; as well as all of the many labmates that I've been able to work with: Annie, Jordi, Xiaosai, Cary, Alice, Jim, Ryan, Monique, Alessandro, Michael, Mark, Alex V., Chi, Surin, Ethan, Justin, Alex M., Peng, Zak, Faycal, Colin, Anthony, Rebecca, Kyle, Guillaume, Tuang, Yuki, Katie, Jessie, Hansol, Zi-Ning, and Massi.

Beyond the lab, I've had steadfast friends that have brightened my days and kept me moving forward: Julie Ralph, Nelson Nogales, Kaja Kaastrup, Byron Kwan, Dan Gui, Eric Zhu, Tiffany Chen, and Nicole Yang.

Most of all, I want to thank my family for their unwavering support: my adorable nephews and niece, Benjamin, Zachary, Matthew, Jonathan, Nicholas, and Annabelle, who each can lift my spirits with just a smile; my sisters, Katherine and Christine, for all of their love and big sister wisdom; and of course, my parents, whose unconditional love and faith in me go beyond what I could ever possibly deserve. To all of them, my heartfelt thanks.

Table of Contents

List of Figures

List of Tables

Chapter 1: Bacterial Toxins for Tumor Targeting

1.1 Anthrax toxin

Many pathogenic microbes invade a host organism and subvert existing defenses and machinery in order to survive and proliferate. To do this, nature has evolved many mechanisms for microbes to deal with and sometimes even take advantage of such defenses, ranging from methods to cross the mucosal barrier to ways of entering into host cells. [1] On a cellular level, microbial toxin agents must interact with or cross the cell membrane in order to attack or access the cytosol.

Across the gamut of pathogens, nature has evolved numerous mechanisms for bacterial toxins to enter and alter cells. *Bacillus anthracis* is one such microbe that has demonstrated high efficiency in infecting animals, including humans. [2] It is a bacterium that typically resides in the soil in the form of a dormant spore. The toxin responsible for *B. anthracis*'s adverse effects on host organisms consists of three separate protein components: protective antigen (PA), lethal factor (LF), and edema factor (EF). [3]

Lethal factor and edema factor are the components of anthrax toxin that mediate its toxicity. LF cleaves and inactivates mitogen-activated protein kinase kinases 1 and 2 (MAPKK1 and MAPKK2), effector proteins that activate other kinases involved in cell proliferation. [4] EF is an adenylate cyclase that increases cAMP levels in the cytosol, causing edema. [5,6] It is not necessary for both toxins to enter the same cell; rather, LF causes damage to cardiomyocites and vascular smooth muscle cells, while EF induces lethality by causing edema in the intestine and liver. [7] However, none of the three protein components of anthrax toxin are toxic as single agents. LF and EF both rely on PA for translocation into the cytosol where they can interact

with their enzymatic targets. [8] The ability of PA to translocate protein is highly dependent on its interaction with the cell surface.

1.2 Protective antigen's role in anthrax toxin

Protective antigen is an 83 kDa protein consisting of four domains. Domain I is capable of interacting with ligands LF or EF, while domain IV is responsible for protective antigen binding to CMG2 and TEM8 on the surface of cells. [9,10] CMG2 and TEM8 are receptors involved in angiogenesis that are ubiquitously expressed in numerous tissue types of animals. [11] TEM8 is present on epithelial cells of the lung, skin, and intestines, while CMG2 is widely expressed in most human tissue. TEM8 is upregulated in endothelial cells during angiogenesis, while CMG2 has been demonstrated as being critical to proliferation of endothelial cells due to its function in capillary formation. [11–13] PA binds CMG2 strongly with a K_d of $1.7e^{-10}$ M, while interaction with TEM8 is much weaker with an affinity that is reported as being between 11 and 1000 times lower than that of CMG2. [14,15] It is hypothesized that this difference in affinity is why CMG2 is the receptor that is primarily responsible for anthrax toxin lethality, while TEM8 plays only a minor role. [16] The high expression of both of these receptors renders most tissues vulnerable to anthrax toxin, contributing to its high potential for lethality.

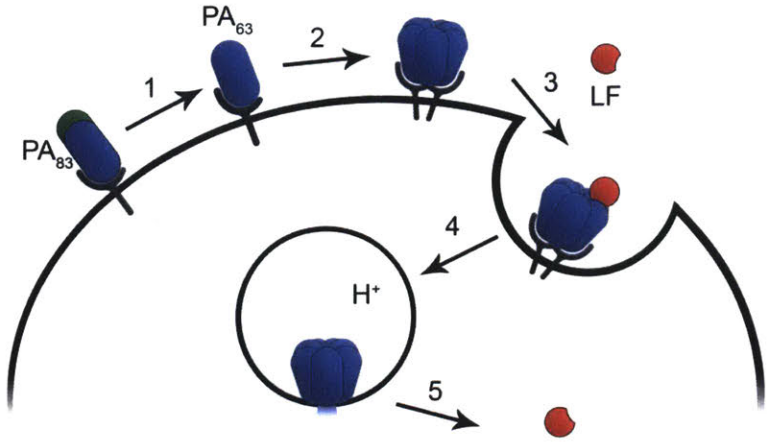

Figure 1.1. Schematic representation of the process of protective antigen-mediated translocation. PA binds to the cell and is cleaved into a 63 kDa form by cell surface proteases. In this form, PA can assemble into heptamers or octamers and associate with cargo such as LF, and the complex is then internalized into the cell. While in the acidic environment endosome, PA forms a pore through which cargo can be translocated into the cytosol.

The binding of PA to either of its receptors brings it in proximity of cell-surface proteases. Upon binding the cell, protective antigen is cleaved by furin into an active 63 kDa form. The 20 kDa fragment, consisting of PA residues 1-167, dissociates and does not play any further role in translocation. [9] This dissociation occurs within 1 minute, and then PA_{63} slowly isomerizes into its active form. [17] In this active form, PA is capable of assembling into a ring-shaped heptamer called the pre-pore. [8] Octameric forms of PA have also been observed and exhibit similar functionality to heptameric complexes. [18] Binding and oligomerization of the anthrax receptor by protective antigen induce its recruitment into lipid rafts on the cell surface, after which the entire complex is internalized via clathrin-dependent endocytosis (Figure 1.1). [19] As part of the process of internalization, anthrax receptors undergo palmitoylation to delay recruitment into lipid rafts, after which E3 ubiquitiin ligase Cbl ubiquitinates the receptors and induces rapid endocytosis of the complex. [20] It has been observed that β-arrestin mediates ubiquitination of the receptors bound to PA, but the mechanism of such external effectors is not fully characterized. [21]

Endocytosis of pre-pore is essential to the translocation activity of protective antigen, as it is the acidity of the endosome that triggers the transition of the pre-pore to a pore through which material can be transported. Specifically, domain II of PA undergoes a pH-dependent conformational change in order to form the pore. [22] The F427 residues of each monomer of PA form a Φ-clamp. [23] The pore is narrowest at this point at 6 Å and as such can only translocate cargo in an unfolded state lacking secondary structure. [24] Translocation is driven by a proton gradient generated by the difference between the acidic endosome and the cytosol. It is theorized that translocation occurs via a charge-state-dependent Brownian ratchet in which interaction with the Φ-clamp and protonation of negative residues of the translocating polypeptide drive transport through the pore. [25]

The high virulence of *B. anthracis* drew national attention in 2001 due to acts of bioterrorism in which active *B. anthracis* spores were intentionally delivered through the mail, resulting in the death of five people. [26] However, each individual component of anthrax toxin is non-lethal in isolation. Protective antigen itself does not cause harm to the targeted cell, and lethal factor and edema factor cannot affect cell processes without being translocated into the cytosol by some mechanism such as protective antigen's pore formation. The modular nature of anthrax toxin provides the opportunity to reengineer it in such a way that payload translocation occurs only under specific conditions or for specific payloads.

1.3 Retargeting bacterial toxins as cancer therapy

There is extensive precedent for the use of bacterially-derived toxins for tumor targeting. [27] Since the primary purpose of these toxins is to induce cell death, they are suited for applications in which cytotoxicity against tumor cells is desired. An obvious disadvantage,

however, is the indiscriminate nature of these toxins, which leads to damage even in non-cancerous host cells. One method of restricting the target of cytotoxic proteins is to conjugate or fuse the toxins to antibodies against targets of interest, forming a class of compounds called immunotoxins. These compounds leverage the wide library of clinically-relevant antibodies to impart upon toxins specificity to virtually any antigen. [28] This strategy has been applied in many studies to find antibody-toxin conjugates that target cancer-relevant receptors like HER2, EGFR, IL-2R, and CD3. [29–31] One immunotoxin, denileukin diftitox (Ontak), which fuses IL-2 to the catalytic domain of diphtheria toxin to target lymphoma, has been approved for the clinic. [32] Several others are in clinical trials. [33]

Further studies have attempted to leverage other naturally-occurring pore forming proteins. A system was recently described in which a pore-forming bacterial protein, perfringolysin-O (PFO), is targeted specifically to epidermal growth factor receptor (EGFR), a surface protein overexpressed in many cancers. [34] In its native form, PFO is unsuited for tumor therapy because it forms pores on all cells, compromising the integrity of the membrane and leading to host cell death. A bispecific complex including an anti-EGFR antibody for targeting and a fibronectin binder to PFO was created, where the binder to PFO inhibited its pore formation until entrance into the endosome. Retargeting PFO and restricting its activity to the endosome dramatically increased its therapeutic window, opening up possibilities for use as a therapy.

The studies in this field validate the strategy of combining naturally occurring cytotoxic agents with engineered or discovered antibodies for a modular system of retargeting bacterial toxins.

1.4 Retargeting protective antigen

A straightforward process of retargeting anthrax toxin's protective antigen was described by Mechaly et. al. and is summarized in Figure 1.2. [35] A double mutation in the receptor-binding domain of PA, N682A/D683A, ablates binding of PA to TEM8 or CMG2 while leaving its pore-forming properties intact. [36] This non-binding mutated PA (mPA) was then given a new fifth domain by recombinant fusion to the ligand for EGFR, EGF. This fusion conferred binding specificity to EGFR while exhibiting none of the previous binding to PA's native receptors. The retargeted PA, mPA-EGF, was shown to be capable of translocating toxins into EGFR-positive cells but had no effect on cells lacking EGFR. PA was also fused to the receptor-binding domain of diphtheria toxin (DTR), and in the case of both mPA-EGF and mPA-DTR, the cytotoxicity of toxins delivered by the PA variants was dependent on the interaction with the fused domain's receptor and independent of binding with anthrax receptor.

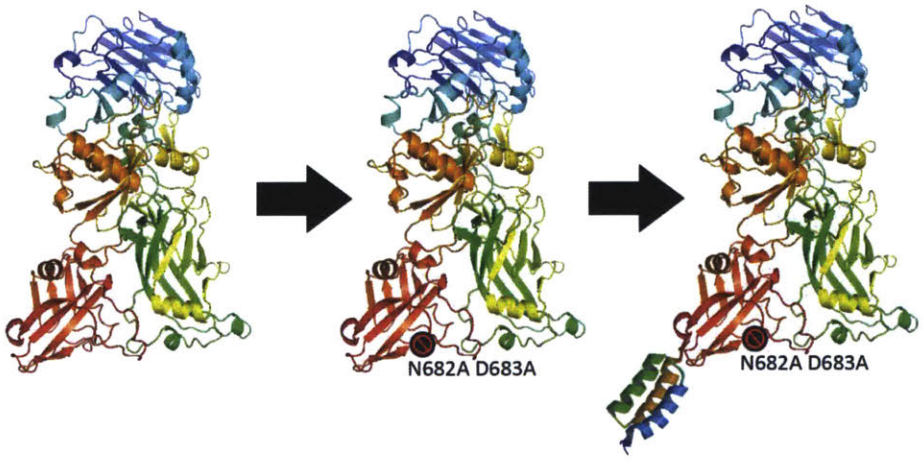

Figure 1.2. Graphical representation of the process of changing the receptor specificity of PA. The double mutant in domain IV, N682A/D683A, ablates binding of PA to its native anthrax receptors. The fusion of additional binding domains such as affibodies confers new targeting specificity to the full construct.

This retargeting strategy was also used in conjunction with engineered protein scaffolds that bind HER2. [37] Affibodies are 6.5 kDa proteins derived from the IgG-binding domain of

Protein A. [38] A previously engineered affibody against HER2 was fused to mPA and was shown to have activity against only HER2-positive cells. By screening a large panel of cell lines with varying levels of HER2, it could be observed that the toxicity of proteins translocated by mPA-ZHER2 correlated strongly with HER2 expression, with the highest-expressing cell lines being most sensitive to the treatment. The modularity of this method is exemplified by further work done by McCluskey et. al. [39] Using sortase-mediated ligation chemistry, fully functional retargeted PA was generated by fusing an affibody or a single chain antibody fragment (scFv) to mPA. Such results confirm that the entire library of binders generated from protein scaffolds such as antibodies or affibodies can be used to retarget PA to any desired antigen.

The specificity of protective antigen for its receptors can also be directly modulated by evolving PA, obviating the need for fusion of a fifth domain. [40,41] Chen et. al. used phage display to screen for PA mutants that selectively bind CMG2 or TEM8. These PA variants were capable of selectively targeting only the cells overexpressing the receptor to which they were engineered for exclusive binding. The cytotoxicity of PA mutated in this manner was then applied to killing of cancer cells, pointing to a receptor-dependent mode of action.

Lastly, a different method of retargeting PA relies on altering the conditions in which PA is proteolytically activated into its 63 kDa form. Liu et. al. describes replacing the furin cleavage site of PA with sequences subject to cleavage by matrix metalloproteases (MMP), which are overexpressed in tumors. This mutation gave PA the property of translocating toxins selectively into MMP-positive cells without harming healthy tissue. [42] The selective nature of the MMP-specific PA translated to a drastic increase in therapeutic window of PA-based therapies in mouse models, with wild-type PA causing widespread toxicity where the retargeted PA acted only on tumors. [43] Reduced uptake and clearance of PA by untargeted cells and mechanisms of

targeting tumor vasculature and inhibiting angiogenesis have been identified as reasons for which the modified PA possesses greater therapeutic effect. [44] PA has also been modified to be activated only by urokinase plasminogen activator, and the combination of these two protease-specific PAs has been used in strategies to engineer PA that exclusively form octamers when bound to tumor cells that express both proteases. [45,46]

1.5 Use of protective antigen to deliver non-native cargo

The heptameric pre-pore of protective antigen associates with up to three EF or LF molecules, with which it can be internalized into the endosome for translocation. [47] The interaction of the pre-pore with LF relies on the first 254 residues of the LF polypeptide, and unfolded regions of LF binds non-specifically to an α-clamp on PA that catalyzes further unfolding. [48,49] Because of the small size of the channel formed by PA, it is only in this unfolded state that proteins can be translocated, precluding the translocation of proteins with secondary structures such as those created by disulfide bonds. [50]

It was discovered that the 254-residue N-terminal fragment of LF (LF_N) was sufficient to translocate *Pseudomonas* exotoxin A that had been fused to LF_N's C-terminus. [48] When translocated in this manner, the exotoxin was fully functional within the cell at mediating cytotoxicity, and the potency was even greater than that of the toxin's native mode of entry into the cell. [51] The ability to deliver non-native cargo using protective antigen's efficient machinery presents a prime opportunity to repurpose PA for delivery of other proteins that must act within the cytosol, potentially for use in therapeutic applications. As long as a protein can be fused to LF_N and can unfold into a single polypeptide chain, it is a candidate for PA-mediated translocation.

Arora and Leppla further investigated the finding of their initial work conducted with *Pseudomonas* exotoxin by fusing LF_N to the active domains of Shiga toxin and diphtheria toxin, again confirming that alternate cargo can be delivered by this strategy. [52] Diphtheria toxin is composed of two subunits, A and B, where DTB associates with cells and mediates translocation of DTA, which causes ADP-ribosylation of eukaryotic elongation factor 2, inhibiting protein synthesis. [53] A cleavage product of subunit A of Shiga toxin also inhibits protein synthesis, but instead targets 28S rRNA, inactivating the ribosome. [52] When either DTA or Shiga toxin A1 were fused to LF_N, the fusion protein intoxicated cells in a PA-dependent manner, confirming with multiple examples that PA could be used to translocate different payloads that retain enzymatic activity. Additionally, the fusion protein LF_N-DTA has further use as a reporter on translocation due to its quick action in being transported into the cell and inhibiting protein synthesis. The degree of translocation can be measured indirectly by measuring protein synthesis. This is done by quantifying incorporation of a radiolabeled amino acid (^{3}H leucine).

Ras/Rap 1-Specific Protease (RRSP) is a subdomain of MARTX toxin of the *Vibrio vulnificus* bacterium that is responsible for the toxin's enzymatic activity. It is a protease that cleaves Ras in the cytosol, and retains this ability when isolated and translocated into the cell by protective antigen. [54] This is a recently discovered toxin that presents another viable route of inhibiting cell growth through use of PA. [55] Other studies have applied the LF_N fusion strategy to other proteins such as ricin, dihydrofolate reductase, β-lactamase, and cytolethal distending toxin B. [37,43,50,56] These translocated cargo performed various functions such as targeting tumor cells or enabling fluorescent-based confirmation of translocation.

Our lab has published studies that expand the known repertoire of cargo that can be delivered into the cytosol by protective antigen. Numerous protein scaffolds have been

engineered to replicate the binding specificity and versatility of antibodies, such as Fn3 domains derived from fibronectin, affibodies, DARPins, and the B1 domain of Protein G. Liao et. al. showed numerous examples of several forms of these scaffolds being translocated into cells by PA and retaining their biological activity, opening up an avenue for protein therapeutics by providing a viable access point for engineered therapies to reach cytosolic components. [57]

Protective antigen also serves as an access point to the cytosol for compounds that are not polypeptide-based, provided that the structure of the cargo complies with the size restraints imposed by PA's pore. Rabideau et. al. demonstrated translocation of clinically relevant small molecules monomethyl auristatin F (MMAF) and doxorubicin, while also noting that the more structurally complex molecule docetaxel was translocated much less efficiently. Additionally, protein cargo bearing backbone or side chain modifications translocated with the same efficiency as traditional peptides, while the introduction of cyclic peptides inhibited translocation likely due to the same size constraints noted previously. [58]

Protective antigen is a possible system for the introduction of proteins composed entirely of D-amino acids. These mirror image proteins are of particular interest due to their increased stability and resistance to naturally occurring proteases. [59] Having the capability to transport D-proteins into the cell opens up new purposes for engineering D-proteins as therapeutics. Furthermore, Rabideau has shown that a single D-amino acid placed at the N-terminus of translocated cargo protects the cargo from degradation in the proteasome by preventing ubiquitination. [60] This application of the N-end rule can be used to extend the half-life of translocated proteins and potentially enhance their therapeutic efficacy. [61]

A novel use of the anthrax toxin delivery system engages $CD4^+$ and $CD8^+$ T cells to induce an antigen-specific immune response. Peptides translocated into the cytosol in this

manner are capable of engaging the MHC class I and class II pathways required for induction of antigen-specific immunity. [62] Such uses illustrate the vast potential of a versatile, tunable system that allows controlled access of proteins and compounds to the cytosol of the cell.

1.6 Thesis Overview

The objective of this thesis is to apply the principles of protein engineering to develop therapeutics that bind specifically to cancer-associated antigens. We approach this by using recombinant fusion of protein binders to pore-forming bacterial toxins. The constructs generated, which use epidermal growth factor receptor (EGFR) or carcinoembryonic antigen (CEA) as a target for anti-cancer therapy, are characterized for their ability to modulate the biology of cancer cell lines, with an emphasis on inhibition of growth signaling and cell proliferation. We then assess the viability of these constructs in controlling tumor growth using mouse models.

In Chapter 2, a novel anti-EGFR antibody we developed from earlier work and described in Appendix 1 is combined with the anthrax toxin transport system, creating a PA construct that can translocate material into EGFR-positive pancreatic cancer cells. This EGFR-targeted PA is characterized using cell assays to assess the effect on growth signaling and proliferation when delivering a Ras protease and diphtheria toxin enzymatic domain. In Chapter 3, a parallel strategy is described in which an existing antibody against CEA is used to retarget PA to the same cancer cells, and that modified PA was then studied to understand the dependence of translocation efficiency on PA's receptor. These two constructs are then used in Chapter 4, which describes preliminary data on their effect as treatments for inhibiting tumors in mice.

Lastly, in Chapter 5, we discuss the impact of the work described and recommend further avenues of study.

Chapter 2: Modified Protective Antigen Targets EGFR to Translocate Cytotoxic Ras Protease into Cancer Cells

2.1 Introduction

Delivery of toxins capable of inhibiting tumors for the treatment of cancer is made challenging by the heterogeneity of cancer cells, the similarity of these cells to host cells, and the difficulty therapies have in accessing the cell cytosol where the majority of tumor-sustaining processes take place. [109] Pancreatic cancer in particular is a notoriously difficult cancer to treat. It is aggressive and fast-moving, and prognosis for patient survival is usually poor. [110] By the time it is detected, the disease is often too far advanced for surgical resection to be an option, and this type of cancer has shown resistance to local therapies. [111] Genomic instability in pancreatic cancer leads to rapid development of acquired resistance, furthering the challenge of treatment. Lastly, these cancers tend to respond poorly to chemotherapy, necessitating the development of effective alternative therapies. [112]

As detailed in Chapter 1, the protective antigen (PA) component of anthrax toxin addresses some of the issues of pancreatic cancer treatment and offers a promising avenue for the development of cancer therapies. [41] PA is one of three components of anthrax toxin, the others being lethal factor (LF) and edema factor (EF). [3] PA assembles on the surface of cells in heptamers, and when internalized into the high acidity environment of the endosome, forms a pore capable of translocating LF and EF into the cytosol, accessing difficult-to-reach growth effectors. [113] Past efforts have demonstrated that the PA-binding domain of LF can be isolated and inactivated (forming LF_N) and fused to protein cargo, enabling PA to translocate the entire fusion protein across the cell membrane. [52]

PA natively targets two ubiquitously expressed cell surface receptors, TEM8 and CMG2, but can be retargeted to other surface markers through use of additional binding domains. [14,114] This modularity allows PA to be used to design targeted toxins for a variety of cancer-specific surface markers, and with careful selection of antigen, the therapy can minimize off-site toxicity effects. The process of retargeting protective antigen has been described previously by Mechaly et. al. In brief, the native binding specificity of protective antigen for CMG2 and TEM8 is ablated by the introduction of a double mutation in domain IV of the protein (N682A and D683A). [35] This mutated PA (mPA) is then fused to an added fifth domain, usually a small protein scaffold engineered to bind to a target of interest, which confers a new specificity to PA. This can then be used to target cancer cells selectively to deliver a cytotoxic payload to the cytosol of those cells. [35,39]

Epidermal growth factor receptor (EGFR) is a well-characterized receptor involved in cell growth, proliferation, and migration. [115] Many cancers bear mutations in the EGFR receptor or in effectors downstream of this pathway, leading to rampant proliferation and driving the growth of these tumors. [81,98] The fact that EGFR is overexpressed on the cell surface in several cancers, and particularly, many types of pancreatic cancer, presents an opportunity to use EGFR as a marker for protective antigen-mediated toxin delivery. [35]

Another common characteristic of pancreatic cancers is an oncogenic mutation in K-ras, leading to sustained tumor growth. Ras is an oncogene that has been identified as a driving force behind many different cancers. Importantly, expression of oncogenic K-ras has been shown to be necessary to sustain certain pancreatic cancers, suggesting this cancer type may be especially vulnerable to Ras inhibition. [116] K-ras mutations in pancreatic cancer can drive mutations in the p53 gene, leading to failed growth arrest and furthering the progression of tumor growth. [117]

Inhibition of Ras in such cancers has led to a significant inhibition of growth of tumors in mouse xenograft models. [118] RRSP is a recently characterized Ras protease derived from the MARTX toxin of the *Vibrio vulnificus* bacterium that has been shown to rapidly cleave Ras when translocated into the cell as a fusion to LF_N. [54] This has been shown to result in the phenotypic effect of cell rounding and inhibition of colony formation. [55] Such findings suggest that this protein has the potential to be useful as a therapy against Ras-driven cancers.

We sought to leverage the combination of powerful targeting and delivery methods offered by EGFR-based PA-mediated translocation and inhibition of Ras signaling as a strategy for halting cell growth. We expressed the novel anti-EGFR antibody described in Appendix 1, E1v3, in the format of a single-chain antibody fragment (scFv) fused to a mutant form of PA. This fusion protein, mPA-E1v3, selectively targeted EGFR-positive pancreatic cancer cells in a receptor-dependent manner, and was able to translocate RRSP into the cytosol of cells where it exhibited Ras protease activity. Our results indicate that this strategy antagonizes the growth signaling cascade downstream of Ras, presenting a viable method for inhibiting tumor cell growth.

2.2 Results

2.2.1 Construction and characterization of a PA-scFv fusion targeting EGFR

Mutant PA bearing the N682A D683A mutation (mPA) was recombinantly expressed as a fusion to the scFv form of E1v3, creating the EGFR-targeted protective antigen construct, mPA-E1v3 (Figure 2.1a). SDS-PAGE analysis showed that under reducing conditions, mPA-E1v3 runs as a 110 kDa monomer as expected (Figure 2.1b). When proteolytically cleaved by trypsin to convert the mPA-E1v3 monomer to its active form, mPA-E1v3 converted to a high

molecular weight oligomer in a pH-dependent manner, consistent with the expectation that PA would assemble into a heptamer to form an SDS-resistant pore (Figure 2.1c). Trypsin treatment also appears to have formed a PA-sized side product that would suggest protease susceptibility of the linker between PA and scFv, but this is not expected to impair the activity of mPA-E1v3 under typical conditions.

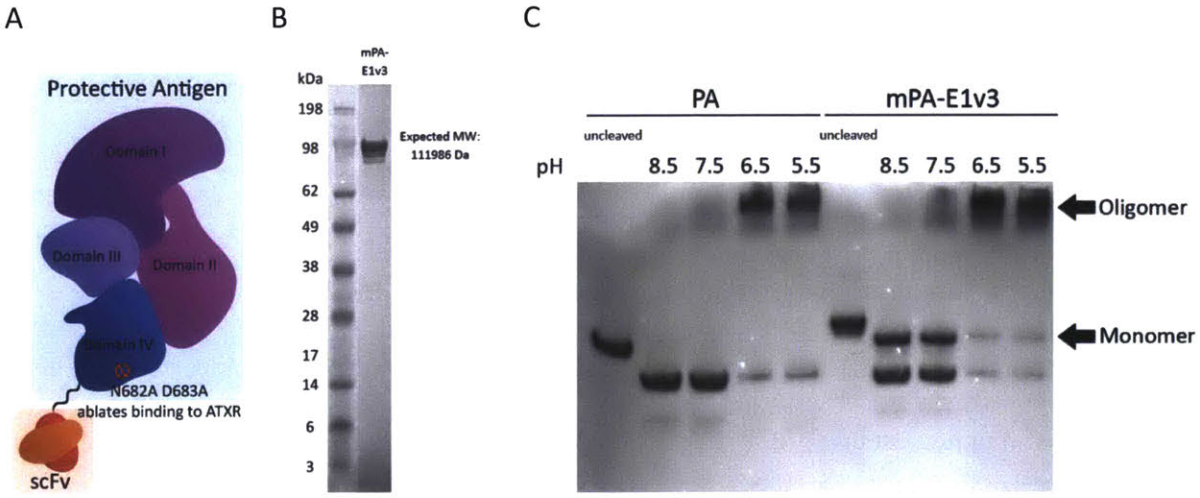

Figure 2.1. Characterization of mPA-E1v3 shows retention of PA's properties in gel electrophoresis. (a) Schematic representation of retargeted protective antigen. The N682A/D683A mutation in domain IV knocks out binding of PA to native receptors TEM8 and CMG2. An additional scFv binding domain is fused to PA at the C-terminus to confer new specificity for EGFR. (b) SDS-PAGE analysis of mPA-E1v3, the mutant PA retargeted to EGFR. (c) SDS-PAGE analysis of the conversion of mPA-E1v3 oligomer to an SDS-resistant pore at varying pH levels.

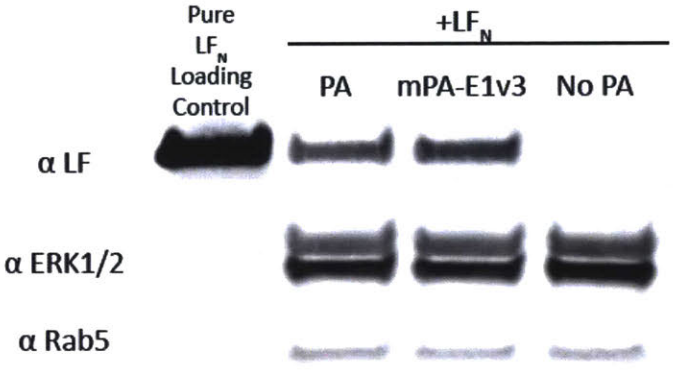

Figure 2.2. Western blot analysis of mPA-E1v3 + LF_N treatment demonstrates translocation activity. AsPC-1 cells were treated with 100 nM LF_N and 50 nM of PA or mPA-E1v3. After 24 hours, cells were washed and trypsinized, then lysed in buffer containing digitonin. Lysates were analyzed by Western blot and stained with goat anti-LF antibody and anti-goat antibody conjugated to 800CW IRDye. In the case of both PA and mPA-E1v3, LF_N can be detected in the cytosol.

mPA-E1v3 was shown to be capable of translocating material across the cell membrane through use of Western blot (Figure 2.2). AsPC-1 cells, an EGFR-positive pancreatic cancer cell line, were treated with PA constructs and LF_N for 24 hours, then subjected to a digitonin buffer to dissociate the cell membrane without disrupting the endosomes. Lysates were analyzed by Western blot stained with anti-LF antibody. The results showed that in the case of both wild-type PA and mPA-E1v3, LF_N can be detected as having been translocated into the cytosol, with bands appearing in the digitonin extraction sample.

A

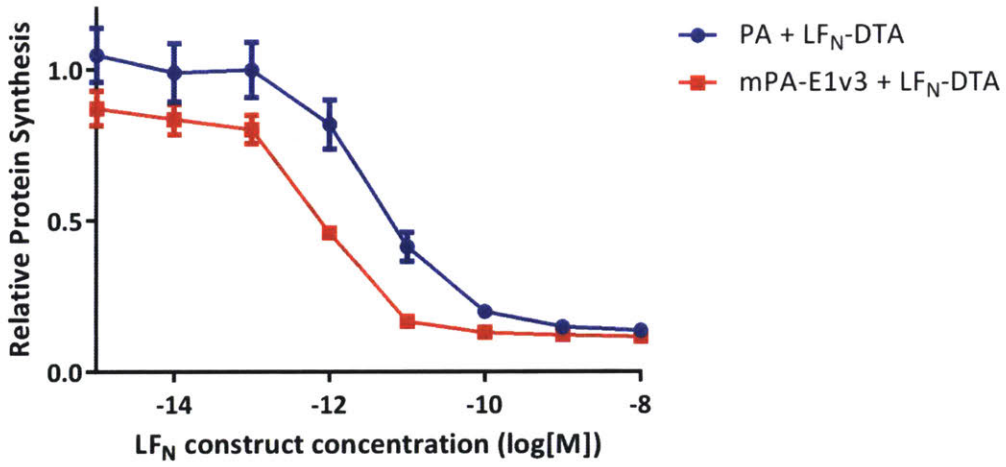

B

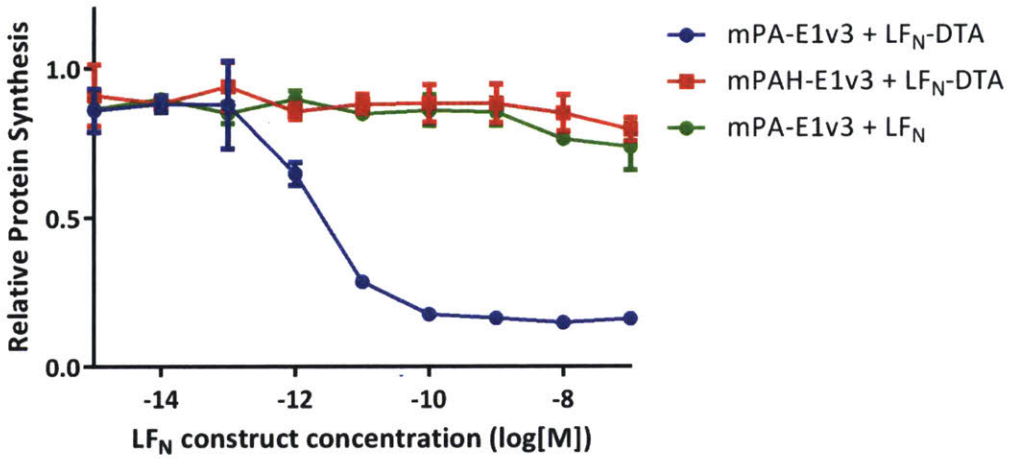

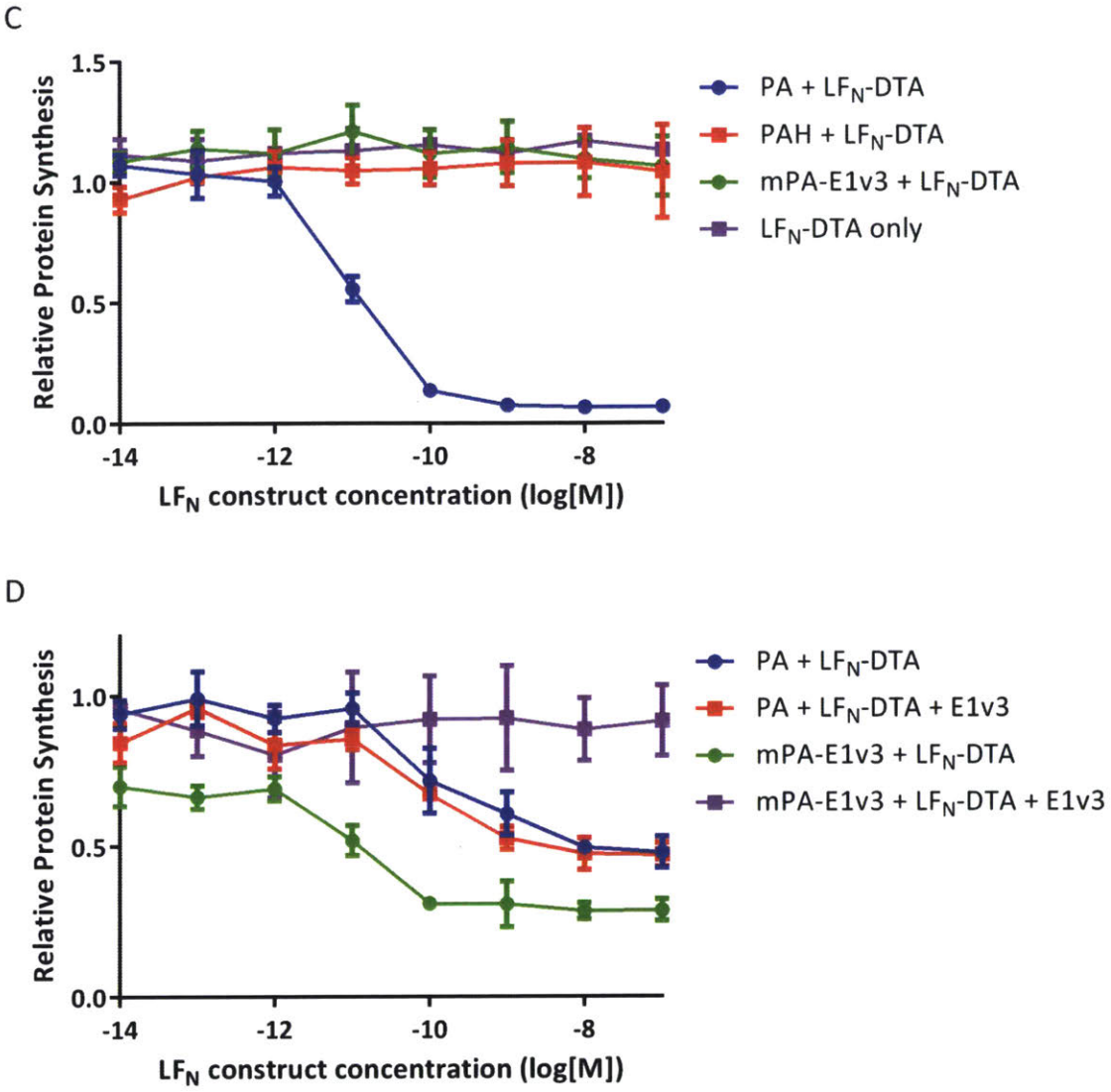

Figure 2.3. Protein synthesis inhibition assay shows biological activity of DTA domain translocated by mPA-E1v3. The ability of PA targeted to EGFR to deliver LF_N-DTA and inhibit protein synthesis was measured. AsPC-1 cells were treated for 30 minutes with 50 nM PA construct and the indicated concentration of LF_N construct. Incorporation of 3H-leucine was measured by liquid scintillation counting. (a) Comparison of PA and mPA-E1v3. (b) Comparison of mPA-E1v3 to translocation-deficient mutant (mPAH-E1v3) or translocated payload without catalytic domain (LF_N). Cells treated with both active PA (PA or mPA-E1v3) and active cargo (LF_N-DTA) showed inhibition of protein synthesis. (c) CHO cells, negative for human EGFR, were treated with LF_N-DTA and either PA, PAH, or, mPA-E1v3. Only PA shows activity. (d) Pre-treatment with E1v3 scFv inhibits the effect of mPA-E1v3.

The ability of mPA-E1v3 to translocate active material into the cell was tested by measuring the activity of translocated LF_N-DTA. LF_N-DTA is a fusion between DTA, the catalytic domain of diphtheria toxin, and LF_N. [119] DTA inhibits protein synthesis via ribosylation

of eukaryotic elongation factor 2. [120] The degree of protein synthesis can be measured by observing the incorporation of ^{3}H-leucine into the cell via scintillation counting (Figure 2.3). When AsPC-1 was treated with mPA-E1v3 and LF_N-DTA, protein synthesis was inhibited compared to the combination of mPA-E1v3 and LF_N (without any catalytic domain) as well as the combination of LF_N-DTA and mPAH-E1v3, an F427H mutant that is incapable of translocating material into the cell (Figure 2.3a and 2.3b). Furthermore, the potency of the EGFR-targeted mPA-E1v3 treatment was greater than that of PA targeted to its native anthrax receptors, showing protein synthesis inhibition at concentrations of LF_N two orders of magnitude below.

This effect was not replicated in CHO cells, which do not express human EGFR, demonstrating that the treatment is dependent on the presence of the targeted receptor on the cells (Figure 2.3c). Additionally, when cells were treated with soluble E1v3 scFv for one hour before treatment with PA, the ability of mPA-E1v3 to inhibit protein synthesis was blocked, again showing that this is receptor specific. (Figure 2.3d)

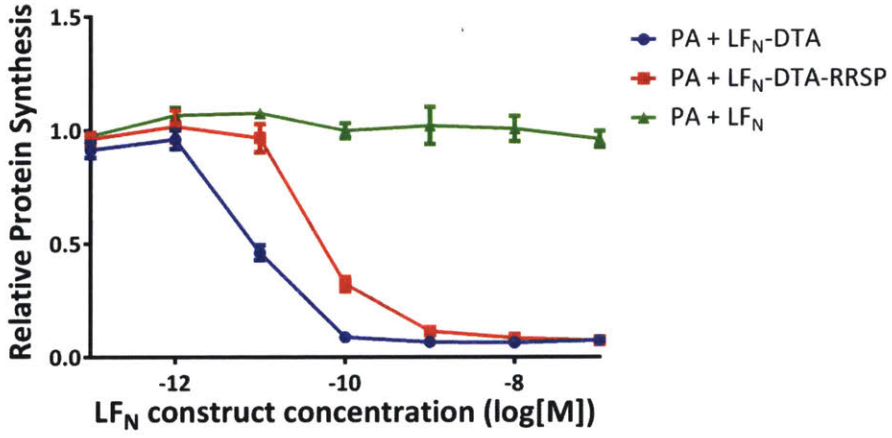

Figure 2.4. Protein synthesis inhibition assay shows RRSP domain can be translocated by PA when expressed as a fusion to LF_N-DTA. Cells were treated with 50 nM PA and the indicated concentration of LF_N, LF_N-DTA, or LF_N-DTA-RRSP. The fusion of RRSP to LF_N-DTA is still translocated into the cell where the DTA domain can actively inhibit protein synthesis, but at a reduced rate compared to LF_N-DTA alone.

2.2.2 RRSP cleaves Ras in cells in the presence of PA

In order to characterize PA-mediated entry of RRSP into the cell, RRSP was fused to the C-terminus of LF_N-DTA. This fusion was used to determine whether the fusion construct was still able to inhibit protein synthesis, an indication that the RRSP domain does not prevent the full construct from being translocated (Figure 2.4). LF_N-DTA-RRSP achieved protein synthesis inhibition, but at a reduced effect compared to LF_N-DTA.

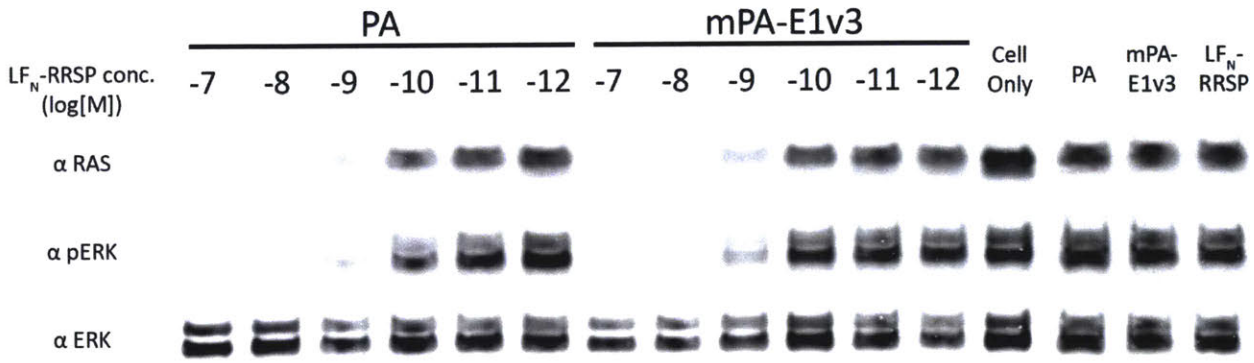

Figure 2.5. Signal inhibition by LF_N-RRSP is detected by Western blot. AsPC-1 cells were treated with 50 nM PA or mPA-E1v3 and the indicated concentration of LF_N-RRSP for 24 hours. Cells were then subjected to total lysis in SDS buffer, then analyzed by Western blot stained for Ras, pERK, and ERK. In a dose-dependent manner, LF_N-RRSP is translocated into the cell where it induces cleavage of Ras. As a result, signaling of ERK is reduced while total levels of ERK remain unchanged.

The biological activity of translocated RRSP was measured in AsPC-1 cells. Cells were treated for 24 hours with combination of PA variants and a range of concentrations of LF_N-RRSP (Figure 2.5). After treatment, cells were lysed and lysates run on Western blots, then stained for internal signal effectors RAS and pERK. If LF_N-RRSP is successfully translocated across the membrane, it induces cleavage of cytosolic RAS, which then inhibits signaling downstream of RAS in the pathway through effector proteins such as pERK. As shown in Figure 2.5, both PA and mPA-E1v3 are capable of mediating RRSP-induced cleavage of RAS within AsPC-1 cells. This results in a decrease in the level of phosphorylated ERK protein within the cell, but does not alter the total levels of ERK protein.

2.2.3 Translocated RRSP inhibits cell growth

To study the effects of PA/RRSP-induced Ras cleavage on the viability of the cell, a cell migration assay was performed in the form of a scratch test. A wound was made by scraping a line of cells from a tissue culture of AsPC-1 cells. The cultures were then grown in media containing PA and LF_N constructs, with images of the cultures taken at the start of the experiment and after 72 hours. The degree to which the wound had been healed, indicated by the regrowth of cells into the vacant area of the tissue culture surface, was compared between the two time points. This qualitative experiment allows for some judgment to be made on the phenotypic response of this treatment.

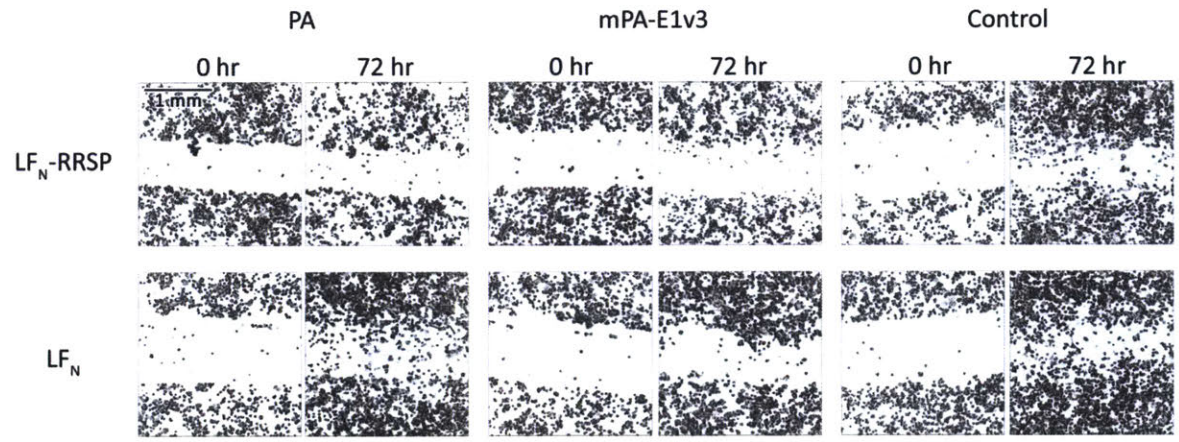

Figure 2.6. Scratch test assay demonstrates mPA-E1v3 inhibits cell proliferation. AsPC-1 cells were grown in a 12-well plate to 90% confluency. A band of cells was scraped away, and cells were treated for 36 hours with 100 nM LF_N-RRSP or LF_N and 50 nM PA and mPA-E1v3. Images were taken at t = 0 and t = 72 hours. Translocated RRSP inhibited migration of cells.

When LF_N-RRSP was translocated using PA or mPA-E1v3, there was little to no change in the width of the scratch before and after the treatment (Figure 2.6). This suggests an inhibition of cell migration that has the potential to translate to an anti-proliferative effect. Notably, when mPA-E1v3 was used to translocate LF_N, a payload lacking any catalytic domain, there was also

an apparent moderate inhibition of cell migration, as the cell front only partially progressed back into the wound in this treatment group compared to the control. This lends credibility to the idea that the inhibition of cell signaling caused by the E1v3 scFv domain may also be contributing to the therapeutic effect of this treatment. It is possible that mPA-E1v3 and LF_N-RRSP together are more potent than the scFv alone or than LF_N-RRSP translocated using wild-type PA.

To quantify the degree to which mPA-E1v3 and LF_N-RRSP modulate the growth processes of these cancer cells, the CellTiter Glo Luminescent Cell Viability Assay (Promega) was employed. Cells grown in a 96-well plate were treated with PA constructs and varying LF_N payloads for three days, after which the metabolic activity of the cells was measured using the CellTiter-Glo kit for quantification of ATP. In the case of both PA and mPA-E1v3, combination treatment with LF_N-DTA and LF_N-RRSP showed inhibition of cell growth. (Figure 2.7) No response was observed in the case of PA and mPA-E1v3 bearing the F427H mutation, which knocks out the ability to translocate material across its pore. Similarly, when no catalytic domain was translocated in the case of LF_N, there was no difference between the metabolic activity of treated cells versus the control. This indicates that mPA-E1v3 can translocate material such as LF_N-RRSP and induce an anti-proliferative response.

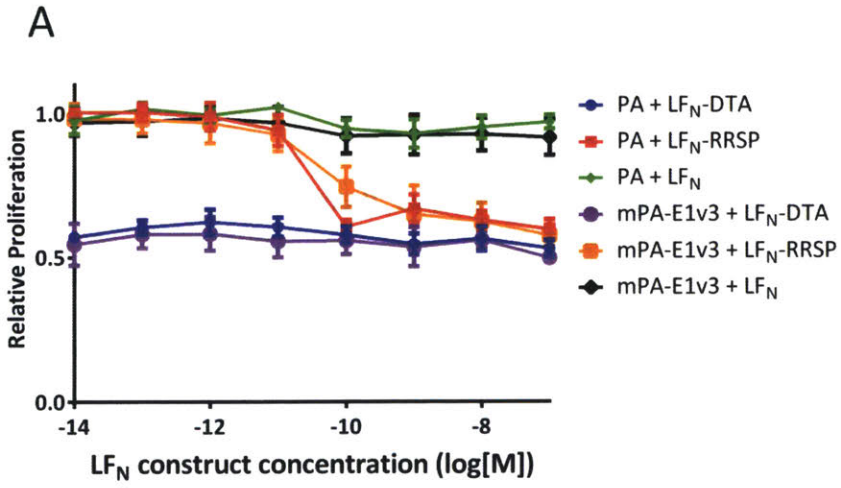

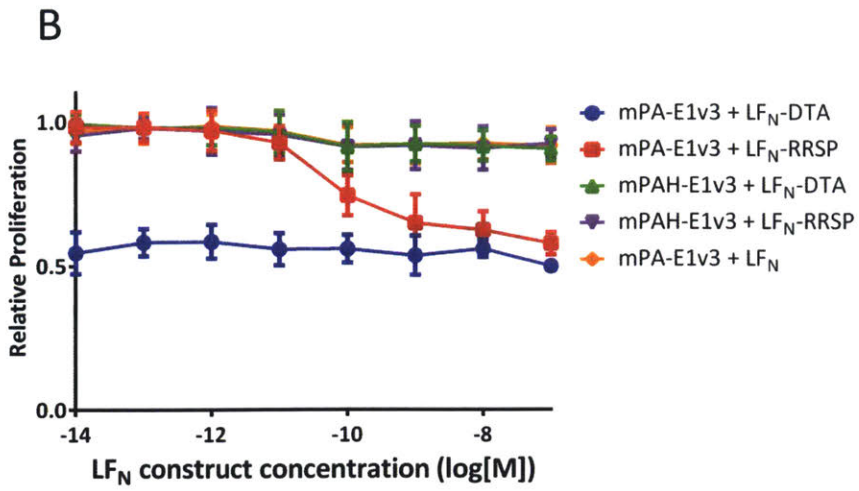

Figure 2.7. CellTiter-Glo assay quantifies cell proliferation inhibition by mPA-E1v3. LF_N-RRSP exhibits an anti-proliferative effect in ATP-quantification experiments. AsPC-1 cells were treated with 50 nM PA, mPA-E1v3, or F427H variant and the indicated concentration of LF_N construct for 72 hours. The amount of ATP in the cells was then quantified using CellTiter-Glo assay (Promega). (a) Comparison of PA and mPA-E1v3 delivering LF_N, LF_N-DTA, or LF_N-RRSP. (b) Comparison of delivery by mPA-E1v3 versus translocation-deficient F427H mutant, mPAH-E1v3. Both PA and mPA-E1v3 exhibited a similar dose response to translocated LF_N-RRSP, with proliferation inhibited at higher concentrations. Translocated LF_N-DTA inhibited proliferation at all concentrations tested.

2.3 Discussion

The pair of anthrax toxin components, PA and LF_N, presents a modular platform that can be engineered to fit a variety of needs. Because the specificity of PA can be altered to any target for which a protein binder exists, this system can easily be applied toward the inhibition of cancer cell growth. Similarly, the versatility of the cytotoxic payload is restricted only to the myriad of disulfide-free proteins that can be fused to LF_N and translocated through the pore.

RRSP, a potent enzyme that nature has effectively engineered to inhibit Ras, is one such protein. As a component of the toxin produced by *V. vulnificus*, it is transported across the cell membrane as part of the larger MARTX toxin, then excised while within the cytosol where it can act upon Ras. This approach would be too unwieldy for use as a therapeutic, but when combined with protective antigen, the isolated RRSP domain can be delivered efficiently and achieve the

same biological effect. Our results show that the strategy of PA-mediated delivery of RRSP can be used to inhibit growth signaling and proliferation of a pancreatic cancer cell line.

The combination of EGFR and Ras-targeted treatment has the potential to synergize and achieve a potent anti-proliferative effect. In this study, EGFR can be used not only as a cell marker, but also as a therapeutic target. If the EGFR targeting domain of mPA is also capable of inhibiting growth signaling at the level of the receptor-ligand interaction, it may serve as part of a two-pronged approach of achieving near-complete signal inhibition. However, this result is not reflected in the data for cell proliferation. As seen in Figure 2.7, the anti-proliferative response of LF_N-RRSP is similar whether it is translocated by wild-type PA or PA targeted to EGFR. This diverges from the result seen in Figure 2.3a, where, under the time frame shown, mPA-E1v3 reaches a greater degree of protein synthesis inhibition compared to wild-type PA. The difference here may be because of the more rapid internalization kinetics of EGFR compared to TEM8 and CMG2, which would lead to quicker internalization of PA construct and subsequently, a greater number of LF_N-DTA proteins entering the cytosol. However, over the timescale of three days, exceeding the internalization half-life of both receptors, translocation of protein into the cell may no longer be the rate-limiting step for Ras cleavage, with sufficient numbers of LF_N-RRSP present to degrade Ras. The effect of receptor identity on the kinetics and efficacy of PA-based therapeutics warrants further investigation.

2.4 Materials and Methods

2.4.1 Synthesis of mPA-E1v3

The E1v3 scFv gene was cloned into an existing plasmid containing the mPA gene. The primers 5'-ATCTTCTCTAAGAAAGGCTACGAAATCGGTGAATTCAGCCCGGGTCATAA-

3' and 5'-TATGGGGTGTCGCCCTTGGGGTTAACCTTACGAGGAGACGGTGACCAGGG-3' were used to create large primers containing the scFv gene, then inserted into the mPA backbone using site-directed mutagenesis (Agilent QuikChange Lightning Mutagenesis Kit). F427H mutants were generated using site-directed mutagenesis with the primers 5'-CTGAACGCTCAGGACGACCACTCTTCCACCCCGATCAC-3' and 5'-CAGTTCAGCCAGCTGGTTGCAGATGTTCTGAGAGGTTTG-3'.

PA constructs were overexpressed in the periplasm of BL21 *E. coli* cells as described previously. [57] Protein was extracted from frozen culture pellets by resuspension in sucrose buffer (20% w/v sucrose, 1 mM EDTA, 20 mM Tris, pH 8.5). This was followed by centrifugation, a wash with 20 mM Tris pH 8.5, centrifugation, and a resuspension of the cell pellet in 5 mM $MgSO_4$. Tris pH 8.5 was added to a concentration of 20 mM, and the final suspension was centrifuged and the supernatant filtered on a .22 micron bottle-top filter.

PA was isolated from the supernatant using anion exchange chromatography (Q HP column, GE Healthcare) from a gradient of 0 to 250 mM NaCl. Protein-containing fractions were pooled, concentrated using 30 kDa MWCO Amicon centrifugal filters (Millipore), and purified again using size-exclusion chromatography on a SuperDex 200 gel filtration column (GE Healthcare). Proteins were analyzed by gel electrophoresis to confirm size (Figure S2.2).

2.4.2 Synthesis of LF_N-RRSP

The DNA encoding RRSP was a generous gift from Karla Satchell's lab at Northwestern University. QuikChange mutagenesis was used to insert this gene into a previously generated plasmid containing the gene for LF_N expressed as a fusion to His-tagged SUMO. DNA for LF_N, LF_N-DTA, and LF_N-RRSP was transformed into BL21 cells and cultured in 1 L of LB medium in

an incubator shaker at 37°C to OD = 0.6, at which point cultures were grown at 30°C and protein expression was induced with 0.4 mM IPTG for 16 hours. Cultures were centrifuged to form cell pellets, then resuspended in Tris-buffered saline (pH 7.5) with a small amount of lysozyme and half a tablet of protease inhibitor cocktail (Roche). The suspension was sonicated to lyse the cells, then centrifuged to remove cell solids. The supernatant was filtered, then passed through a HisTrap FF Ni-NTA column to allow the SUMO fusion to bind the column. Protein was eluted with Tris-buffered saline and 500 mM imidazole, then desalted via HiTrap Desalting Column (GE Healthcare). SUMO was cleaved from LF_N by reacting with SUMO protease for 1 hour at room temperature, and soluble LF_N construct was purified by collecting the flowthrough from a second pass through a HisTrap FF Ni-NTA column. Proteins were analyzed by gel electrophoresis to confirm size (Figure S2.2).

2.4.3 Cell culture

AsPC-1 cells were obtained from American Type Culture Collection (CRL 1682). Cells were maintained in a tissue culture incubator and grown in RPMI medium supplemented with 10% fetal bovine serum, 100 units/mL penicillin, and 100 μg/mL streptomycin.

2.4.4 Protein synthesis inhibition assay

AsPC-1 cells were seeded in a 96-well tissue culture plate at 50,000 cells per well and grown overnight. Cells were then treated with media containing LF_N, LF_N-DTA, or LF_N-DTA-

RRSP at varying concentrations as well as 50 nM PA, mPA-E1v3, or F427H variants. The plate was incubated at 37°C for 30 minutes, then washed three times with phosphate-buffered saline (PBS) and incubated at 37°C for 1 hour in leucine-deficient medium supplemented with ^{3}H-leucine at 1 μCi/mL. Cells were washed three times with PBS, then lysed using scintillation fluid. Protein synthesis levels were measured by determining incorporation of ^{3}H-leucine using a 1450 Microbeta Luminescence and Liquid Scintillation Counter (Perkin Elmer Life Sciences).

2.4.5 Western blotting analysis

For Ras cleavage and signaling pathway analysis, AsPC-1 cells were grown in a 12-well tissue culture plate until 80% confluency. Cells were treated with media containing 100 nM LF_N, LF_N-DTA, or LF_N-RRSP and 50 nM PA or mPA-E1v3 for 24 hours at 37°C. After this step, cells were washed with PBS, then lysed using SDS buffer (50 mM Tris HCl, 2% SDS, 5% glycerol, 5 mM EDTA with protease and phosphatase inhibitors). The lysates were filtered using AcroPrep Filter Plates with Bio-Inert Membranes (Pall Life Sciences), then run on SDS PAGE gels and transferred to Western blot membranes. Western blots were sequentially incubated with anti-Ras antibody, anti-pERK antibody, and anti ERK antibody (Cell Signaling Technologies), then incubated with anti-rabbit antibody labeled with IRDye and imaged on an Odyssey Imaging System (LI-COR Biosciences).

For translocation quantification, AsPC-1 cells were treated for 24 hours with 50 nM PA or mPA-E1v3 and 100 nM of LF_N. Cells were then washed with PBS and trypsinized. The outer membrane was dissociated with digitonin buffer (50 μg/mL digitonin, 1 mM NaH_2PO_4, 75 mM NaCl, 8 mM Na_2HPO_4, 250 mM sucrose, protease inhibitor cocktail, pH 7.7) and centrifuged, and the supernatant was run on SDS-PAGE gels and transferred to Western blot membranes.

Western blots were stained with goat anti-LF antibody (Santa Cruz Biotechnology) followed by anti-goat antibody 800CW IRDye, then imaged on an Odyssey Imaging System.

2.4.6 Scratch test

AsPC-1 cells were grown in 12-well plates to 90% confluency. A portion of the cells was then removed using a 200 μL pipet tip to form a scratch in a single line across the culture surface. In each well, a mark was made to allow for the same region of the plate to be photographed at different time points. The media was then replaced with fresh media containing 50 nM PA or mPA-E1v3 and 100 nM of LF_N or LF_N-RRSP. Images were taken using the microscope and an AmScope MU300 camera at the start of the experiment and after incubating at 37°C for 72 hours. To improve visibility of cells, a "Find Edges" Photoshop filter was applied to the image. The original image is shown in Figure S2.3.

2.4.7 Proliferation assay

AsPC-1 cells were seeded in a 96-well tissue culture plate at 10,000 cells per well and grown overnight. Cells were then treated with media containing LF_N, LF_N-DTA, or LF_N-RRSP at varying concentrations as well as 50 nM PA, mPA-E1v3, or F427H variants. The plate was incubated at 37°C for three days.

Quantification of ATP in cells was carried out using the CellTiter-Glo Luminescent Viability Assay (Promega) according to manufacturer's protocols. The tissue culture plate was cooled to room temperature, and 100 μL of resuspended CellTiter-Glo reagent was added to each

well. Cells were shaken in order to mix the reagent and lyse the cells, then incubated at room temperature for 10 minutes. Luminescence was quantified using a 1450 Microbeta Luminescence and Liquid Scintillation Counter (Perkin Elmer Life Sciences).

Chapter 3: CEA-targeted cytosolic delivery of anti-cancer toxins is influenced by receptor kinetics

3.1 Introduction

Cancer cells bear strong similarities to healthy cells, invalidating the viability of many cytotoxic treatments due to the risk of unacceptable off-site toxicity. [121] Such a challenge is alleviated by targeting cancer surface markers with expression profiles that differ greatly from that of host cells. [109] Because the field of protein engineering is capable of generating binding domains against targets of interest, existing toxins found in nature can now be coopted for use against such cells bearing unique cancer-associated antigens. [35]

Carcinoembryonic antigen (CEA) is one such surface antigen. A member of the carcinoembryonic antigen family, it is principally involved in processes relating to cell adhesion. [122] During the development of the fetus, this antigen is widely expressed in the gastrointestinal tract, but in adulthood, expression is typically only found in the case of certain cancers. [123] This property makes it a useful cancer marker, and has led to its use in various imaging technologies. [124] It has been less effective to use CEA as a therapeutic target, with most efforts towards raising antibody responses against CEA as part of anti-cancer vaccine design showing minimal success. [125,126] This suggests that while targeting CEA to inhibit its biological activity may not affect tumor growth, it may be useful to use CEA to target specifically tumor cells and deliver a toxin that can induce cell death independent of CEA.

Protective antigen (PA) has been retargeted to cancer-associated antigens such as HER2 and EGFR, but it has not yet been used in the context of CEA. [35,37] PA is the pore-forming component of anthrax toxin and binds to TEM8 and CMG2, which are widely expressed on most

human cells. [14] When bound to the surface, PA is cleaved into an active form that can then oligomerize, and when it is endocytosed into the cell, the low pH of the endosome causes the oligomer to form a pore that can then translocate cargo across the cell membrane. [19] This system can be hijacked to translocate other proteins of interest by fusing those proteins to the PA-binding domain of LF (LF_N). [113] Moreover, the specificity of PA can be altered by knocking out its native binding for TEM8 and CMG2 with a double mutation (N682A and D683A), and then adding a new fifth binding domain specific for the desired target. [35] Through this strategy, PA can be used to target cancer-specific surface receptors, such as CEA, that could alleviate the effects of off-site toxicity.

In this study, we sought to combine the favorable expression profile of CEA with PA-based toxin delivery in order to develop a highly specific toxin. Through recombinant expression, PA was mutated to ablate its native binding activity, then fused to an anti-CEA antibody first described by Graff. et al, sm3e, in single-chain antibody fragment format (scFv). [127] The resulting construct, mPA-sm3e, translocated cytotoxic material selectively into CEA-positive tumor cells and inhibited cell growth, demonstrating a potential therapeutic strategy for cancer treatment.

3.2 Results

3.2.1 Construction of PA-scFv fusion targeting CEA

The engineering and characterization of the anti-CEA single chain variable fragment (scFv), sm3e, was described by Graff et. al. [127] This protein binds with picomolar affinity to CEA, but is not known to bear any biological or therapeutic effect on its own. Mutant PA bearing the N682A D683A mutation (mPA) was recombinantly expressed as a fusion to sm3e,

creating the CEA-targeted protective antigen construct, mPA-sm3e (Figure 3.1). The ability of mPA-sm3e to form an SDS-resistant pore was compared to that of wild-type PA. Both PA constructs were proteolytically cleaved by trypsin to remove the 20 kDa fragment and activate the monomer. This cleaved form of PA was subjected to varying pH and run on SDS-PAGE, showing the formation of a high molecular weight aggregate indicative of formation of an oligomer characteristic of a pore. Trypsin treatment also appears to have formed a PA-sized side product that would suggest protease susceptibility of the linker between PA and scFv, but this is not expected to impair the activity of mPA-E1v3 under typical conditions.

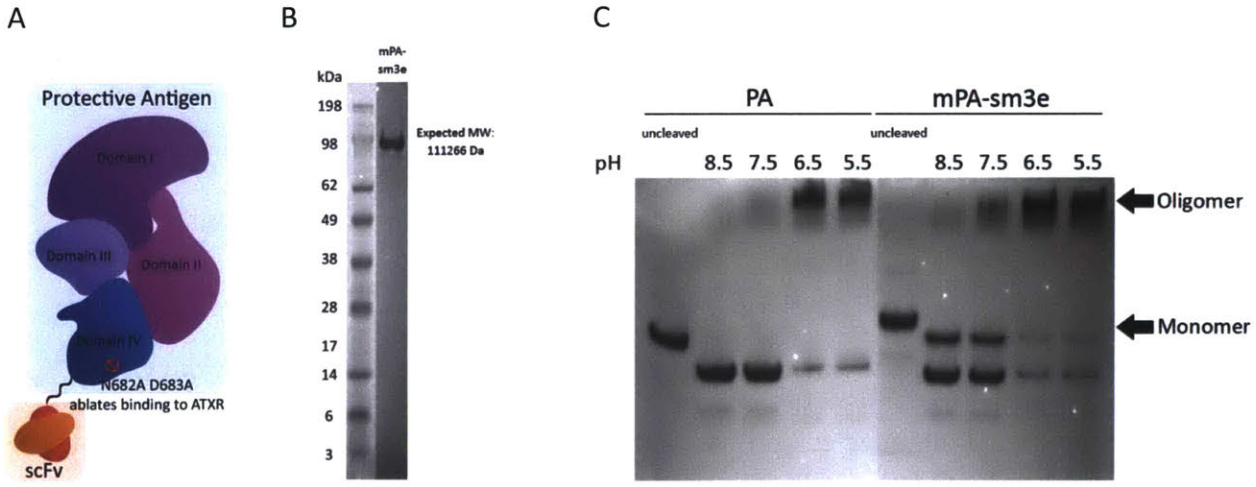

Figure 3.1. Characterization of mPA-sm3e shows retention of PA's properties in gel electrophoresis. (a) Schematic representation of retargeted protective antigen. The N682A/D683A mutation in domain IV knocks out binding of PA to native receptors TEM8 and CMG2. An additional scFv binding domain is fused to PA at the C-terminus to confer new specificity for CEA. (b) SDS-PAGE analysis of mPA-sm3e, the mutant PA retargeted to CEA. (c) SDS-PAGE analysis of the conversion of mPA-sm3e oligomer to an SDS-resistant pore at varying pH levels.

The activity of mPA-sm3e was confirmed by Western blot detection of translocated protein. A CEA-positive cell line, AsPC-1, was treated with LF_N and either PA or mPA-sm3e for 24 hours. Cells were then lysed with buffer containing digitonin, a mild detergent that disrupts the cell membrane but not the endosomes. Lysates were analyzed by Western blot

stained with anti-LF antibody (Figure 3.2). The results showed that in the case of both wild-type PA and mPA-sm3e, LF_N was translocated into the cell.

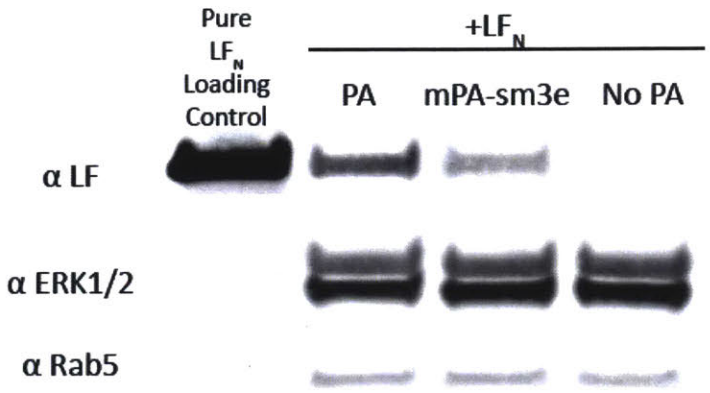

Figure 3.2. Western blot analysis of mPA-sm3e + LF_N treatment demonstrates translocation activity. AsPC-1 cells were treated with 100 nM LF_N and 50 nM of PA or mPA-sm3e. After 24 hours, cells were washed and trypsinized, then lysed in buffer containing digitonin. Lysates were analyzed by Western blot and stained with goat anti-LF and anti-goat antibody conjugated to 800CW IRDye. In the case of both PA and mPA-sm3e, LF_N can be detected in the cytosol.

A

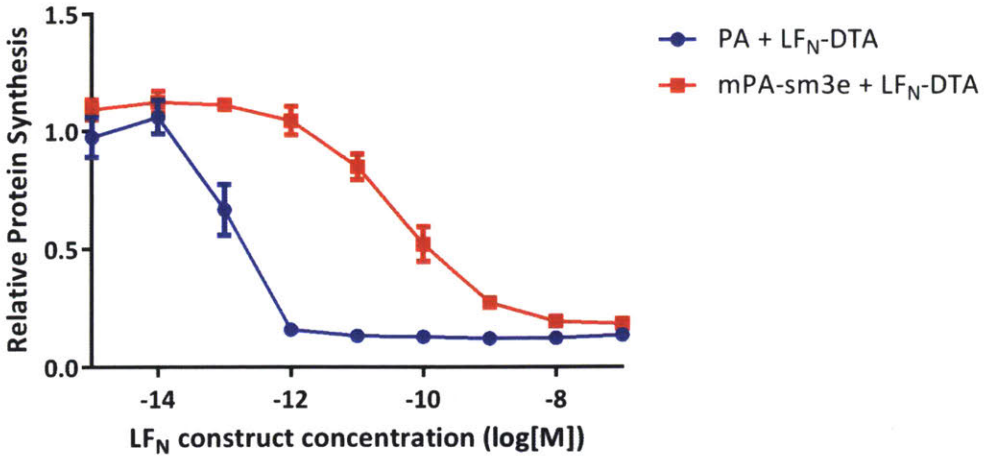
Relative Protein Synthesis
1.5
1.0
0.5
0.0
-14
-12
-10
-8
LF$_N$ construct concentration (log[M])
PA + LF$_N$-DTA
mPA-sm3e + LF$_N$-DTA

B

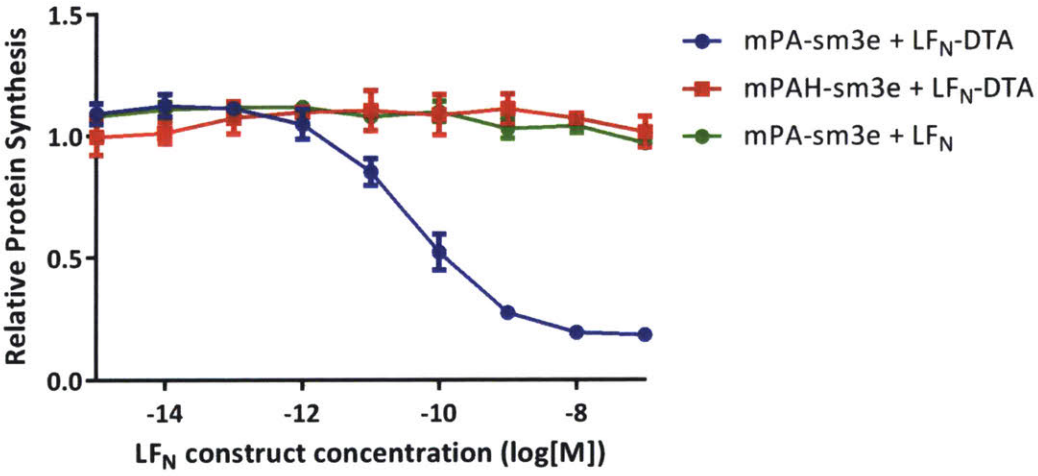
Relative Protein Synthesis
1.5
1.0
0.5
0.0
-14
-12
-10
-8
LF$_N$ construct concentration (log[M])
mPA-sm3e + LF$_N$-DTA
mPAH-sm3e + LF$_N$-DTA
mPA-sm3e + LF$_N$

C

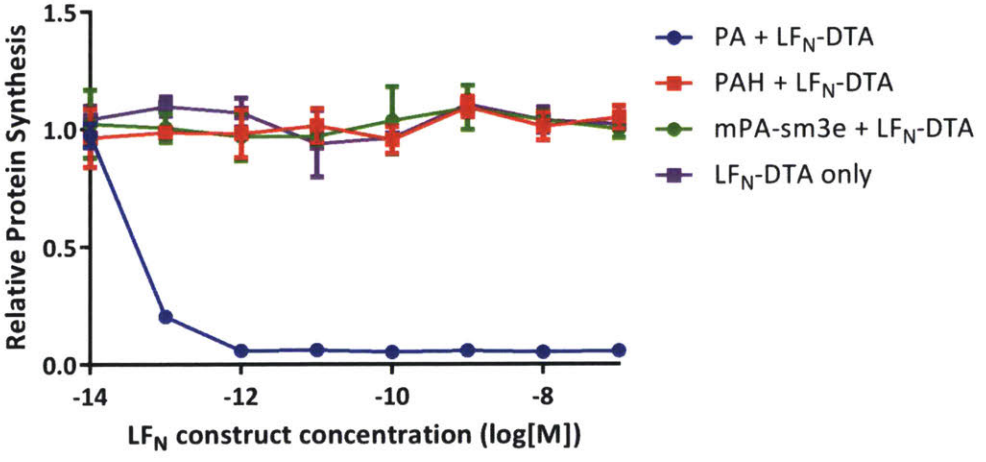
Relative Protein Synthesis
1.5
1.0
0.5
0.0
-14
-12
-10
-8
LF$_N$ construct concentration (log[M])
PA + LF$_N$-DTA
PAH + LF$_N$-DTA
mPA-sm3e + LF$_N$-DTA
LF$_N$-DTA only

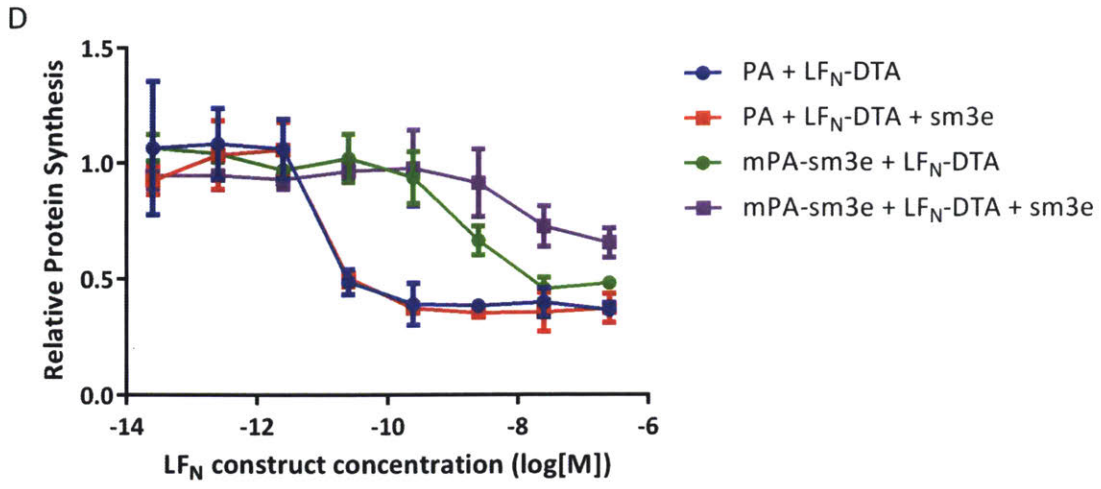

Figure 3.3. Protein synthesis inhibition assay shows biological activity of DTA domain translocated by mPA-sm3e. AsPC-1 cells were treated for 4 hours with 50 nM PA construct and the indicated concentration of LF_N construct. Incorporation of 3H-leucine was measured by liquid scintillation counting. (a) Comparison of PA and mPA-sm3e. (b) Comparison of mPA-sm3e to translocation-deficient mutant (mPAH-sm3e) or translocated payload without catalytic domain (LF_N). Cells treated with both active PA (PA or mPA-sm3e) and active cargo (LF_N-DTA) showed inhibition of protein synthesis, but mPA-sm3e showed reduced potency at lower concentrations of LF_N-DTA. (c) CHO cells negative for human CEA were treated with LF_N-DTA and either wild-type PA, PAH, or mPA-sm3e. Only PA showed activity in these cells. (d) Pre-treatment with soluble sm3e scFv diminishes the activity of mPA-sm3e but not wild-type PA.

3.2.2 Confirmation of activity of toxin payload translocated by mPA-sm3e

DTA is the catalytic domain of diphtheria toxin that disrupts protein synthesis through ribosylation of eukaryotic elongation factor 2. [119] When fused to LF_N, DTA can serve as a measure of translocation since levels of protein synthesis inhibition can be quantified via incorporation of ^{3}H-leucine, measurable by scintillation counting. The activity of PA and mPA-sm3e in CEA-positive AsPC-1 cells were compared using this assay (Figure 3.3). Variants of these constructs bearing the F427H mutation were also tested. This mutation completely blocks the ability of PA to translocate material through its pore. The combination of PA and LF_N-DTA completely inhibited protein synthesis at concentrations of LF_N-DTA above 0.1 pM, whereas PAH and LF_N-DTA or PA and LF_N did not (Figure 3.3a and 3.3b). mPA-sm3e and LF_N-DTA together also inhibited protein synthesis, but only at concentrations of LF_N above 1 nM.

CHO cells that do not express human CEA were also tested using this experiment. As expected, mPA-sm3e did not have any activity in this cell line, demonstrating this system's dependence on the expression of the target antigen (Figure 3.3c). Similarly, when AsPC-1 cells were pre-incubated with soluble sm3e scFv for three hours, then treated with either PA or mPA-sm3e with LF_N-DTA, the activity of mPA-sm3e was reduced by up to 49% compared to cells that were not treated with sm3e (Figure 3.3d). No change in activity was observed in cells treated with wild-type PA, again confirming the importance of CEA-targeting for this therapy.

3.2.3 Influence of receptor dynamics on translocation efficiency

The difference in potency between wild-type PA and mPA-sm3e (Figure 3.3a) could possibly be attributed to disparities in the affinity of mPA-sm3e for CEA versus wild-type PA for its two anthrax receptors (ATXR) or differing receptor expression levels and trafficking mechanics of CEA when compared to ATXR. The pH-dependence of translocation is hypothesized to be influenced by the affinity of PA for its receptor, where higher affinity interactions require lower pHs to dissociate PA from the bound receptor, an event that is required for the formation of the pore. [128] Wild-type PA's affinity for CMG2 is K_D = 170 pM, which may explain why a lower pH is required for translocation through PA pores associated with CMG2. [129] sm3e is engineered as a high-affinity CEA binder (K_D = 30 pM), which may inhibit translocation if mPA-sm3e fails to efficiently dissociate from the receptor and allow the pore to form. Regarding trafficking, CEA bears a kinetic profile that differs from PA's native receptors TEM8 and CMG2 as well as previously described targets HER2 and EGFR. It does not undergo a fast cycle of internalization, and the binding of antibody, in most cases, does not induce endocytosis of the surface antigen. [130] The activity of PA is dependent on its internalization into

the endosome, so if mPA-sm3e is not internalized as quickly, it could delay its activity in translocating cargo.

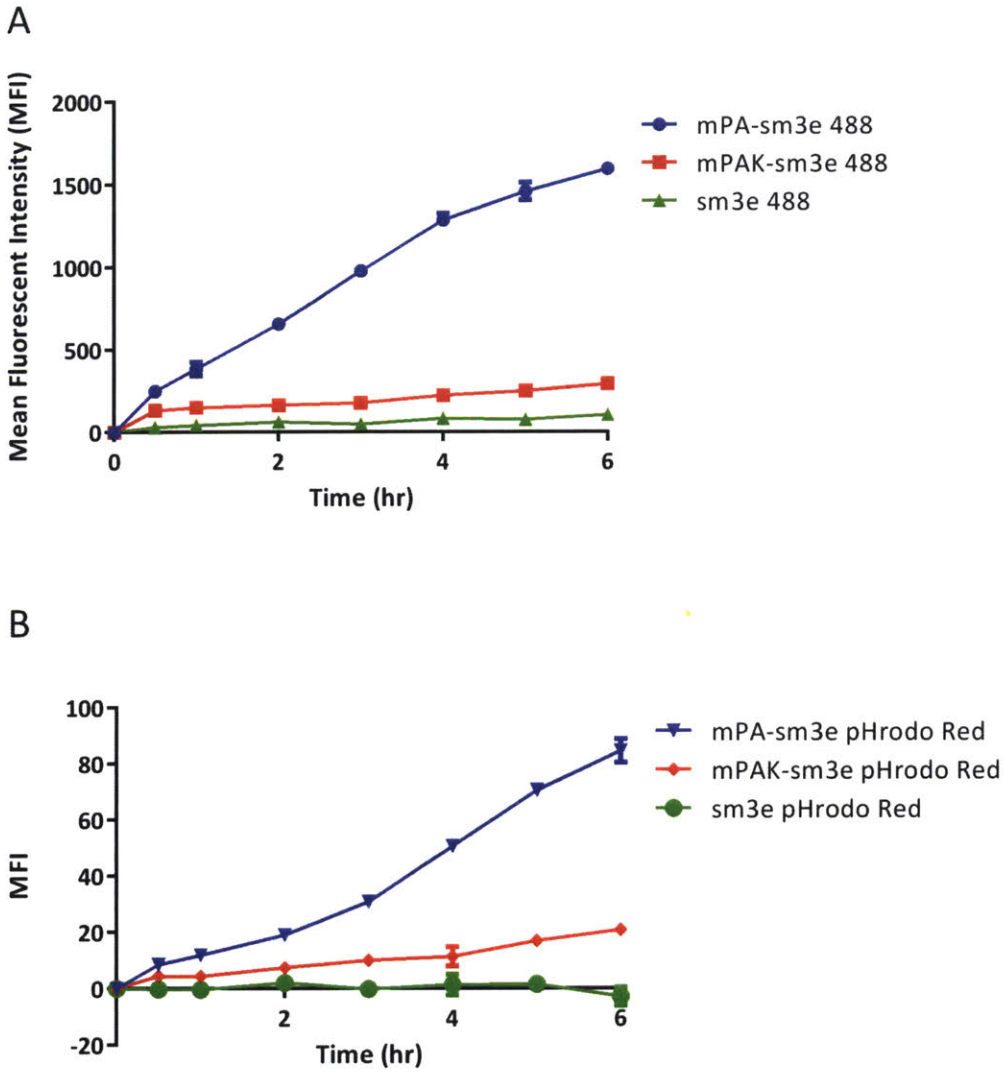

Figure 3.4. Measurement of internalization by flow cytometry shows PA increases the internalization rate of CEA-binding sm3e. AsPC-1 cells were treated with fluorophore-labeled mPA-sm3e, non-oligomerizing mPAK-sm3e (D512K mutant), or sm3e scFv at various time points over the course of 6 hours. Fluorescence was measured using flow cytometry. (a) Signal from cells labeled with Alexa Fluor 488, showing total binding of mPA-sm3e, mPAK-sm3e, or sm3e scFv. (b) Signal from cells labeled with pHrodo Red, showing internalized mPA-sm3e, mPAK-sm3e, or scFv.

The latter possibility of receptor kinetics altering PA activity was investigated using flow cytometry to measure trafficking of protective antigen constructs from the surface to the

endosome of the cell. Using maleimide conjugation chemistry, PA targeted to CEA was fluorescently labeled, and cells were treated with labeled PA at varying time points over 6 hours to determine the number of receptor-bound PA on either the surface of the cell or within the endosome as a function of time (Figure 3.4). A pH-sensitive fluorescent label, pHrodo (Life Technologies), was used to determine the extent to which mPA-sm3e or a non-oligomerizing variant, mPAK-sm3e (bearing the D512K mutation), was internalized. These results indicate that mPA-sm3e is actually internalized at a steady rate, contrary to the understanding of how CEA-bound sm3e is trafficked in the cell. [130] In comparison, both the non-oligomerizing mPAK-sm3e and soluble sm3e scFv bind to the cell and quickly saturates the surface antigen, but are not significantly internalized over the course of 6 hours. This strongly suggests that the property of PA that allows it to assemble into a prepore is capable of driving internalization of CEA, a surface antigen that normally does not internalize quickly.

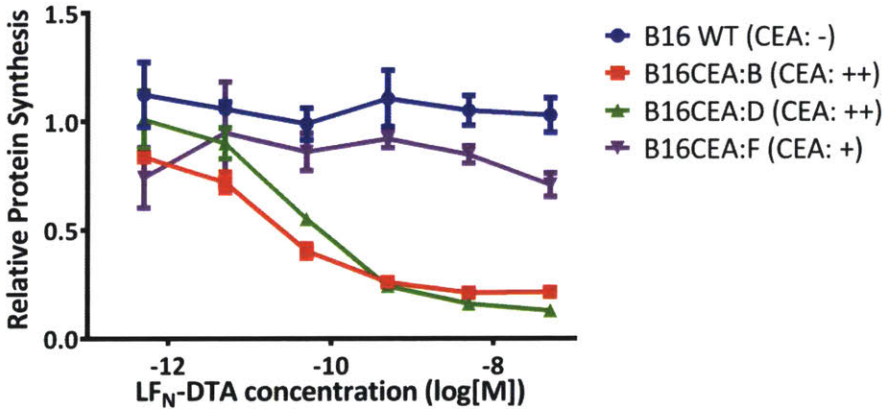

Figure 3.5. Protein synthesis inhibition by mPA-sm3e depends on receptor expression level. Stably-transfected B16F10 cells were treated with 50 nM mPA-sm3e and varying concentrations of LF_N-DTA for 4 hours. Incorporation of 3H-leucine was measured by liquid scintillation counting. Cells expressing higher surface CEA (B, D) showed a greater level of protein synthesis inhibition compared to wild-type cells or lower-expressing cells (F).

The role that antigen expression level plays in the efficacy of LF_N-DTA translocation was investigated using genetically engineered cell lines. A panel of the CEA-negative B16F10 cell

line and three B16F10 variants stably transfected to express CEA were used. The three modified clones express human CEA at 10^5 CEA per cell (clone F) or 10^6 CEA per cell (clone B and D). Each cell line was treated with LF_N-DTA and mPA-sm3e for 4 hours (Figure 3.5). The clones with higher CEA expression, B and D, exhibited greater protein synthesis inhibition compared to the lower-expressing clone, F, with wild-type B16F10 cells showing no response at all. This suggests that a higher antigen count on the surface of the cell enhances the ability of PA to enter the endosome and translocate material. This result is consistent with the published finding that receptor expression influences the lethality of edema factor delivered by protective antigen. [131]

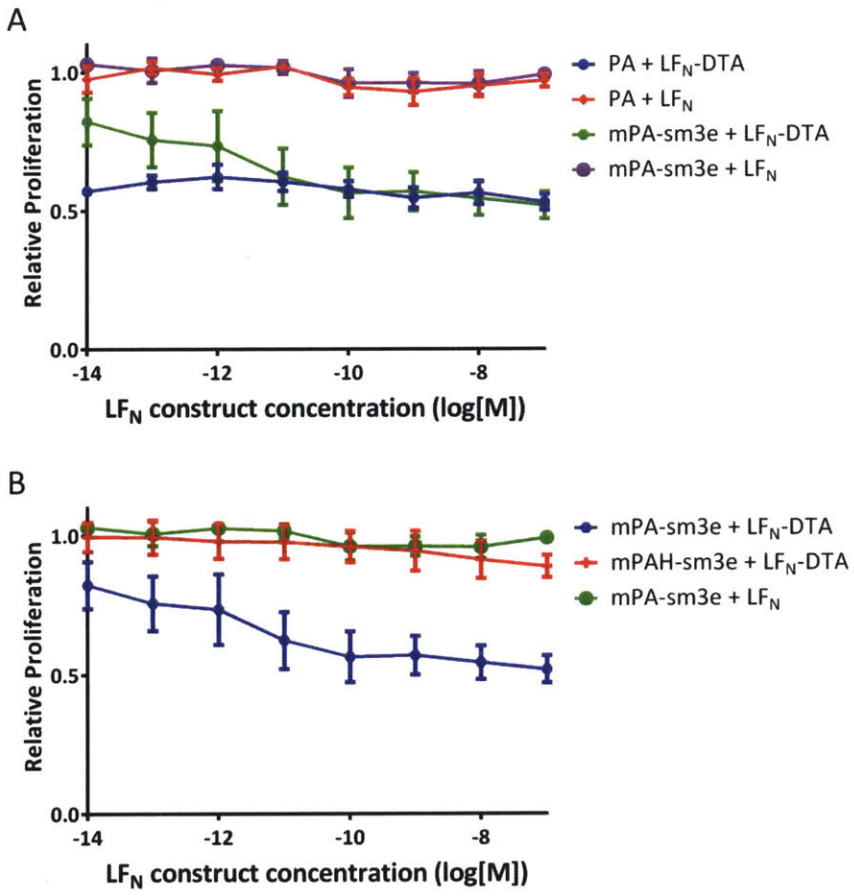

Figure 3.6. CellTiter-Glo assay quantifies cell proliferation inhibition by mPA-sm3e. AsPC-1 cells were treated with 50 nM PA, mPA-sm3e, or F427H variant and the indicated concentration of LF_N construct for 72 hours. (a) PA and mPA-sm3e treated with either LF_N or LF_N-DTA. (b) Comparison of mPA-sm3e to F427H mutant, mPAH-sm3e. The amount of ATP in the cells was quantified using CellTiter-Glo assay (Promega). The combination of mPA-sm3e and LF_N-DTA exhibits an anti-proliferative effect.

3.2.4 Influence of mPA-sm3e on tumor growth

The ability of mPA-sm3e and LF_N-DTA to inhibit cell proliferation was tested using CellTiter-Glo Luminescent Cell Viability Assay (Promega). Cells were grown in a 96-well plate and treated with either PA, mPA-sm3e, or F427H variants, combined with LF_N or LF_N-DTA payloads for three days, after which the metabolic activity of the cells was measured using the CellTiter-Glo kit for quantification of ATP (Figure 3.6). mPA-sm3e with LF_N-DTA showed cell proliferation inhibition, but at lower concentrations, the effect was reduced compared to wild-type PA with LF_N-DTA (Figure 3.6a). In all of the control cases (F427H variants or LF_N as a payload), proliferation was unaffected (Figure 3.6b).

3.3 Discussion

Previous studies have shown that CEA could be targeted by scFvs in immunotoxin format to cause cytotoxicity in tumor cells. [132] Recent work involved use of CEA as a targeting epitope for a cell-penetrating peptide delivering a toxin, which resulted in a delay in growth of tumors. [133] In another study, an antibody recognizing CEA induced antibody-dependent cell-mediated cytotoxicity against CEA-positive tumors. [134] An adoptive T cell therapy directed against CEA induced regression of a colorectal tumor in one patient. [135] All of these point to a strategy in which CEA's favorable expression profile is leveraged to direct therapies to the site of a tumor, while the biological action of the therapy itself does not involve CEA at all.

The work described here uses this same strategy to redirect protective antigen, a pore-forming protein that can translocate protein toxins into the cytosol of the cell. The fact that the receptors for wild-type PA, TEM8 and CMG2, are ubiquitously expressed poses a problem for therapies that must be localized to tumors in a patient. Retargeting PA to CEA, with its high

ratio of expression in cancers versus other tissue, resolves this issue. However, the efficacy of mPA-sm3e and its trafficking into the cell are unexpected given the slow rate of internalization of CEA. It is likely that the oligomerization state of protective antigen allows for mPA-sm3e to bypass the typical trafficking profile of CEA and induce internalization just as wild-type PA would. Further study of the mechanism of mPA-sm3e internalization, and in particular, to determine whether the behavior of recruitment into lipid rafts for clathrin-dependent endocytosis is retained, may be warranted.

The potency of antibody-drug conjugates is often strongly influenced by its ability to be internalized into the target cell. [136] Typically, CEA would not be a candidate target for such therapies because most antibodies do not induce internalization when bound to CEA. [130] mPA-sm3e may represent new opportunities for therapies such as antibody-drug conjugates where only internalization into the endosome is necessary.

3.4 Materials and Methods

3.4.1 Synthesis of mPA-sm3e

The sm3e scFv gene was a generous gift from K. Dane Wittrup (Massachusetts Institute of Technology). The gene was cloned into an existing plasmid containing the mPA gene using the primers 5'-GAATTCAGCCCGGGTCATAAAACCCAGCCGCAAGTTAAACTGGAACAGTC-3' and 5'-TCAGTGGTGGTGGTGGTGGTGCTCGAGTTACTTGATTTCCAACTTCGTTC-3' to create large primers containing the scFv gene. This extended DNA fragment was inserted into the mPA backbone using site-directed mutagenesis (Agilent QuikChange Lightning Mutagenesis Kit). F427H mutants were generated using site-directed mutagenesis with the primers 5'-

CTGAACGCTCAGGACGACCACTCTTCCACCCCGATCAC-3' and 5'-CAGTTCAGCCAGCTGGTTGCAGATGTTCTGAGAGGTTTG-3'. K563C mutants were generated using the primers 5'-CAAACCTCTCAGAACATCTGCAACCAGCTGGCTGAACTG-3' and 5'-CAGTTCAGCCAGCTGGTTGCAGATGTTCTGAGAGGTTTG-3'.

PA constructs were overexpressed in the periplasm of BL21 *E. coli* cells as described previously. [57] Protein was extracted from frozen culture pellets by resuspension in sucrose buffer (20% w/v sucrose, 1 mM EDTA, 20 mM Tris, pH 8.5). This was followed by centrifugation, a wash with 20 mM Tris pH 8.5, centrifugation, and a resuspension of the cell pellet in 5 mM $MgSO_4$. Tris pH 8.5 was added to a concentration of 20 mM, and the final suspension was centrifuged and the supernatant filtered on a .22 micron bottle-top filter.

PA was isolated from the supernatant using anion exchange chromatography (Q HP column, GE Healthcare) from a gradient of 0 to 250 mM NaCl. Protein-containing fractions were pooled, concentrated using 30 kDa MWCO Amicon centrifugal filters (Millipore), and purified again using size-exclusion chromatography on a SuperDex 200 gel filtration column (GE Healthcare). Proteins were analyzed by gel electrophoresis to confirm size (Figure S3.1).

3.4.2 Synthesis of LF_N-DTA

pET SUMO plasmid expression constructs for LF_N or LF_N-DTA was transformed into BL21 cells and cultured in 1 L of LB medium in an incubator shaker (225 RPM) at 37°C to OD = 0.6, at which point cultures were grown at 30°C and protein expression was induced with 0.4 mM IPTG for 16 hours. Cultures were centrifuged to form cell pellets, then resuspended in Tris-buffered saline (pH 7.5) with a small amount of lysozyme and half a tablet of protease inhibitor

cocktail (Roche). The suspension was sonicated to lyse the cells, then centrifuged to remove cell solids. The supernatant was filtered through a .22 μm bottle-top filter, then passed through a HisTrap FF Ni-NTA column to allow the SUMO fusion to bind the column. Protein was eluted with tris-buffered saline and 500 mM imidazole, then desalted via HiTrap Desalting Column (GE Healthcare). SUMO was cleaved from LF_N by reacting with SUMO protease for 1 hour at room temperature, and soluble LF_N construct was purified by collecting the flowthrough from a second pass through a HisTrap FF Ni-NTA column. Proteins were analyzed by gel electrophoresis to confirm size (Figure S3.1).

3.4.3 Cell culture

AsPC-1 cells were obtained from American Type Culture Collection (CRL 1682). Cells were maintained in a tissue culture incubator and grown in RPMI medium supplemented with 10% fetal bovine serum, 100 units/mL penicillin, and 100 μg/mL streptomycin.

Wild-type B16F10 cells and B16F10 cells stably transfected with CEA (clones B, D, and F), were a generous gift from Cary Opel (Wittrup Lab, Massachusetts Institute of Technology). Cells were maintained in a tissue culture incubator and grown in DMEM medium supplemented with 10% fetal bovine serum, 100 units/mL penicillin, and 100 μg/mL streptomycin.

3.4.4 Protein synthesis inhibition assay

AsPC-1 cells were seeded in a 96-well tissue culture plate at 50,000 cells per well and grown overnight at 37°C. Cells were then treated with media containing LF_N or LF_N-DTA at varying concentrations as well as 50 nM PA, mPA-sm3e, or F427H variants. The plate was incubated at 37°C for 30 minutes, then washed three times with phosphate-buffered saline (PBS)

and incubated at 37°C for 1 hour in leucine-deficient medium supplemented with ^{3}H-leucine at 1 μCi/mL. Cells were washed three times with PBS, then lysed using scintillation fluid. Protein synthesis levels were measured by determining incorporation of ^{3}H-leucine using a 1450 Microbeta Luminescence and Liquid Scintillation Counter (Perkin Elmer Life Sciences).

3.4.5 Western blotting analysis

AsPC-1 cells were treated for 24 hours with 50 nM PA or mPA-sm3e and 100 nM of LF_N. Cells were then washed with PBS and trypsinized. The outer membrane was dissociated with digitonin buffer (50 μg/mL digitonin, 1 mM NaH_2PO_4, 75 mM NaCl, 8 mM Na_2HPO_4, 250 mM sucrose, protease inhibitor cocktail, pH 7.7) and centrifuged, and the supernatant was run on SDS-PAGE gels and transferred to Western blot membranes. Western blots were stained with goat anti-LF antibody (Santa Cruz Biotechnology) followed by anti-goat antibody 800CW IRDye, then imaged on an Odyssey Imaging System.

3.4.6 Proliferation assay

AsPC-1 cells were seeded in a 96-well tissue culture plate at 10,000 cells per well and grown overnight. Cells were then treated with media containing LF_N or LF_N-DTA at varying concentrations as well as 50 nM PA, mPA-sm3e, or F427H variants. The plate was incubated at 37°C for three days.

Quantification of ATP in cells was carried out using the CellTiter-Glo Luminescent Viability Assay (Promega) according to manufacturer's protocols. The tissue culture plate was cooled to room temperature, and 100 μL of resuspended CellTiter-Glo reagent was added to each well. Cells were shaken in order to mix the reagent and lyse the cells, then incubated at room

temperature for 10 minutes. Luminescence was quantified using a 1450 Microbeta Luminescence and Liquid Scintillation Counter (Perkin Elmer Life Sciences).

3.4.7 Flow cytometry

AsPC-1 cells were incubated with fluorescently-labeled PA constructs or singly biotinylated sm3e complexed with fluorophore-labeled avidin, then washed with PBS and dissociated from the tissue culture plate using Cell Dissociation Buffer (Thermo Fisher Scientific). Cells were analyzed using an Accuri C6 flow cytometer (BD Biosciences). Fluorescence levels for triplicate samples were averaged.

Chapter 4: Targeted Delivery of Toxins to Tumors in Mouse Models

4.1 Introduction

In vitro assays in which cancer cell lines are exposed to therapies in tissue culture are very useful for investigating lower level cellular responses to toxins. Once promising candidates are identified from *in vitro* studies, further representation of cancer can involve the use of animal models, which can more closely replicate the biological complexity of human patients, allowing tumors implanted in the animal to develop more complex morphologies, with their own vasculatures and transport phenomena. [137–139] Athymic nude mice are frequently used in such experiments. [140] Because these mice lack a thymus, they are unable to produce T cells, which in turn also render the immune system's B cells less effective and allow formation of xenografts from human tissue. [141] In our case, nude mice can be used in a model where a human pancreatic cancer cell line, AsPC-1, is implanted subcutaneously in the flank of the mouse. This enables design of a model in which a tumor expressing human antigens, epidermal growth factor receptor (EGFR) and carcinoembryonic antigen (CEA), are expressed and can be used as targeting epitopes.

This study models pancreatic cancer, an aggressive form of cancer that often moves too quickly for surgical resection or chemotherapy to be effective, leading to poor prognosis for patients. [110–112] As described in Chapters 2 and 3, protective antigen (PA) variants that have been retargeted to cancer-associated antigens have translocated toxins and inhibited the growth of tumors when evaluated via *in vitro* assays. It is not yet known if this growth inhibition will apply to tumors in a xenograft model.

The behavior of protective antigen in an animal has primarily been investigated for the purpose of vaccine development. [142] More recent studies have examined the effect of forms of protective antigen and lethal factor as a cancer therapy, with the combination capable of inducing tumor regression of melanoma and neuroblastoma. [143,144] Other strategies for utilizing protective antigen have leveraged an engineering method in which two different tumor-associated proteases are required in order to proteolytically activate PA. [41] These demonstrated the viability of PA in mouse therapies, but the translocation and delivery of payloads other than lethal factor were not investigated.

In Chapter 2, we described the design and characterization of mPA-E1v3, a protective antigen variant that is fused to the scFv, E1v3, to retarget the protein to epidermal growth factor receptor (EGFR). mPA-E1v3 was used to deliver both LF_N-DTA, a fusion of the N-terminus of lethal factor to a subunit of diphtheria toxin, and LF_N-RRSP, a fusion to a recently discovered Ras protease from the *V. vulnificus* bacteria. [54] mPA-E1v3 was able to target AsPC-1 pancreatic cancer cells and translocate both toxins in tissue culture experiments, resulting in inhibition of cell growth.

Additionally, we characterized mPA-sm3e, which targets carcinoembryonic antigen (CEA) using the sm3e scFv. Despite the fact that CEA is normally not rapidly internalized and protective antigen requires internalization for activity, mPA-sm3e showed activity in targeting CEA on AsPC-1 cells and translocating LF_N-DTA to inhibit cell growth in our *in vitro* assays.

The ability of these retargeted PA constructs to significantly inhibit cell proliferation highlights the potential of using this approach for the development of novel cancer therapies. To further investigate the efficacy of these constructs for inhibiting tumor growth, a pre-clinical model using human pancreatic cancer xenografts in mice was used. We first assayed for

potential toxicity of LF_N-DTA or LF_N-RRSP delivered by mPA-E1v3 or mPA-sm3e to determine the maximum tolerated dose of our treatment. Once this was established, we proceeded to treat mice bearing subcutaneous flank tumors of AsPC-1 cells to determine if our treatments could modulate tumor growth.

4.2 Results

4.2.1 Mouse tolerance for protective antigen and LF_N construct doses

Because DTA is a potent toxin and poses a risk of causing damage to healthy tissue, the protein therapeutics were tested in their proposed combinations to determine if these toxins would be well-tolerated in mice. Nude mice were injected twice, three days apart, with 0.25 mg/kg of PA construct and 0.025 mg/kg of LF_N construct by tail vein injection. Mouse weights were measured regularly over seven days to determine if any adverse effects resulted from exposure to the combination treatment (Figure 4.1). No reduction in weight was observed, which would suggest that the mice did not experience any toxicity from most of the treatments. Surprisingly, however, mice treated with both mPA-E1v3 and LF_N-DTA did not survive past the third day after the initial injection with treatment.

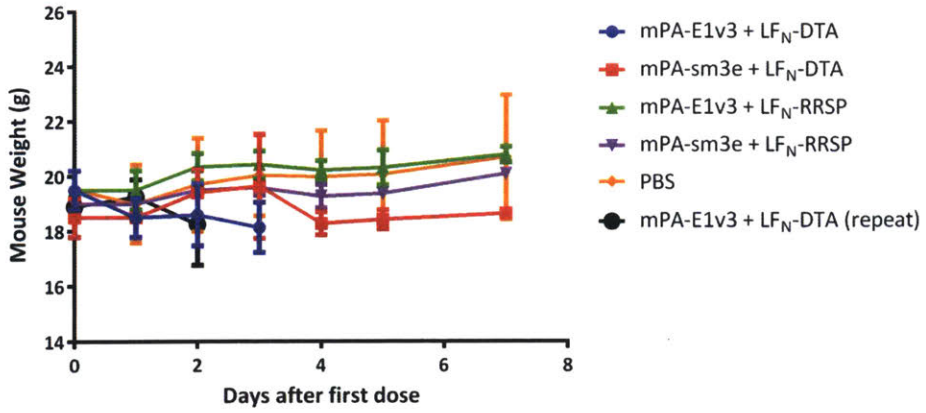

Figure 4.1. Determination of treatment toxicity. Nude mice were injected twice, three days apart, with 0.25 mg/kg PA construct and 0.025 mg/kg LF_N construct. Mice weights were measured to determine toxicity. No significant change in weight was observed; however, mice treated with mPA-E1v3 + LF_N-DTA did not survive past the third day.

Because the combination of mPA-E1v3 and LF_N-DTA was lethal to the mice, a lower dosage was required. To determine a tolerated dose of the treatment, mice were injected with varying amounts of mPA-E1v3 and LF_N-DTA from 0.0064 mg/kg to 0.1 mg/kg mPA-E1v3 and 0.00064 mg/kg to 0.01 mg/kg LF_N-DTA, and mouse weights were measured over six days (Figure 4.2). Based on the results, it was concluded that dosages of 0.1 mg/kg mPA-E1v3 and 0.01 mg/kg LF_N-DTA could be tolerated by mice.

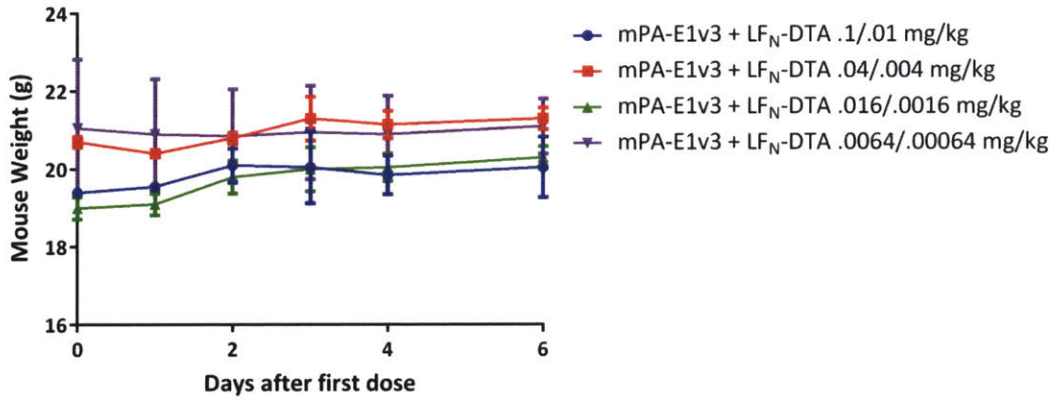

Figure 4.2. Determination of maximum tolerated dose. Maximum tolerated dose study for the combination of mPA-E1v3 and LF_N-DTA showed that the treatment is nonlethal at all doses tested. Nude mice were injected twice, three days apart, with the indicated dosages of mPA-E1v3 and LF_N-DTA. No change in weight or other signs of morbidity were observed.

4.2.2 EGFR-based inhibition of pancreatic cancer xenografts

To characterize mPA-E1v3's effects on pancreatic cancer cells *in vivo*, nude mice were injected in the flank with AsPC-1 cells to establish subcutaneous tumors. Mice were then treated with mPA-E1v3 and LF_N-DTA or LF_N-RRSP, and tumor growth was measured by digital caliper (Figure 4.3).

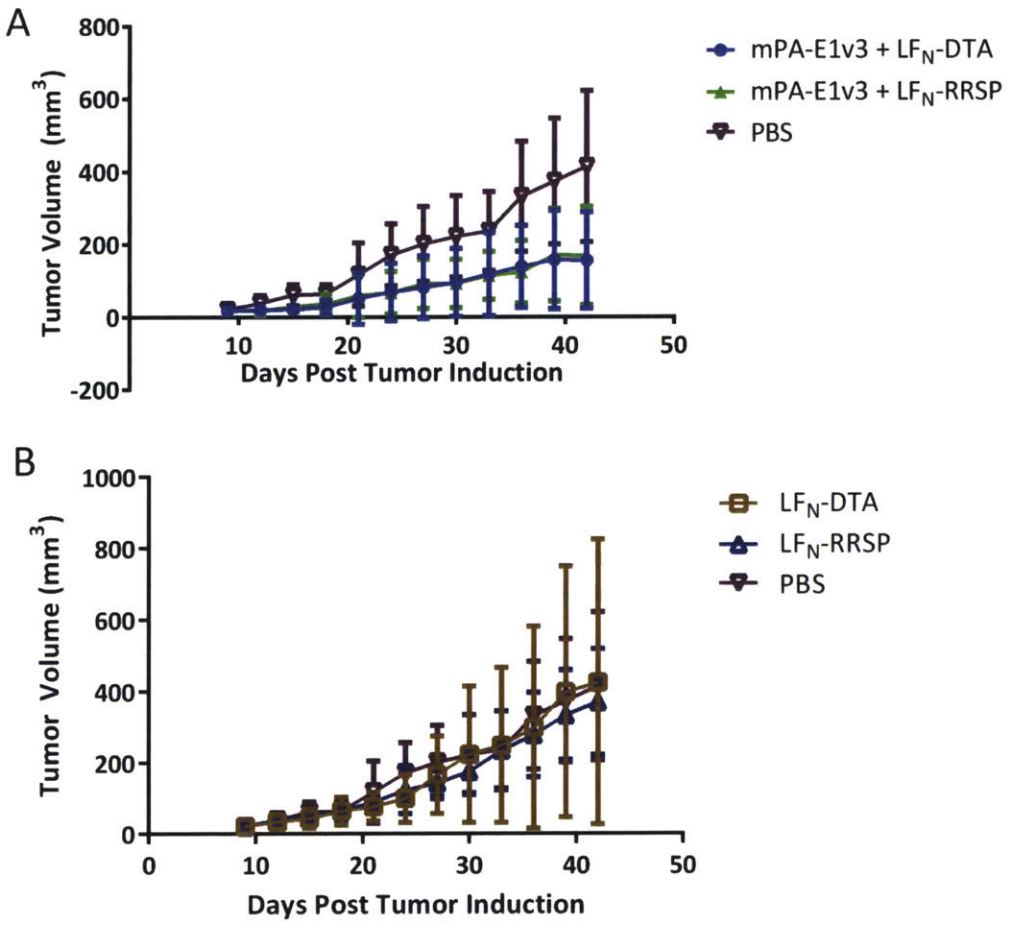

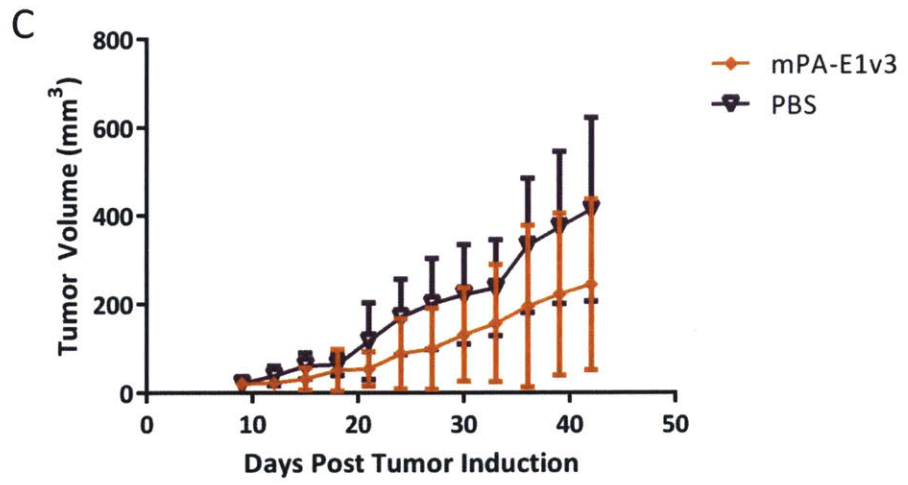

Figure 4.3. Treatment of AsPC-1 subcutaneous tumors by toxins delivered by mPA-E1v3. (a) Mice were treated every 3 days with 0.08 mg/kg of mPA-E1v3 and 0.008 mg/kg of LF_N-DTA, or 0.25 mg/kg of mPA-E1v3 and 0.025 mg/kg of LF_N-RRSP and tumor growth was compared to control. (b) Comparison of control mice treated with 0.025 mg/kg LF_N-DTA or 0.025 mg/kg LF_N-RRSP. The average tumor volume is similar across all three controls. (c) Comparison of mice treated with 0.25 mg/kg mPA-E1v3 and untreated mice.

High variability in tumor sizes was observed across all treatments in this mouse study. After 31 days of treatment, the mean tumor sizes of mice treated with either mPA-E1v3 and LF_N-DTA or mPA-E1v3 and LF_N-RRSP were lower than that of the untreated mice (157 mm^3 for mice treated with mPA-E1v3 + LF_N-DTA and 169 mm^3 for mice treated with mPA-E1v3 + LF_N-RRSP versus 415 mm^3 for untreated mice) (Figure 4.3a). The mean tumor sizes of mice treated with only LF_N-DTA (425 mm^3) or only LF_N-RRSP (371 mm^3) were similar to that of the untreated control mice (Figure 4.3b). Finally, mice treated with mPA-E1v3 also showed lower average tumor size (245 mm^3) compared to the untreated controls (Figure 4.3c). These results indicate that tumor growth can be inhibited through delivery of the tested toxins by mPA-E1v3, and that mPA-E1v3 alone may also have some effect in controlling tumor growth. However, future work should be aimed at confirming these results and minimizing the high variability in response rate observed in these initial experiments.

Because of the wide range of tumor sizes observed even in the control mice, it is likely that the variability originates from the method of tumor induction. A reevaluation of both the AsPC-1 cell line used and the experimental technique for inducing the subcutaneous tumors may help reduce the variability in future experiments.

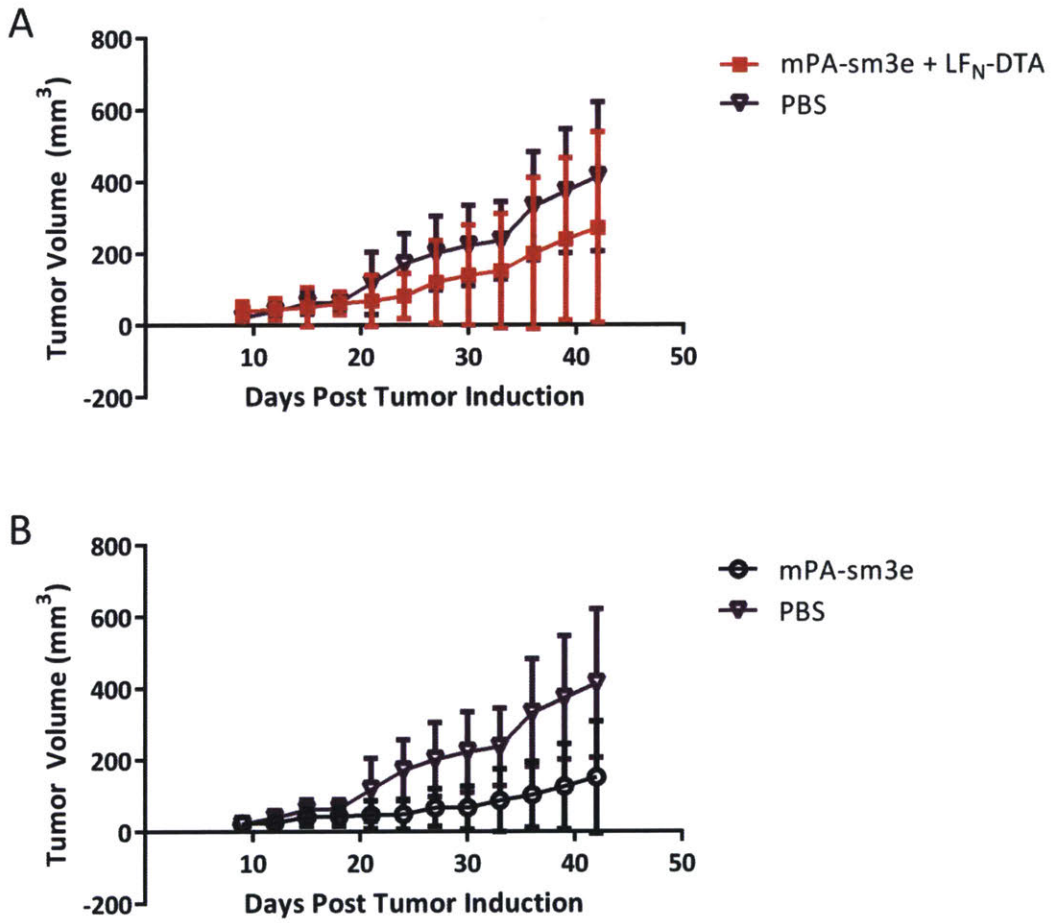

Figure 4.4. Treatment of AsPC-1 subcutaneous tumors by toxins delivered by mPA-sm3e. (a) Mice were treated every 3 days with 0.25 mg/kg of mPA-sm3e and 0.025 mg/kg of LF_N-DTA and tumor growth was compared to control. (b) Comparison of mice treated with 0.25 mg/kg mPA-sm3e only and untreated mice.

4.2.3 CEA-based inhibition of xenografts

The effect of LF_N-DTA delivered into cells by mPA-sm3e was also investigated. Nude mice were injected in the flank with AsPC-1 cells to establish subcutaneous tumors. Mice were then treated with mPA-sm3e and LF_N-DTA, and tumor growth was measured by digital caliper.

The mean tumor size of mice treated with mPA-sm3e and LF_N-DTA was 272 mm^3 versus 415 mm^3 for the control mice (Figure 4.4a). The mean tumor size of mice treated with only mPA-sm3e was 152 mm^3. As with the results for mPA-E1v3, tumors treated with mPA-sm3e and LF_N-DTA also exhibited high variability in growth rates and warrants further study of this treatment group to minimize variability.

In this xenograft experiment, high variability in the size and growth of the AsPC-1 tumors was observed. The efficacy of the treatment may be dependent on the size and growth rate of the tumor at the initiation of treatment, leading to certain tumors appearing to be responsive to the therapy while others have progressed too far for treatment to be effective. Further investigation with a tumor cell line capable of forming more consistent tumor sizes may be helpful in fully assessing whether these treatments are effective in inhibiting cancer growth.

4.2.4 Adverse effects of LF_N-DTA treatment

Although the mPA-E1v3 + LF_N-DTA combination did not immediately cause signs of morbidity, a significant difference in weight emerged in mice treated with this combination compared to all other treatments (Figure 4.5). While mice in every other treatment group gained weight over 30 days as they aged, mice in the mPA-E1v3 + LF_N-DTA treatment actually lost weight, with the most severe weight loss at approximately 10% of the original body weight. Additionally, mice in this treatment group exhibited severe skin irritation in the tail at the site of injection. This is consistent with the previous finding that higher doses of this combination were lethal to the mice. mPA-E1v3 was engineered to bind to human EGFR, but it is likely that it is also cross-reactive with mouse EGFR. Therefore, it is likely that mPA-E1v3 is targeting healthy tissue in the mice, causing off-site toxicity that is diminishing the health of the mouse. This

finding underscores the importance of finding a highly specific tumor-targeting construct, and it suggests further engineering may be required to increase the therapeutic window of mPA-E1v3 in order to minimize unwanted adverse effects.

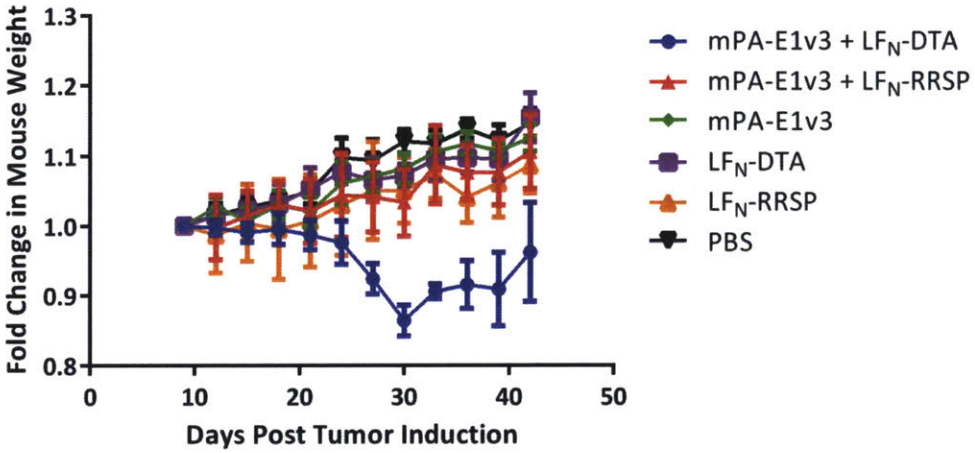

Figure 4.5. Measurement of mouse weights during treatment. Treatment with mPA-E1v3 and LF_N-DTA exhibits adverse effects on mouse health. Mice were weighed during the course of the tumor study in which the indicated treatments were given every 3 days. The combination of 0.08 mg/kg mPA-E1v3 and 0.008 mg/kg LF_N-DTA resulted in a decrease in average mouse weight approximately two weeks after treatment was initiated.

4.3 Discussion

Two parallel therapeutic strategies were investigated: delivery of toxins to tumors by EGFR-targeted PA or by CEA-targeted PA. The ability of these therapies to inhibit growth of pancreatic cancer cells *in vitro* was described in previous chapters. This work involved the application of these treatments to the more challenging *in vivo* model.

The EGFR-targeted treatment, mPA-E1v3, in combination with the diphtheria toxin-based LF_N-DTA or the Ras protease LF_N-RRSP, displayed a reduction in the growth of tumors based on mean tumor sizes observed. However, due to the large variability in tumor size, additional studies must be performed to validate these initial results. Our data also suggests the presence of off-target toxicity effects associated with the delivery of LF_N-DTA by mPA-E1v3.

E1v3 was engineered to target human EGFR, but cross-reactivity with mouse EGFR was not investigated.

Though not specifically observed in this experiment, there are other potential obstacles to the use of protective antigen in animals. PA is a large protein at 83 kDa and is derived from bacteria, making it subject to unfavorable pharmacokinetics as well as neutralization by the immune system. Protective antigen is indeed immunogenic, and recombinant protective antigen injected into mice with adjuvant is capable of producing a strong neutralizing response. [145] It is for this reason that PA is a candidate for the development of vaccines to protect against anthrax toxin, but this also poses problems for therapeutic strategies that require repeated dosing of PA. In immunocompetent animals, raising a neutralizing IgG response could inhibit the tumor inhibition effect of PA. Additionally, mouse experiments in particular may be hampered by the fact that PA is cleaved in the serum of mouse and rats independent of its binding to cells, resulting in quicker clearance from the blood. [146] A reengineering of the furin cleavage site of PA may help raise PA's resistance to serum proteases and allow it to be activated only at the site of the tumor.

In studying the use of PA in treating solid tumors, one may expect the therapeutic efficacy of PA could also be transport-limited. Compounds that are internalized quickly have poor tumor penetration due to rapid depletion in the outer areas of the tumor. [147] This could lead to the phenomenon in which smaller tumors, for which the distance to reach the center of the tumor is much lower, are more susceptible to PA-based treatment, whereas larger tumors may no longer be responsive.

One further property that may alter the efficacy of the retargeted PA constructs in this study is the dosing regimen. Only a single dose was tested for each combination treatment, and

all doses were at a 10:1 ratio of PA to LF_N construct. More potent growth inhibition may occur if a different dosing strategy is used. It is also known that the timing of the injection of PA relative to lethal factor alters the toxicity of the treatment. Doses of lethal factor injected within 8 hours of the initial PA dose were lethal, while those after 10 hours did not demonstrate toxicity. [146] It may be beneficial to investigate alternate methods of dosing the two components of this system beyond simply giving two sequential bolus doses together.

4.4 Materials and Methods

4.4.1 Expression of protective antigen variants

PA constructs were overexpressed in the periplasm of BL21 *E. coli* cells as described previously. [57] Protein was extracted from frozen culture pellets by resuspension in sucrose buffer (20% w/v sucrose, 1 mM EDTA, 20 mM Tris, pH 8.5). This was followed by centrifugation, a wash with 20 mM Tris pH 8.5, centrifugation, and a resuspension of the cell pellet in 5 mM $MgSO_4$. Tris pH 8.5 was added to a concentration of 20 mM, and the final suspension was centrifuged and the supernatant filtered on a .22 micron bottle-top filter.

PA was isolated from the supernatant using anion exchange chromatography (Q HP column, GE Healthcare) from a gradient of 0 to 250 mM NaCl. Protein-containing fractions were pooled, concentrated using 30 kDa MWCO Amicon centrifugal filters (Millipore), and purified again using size-exclusion chromatography on a SuperDex 200 gel filtration column (GE Healthcare). To remove endotoxin, PA was incubated for 1 hour at room temperature in Pierce High Capacity Endotoxin Removal Resin (Thermo Fisher) in spin column format. The resin was then centrifuged and the flowthrough recovered. Endotoxin levels of the samples were quantified using Pierce LAL Chromogenic Endotoxin Quantitation Kit (Thermo Fisher).

4.4.2 Expression of LF_N fusion proteins

Plasmid expression constructs for pET-SUMO-LF_N-DTA and pET-SUMO-LF_N-RRSP was transformed into ClearColi BL21(DE3) cells (Lucigen) by electroporation. This bacterial strain is engineered to express modified LPS that does not activate the innate immune system. Transformed cells were cultured in 1 L of LB medium in an incubator shaker at 37°C to OD = 0.6, at which point cultures were grown at 30°C and protein expression was induced with 0.4 mM IPTG for 16 hours. All glassware, centrifuge bottles, and purification columns were treated with 1M NaOH prior to use in order to destroy exogenous endotoxin. Cultures were centrifuged to form cell pellets, then resuspended in Tris-buffered saline (pH 7.5) with a small amount of lysozyme and half a tablet of protease inhibitor cocktail (Roche). The suspension was sonicated to lyse the cells, then centrifuged to remove cell solids. The supernatant was filtered, then passed through a HisTrap FF Ni-NTA column to allow the SUMO fusion to bind the column. Protein was eluted with Tris-buffered saline and 500 mM imidazole, then desalted via HiTrap Desalting Column (GE Healthcare). SUMO was cleaved from LF_N by reacting with SUMO protease for 1 hour at room temperature, and soluble LF_N construct was purified by collecting the flowthrough from a second pass through a HisTrap FF Ni-NTA column. Endotoxin for proteins produced in ClearColi was quantified using HEK-Blue LPS Detection Kit (Invivogen).

4.4.3 Cell culture

AsPC-1 cells were obtained from American Type Culture Collection (CRL 1682). Cells were maintained in a tissue culture incubator and grown in RPMI medium supplemented with 10% fetal bovine serum, 100 units/mL penicillin, and 100 μg/mL streptomycin.

4.4.4 Toxicity assay

To determine if combination treatments were tolerated, NCr nude mice were injected with both 0.25 mg/kg of PA construct and 0.025 mg/kg of LF_N construct, with two mice per treatment group. Dosages were given twice with three days between each injection. Weights were measured daily for 6 days and mice were observed for signs of morbidity.

To determine maximum tolerated dose of the combination of mPA-E1v3 and LF_N-DTA, mice were injected twice, three days apart, with varying dosages of the combination treatment. Weights were measured daily for 6 days.

4.4.5 Tumor inhibition assay

Female 6 week-old NCr nude mice were subcutaneously injected in the flank with $1x10^6$ AsPC-1 cells. Tumors were allowed to establish over 9 days, after which treatment was given via tail vein injection every three days. 0.25 mg/kg or 0.08 mg/kg PA construct and 0.025 mg/kg or 0.008 mg/kg LF_N construct were given as two separate tail vein injections, with five mice in each treatment group. Subcutaneous tumors were measured via caliper, and tumor volume calculated as ½ x length x $width^2$.

Chapter 5: Conclusions and Future Recommendations

5.1 Summary of work

The primary goal of our work was to apply protein engineering techniques to the development of therapeutics specifically targeted to cancer-associated antigens. We accomplished this through two methods: directed evolution of antibodies obtained *de novo* from naïve scFv libraries (described in detail in Appendix 1), and fusion modifications to retarget existing bacterial toxins. This parallel strategy leveraged established technologies of yeast display and anthrax toxin engineering to target epidermal growth factor receptor (EGFR) and carcinoembryonic antigen (CEA) in a novel format.

The main body of this work focused on leveraging the anthrax toxin system for tumor targeting. However, one of our starting points was a novel antibody targeting EGFR, which we developed from earlier work and is detailed in Appendix 1. For this earlier work, we first targeted and antagonized EGFR directly to modulate the biological processes driving tumor cell growth. We leveraged the published finding that signaling pathways downstream of EGFR are activated even at ligand concentrations that do not phosphorylate EGFR itself at detectable levels, and engineered an antibody that could achieve complete ligand blocking to inhibit this trace growth signal. [105] Using a yeast display library, we isolated a new antibody that binds to EGFR, which we then subjected to successive rounds of random mutagenesis in order to affinity mature the antibody. Through characterization with cancer cells, we determined that this new antibody, E1v3, bound to EGFR in a manner that is competitive with its ligand, EGF. This property allowed E1v3 to reduce growth signaling initiated by EGF, which resulted in inhibition of proliferation of NCI-H292 lung cancer cells in *in vitro* assays.

In our current work, we then used the E1v3 antibody to retarget the protective antigen (PA) component of anthrax toxin. The ability to change the binding specificity of PA to surface receptors overexpressed by cancer cells opens the anthrax-based translocation system for use against any target for which a binder can be generated. [35] A vast library of protein binders already exists, and as detailed in Appendix 1, new protein binders can be engineered to be used with PA, effectively allowing PA to be repurposed for a wide variety of surface receptors. In Chapter 2, we demonstrated that the fusion of PA and E1v3, mPA-E1v3, is an effective mediator of translocation. mPA-E1v3 can transport diphtheria toxin chain A (DTA) as a fusion to the N-terminus of lethal factor (LF_N) into the cytosol of cancer cells to inhibit protein synthesis, leading to cell death. Additionally, in collaboration with Professor Karla Satchell of Northwestern University, we used mPA-E1v3 to translocate a naturally occurring Ras protease, RRSP, into EGFR-positive pancreatic cancer cells (AsPC-1), which inhibited growth signaling and cell proliferation.

As described in Chapter 3, we applied the same retargeting strategy using an existing antibody binder against carcinoembryonic antigen (CEA), forming a fusion protein, mPA-sm3e, capable of translocating material into tumor cells. Previous reports had indicated that sm3e, as well as most other anti-CEA antibodies, do not induce internalization of surface CEA. [130] We showed that mPA-sm3e was still able to induce internalization and retained the properties of pore formation and translocation. We used mPA-sm3e to translocate LF_N-DTA into cancer cells and inhibit proliferation.

Lastly, we performed initial characterizations of our retargeted PA variants, mPA-E1v3 and mPA-sm3e, in tumor models using nude mice, with preliminary data provided in Chapter 4. Xenografts were established by inoculating mice with AsPC-1 cells injected subcutaneously in

the flank. Mice were then treated with combinations of mPA-E1v3 and LF_N-DTA or LF_N-RRSP, or mPA-sm3e and LF_N-DTA, every three days via tail vein injection. Despite large variability in tumor sizes across all treatments in our study, initial results indicate a potential for tumor inhibition and, as such, warrant further study.

The field of antibody engineering has been well-developed, and a vast library of candidate antibodies have been produced to target tumor cells. In this project, we have shown that by expressing antibodies in scFv format, antibodies can be converted for use with the protective antigen system, presenting a simple and flexible method of generating retargeted PA variants. We have also demonstrated that the two specific PA proteins developed in this work show anti-tumor activity in cell culture assays. We believe that this demonstrates the power and versatility of this protein engineering methodology, and there remains great potential in applying this strategy against further targets and payloads relevant to cancer.

5.2 Future recommendations

Much of the remaining uncertainty surrounding the two PA constructs, mPA-E1v3 and mPA-sm3e, concerns its efficacy *in vivo*. The mouse experiments should be repeated and further consideration should be given to establishing tumors of consistent growth rate, either by altering the induction technique or by selecting a different cell line. Beyond this, the PA proteins can be characterized in other ways to understand its behavior in an animal. Biodistribution studies can be performed to determine if there is any difficulty for intravenously dosed proteins in reaching the site of the tumor, and pharmacokinetics of the protein should also be studied to determine if outside factors alter the clearance rate of the proteins. Both the route and dose of treatments can

also be optimized. Other animal studies involving PA have used intraperitoneal injections and at different doses, which may alter the amount of material that reaches the tumor. [43]

The stability of PA in the blood of mice should also be further examined, since studies have shown that PA can be cleaved in the blood independent of binding to the cells. [146] Our data on proteolytic activation of mPA-E1v3 and mPA-sm3e suggests that there may be additional cleavage of PA that removes the scFv domain from the construct, which would completely ablate the ability of the construct to bind to tumor cells. An assessment of linker stability may be necessary to obtain a PA construct that resists serum proteases and retains activity after entrance into the bloodstream.

Engineering for resistance to proteases may also be a viable strategy for enhancing the biological activity of our therapies. Previous work in our lab has established that a D-amino acid capping the N-terminus of translocated payloads dramatically extends the half-life of the protein while in the cytosol. This is due to protection from ubiquitination, which would otherwise direct the proteins to the degradation pathway. [60] Applying this to the construction of cytotoxic payloads such as LF_N-RRSP may increase the therapeutic efficacy of these treatments.

We believe in particular that RRSP, an enzymatic domain that has only recently been characterized, possesses great potential as an anti-cancer therapeutic. Its target, Ras, is a driving force behind many cancers, and having an effective Ras inhibitor that can be transported into the cell with ease presents many opportunities. Ras is likewise a component of the critical signaling network that also encompasses EGFR, MEK, ERK, and Raf, all of which are therapeutic targets. [148] We recommend exploring methods of simultaneously inhibiting multiple members of this network using EGFR-targeted PA and a combination of inhibitory payloads. Shutting down this

signaling network from multiple points may induce a synergistic effect that could completely ablate growth signaling in cancer cells dependent on this pathway.

Appendix 1: A Novel Anti-EGFR Antibody Blocks Ligand-Binding and Inhibits Tumor Cell Proliferation

A1.1 Introduction

A1.1.1 Monoclonal antibodies for cancer therapy

The development of new therapies for treating cancer presents many significant challenges. Cancer cells originate from the host's own healthy cells and have undergone some modification that results in excessive proliferation. There can be great difficulty in distinguishing such cells from normal tissue; therefore, cancer treatments must carefully and selectively target only tumor cells or risk unacceptable levels of off-target specificity. [63] Additionally, anti-cancer drugs are often transport-limited, with unfavorable pharmacokinetics resulting in clearance of the drug from the target area prior to achieving its full effect. This severely diminishes the efficacy of the treatment since the dosage reaches the tumor in insufficient doses or durations. [64]

Monoclonal antibody therapies have seen some success in addressing these issues. Produced by B cells, antibodies serve as a means for the immune system to tag targets of interest for clearance from an organism. Antibodies have two functional domains: the antigen binding fragment (Fab) and the crystallizable fragment (Fc). The Fab region is responsible for the unique recognition ability of an individual antibody, with high amounts of variability characterizing the three complementarity-determining regions (CDRs) found within. The interaction between antibody and antigen can be highly specific, allowing for selective targeting of pathogens without causing harm to normal tissue. [65] The IgG antibody's Fc domain allows the antibody to interact with the neonatal FcR, which protects the antibody from proceeding to the degradation

pathway and therefore allows it to persist in the system. [66] Antibodies play a critical role in the immune response, interacting with the innate and adaptive immune system to further enhance their potency.

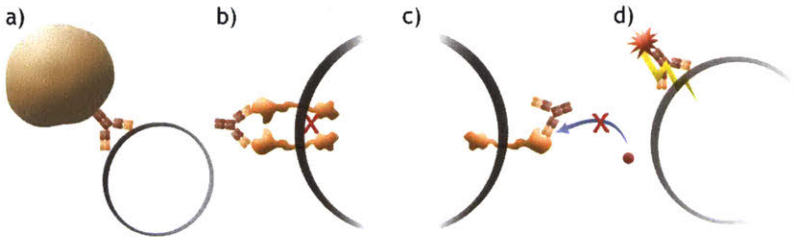

Figure A1.1. Summary of possible cytotoxic action of antibodies. Antibodies targeting tumor cells can enact anti-proliferative effects in several ways, some of which are depicted here. a) Recruitment of immune cells through interaction with the antibody Fc domain can induce apoptosis in the targeted cell. b) Antibodies can bind to growth-related receptors in an antagonistic way, preventing dimerization necessary for signaling or c) preventing a stimulatory ligand from binding to the receptor. d) Antibodies can be conjugated to cytotoxic compounds (antibody drug conjugates or ADCs) to deliver a targeted dose of therapeutic.

As a cancer therapy, antibodies can exert therapeutic effects against tumors via multiple mechanisms (Figure A1.1). Several effective antibody therapies engage the immune system in the same way organisms naturally utilize antibodies. A key function of antibodies is their ability to effect antibody-dependent cell-mediated cytotoxicity (ADCC). Antibodies label target cells, and the Fc domain can interact immune effector cells. Natural killer cells, neutrophils, macrophages, and other immune cells express Fc receptors that allow them to engage antibody-coated target cells and to initiate some form of cytotoxic effect on the target, eliminating the pathogen. [67]

Antibodies also play an important role in engaging the innate immune system. When an antibody binds to a cell, its Fc region can engage C1q, which initiates a cascade for the complement-dependent cytotoxicity (CDC) pathway. The end result of this cascade is usually formation of the membrane attack complex (MAC), which forms pores on the cell membrane of the target cell, ultimately leading to its death. The CDC pathway also recruits immune effector

cells that carry out a variety of functions, such as macrophages and neutrophils. [68] In some cases, complement is a critical component of a therapeutic antibody's function. With rituximab, an anti-CD20 antibody for the treatment of B-cell non-Hodgkin lymphomas, efficacy was completely ablated in C1q knockout mice. [69]

The immune system can also be directly modulated by antibody therapies, specifically by engaging activating and inhibitory receptors. Antibodies that block CTLA-4 or PD-1, inhibitory receptors expressed on T cells, or PD-L1, the ligand for PD-1 are currently under investigation, with clinical evidence demonstrating their abilities to enhance immune responses against tumors. [70–72]

Monoclonal antibodies can also be engineered to effect change on a target cell's viability without the involvement of the immune system, primarily through disruption of a signaling pathway. The binding of an antibody to a receptor may inhibit its ability to assume a conformation necessary for signaling, or alter its trafficking within the cell such that the expression levels of the receptor are altered. Additionally, an antibody can abrogate signaling through a key pathway by competing with ligand for a certain receptor epitope, as is the case with cetuximab, an antibody that targets epidermal growth factor receptor. [65]

Given their targeting specificity, favorable pharmacokinetics, and ability to synergize with the immune system, engineering of monoclonal antibodies is a highly active field that shows a great deal of promise as a cancer treatment. These desirable properties have led to the development of numerous monoclonal antibody cancer therapies. As of 2014, there are over forty monoclonal antibody therapies approved for use in treating malignancies. [73]

A1.1.2 Yeast display for antibody engineering

The first advance in monoclonal antibody generation involved immunization of mice with antigen followed by generation of hybridomas capable of expressing monoclonal antibodies. [74] Since then, many protein engineering methods have been developed that do not rely on the use of live animals. Starting with phage display, these engineering systems display large libraries of candidate binders that can be sorted through using a panning procedure to isolate individual clones with high affinity towards a target of interest. [75,76] Other display systems such as ribosome display and mRNA display eliminate living cells from the process completely and are able to achieve even larger library sizes. [77]

With yeast display, a library of single chain antibody (scFv) binders is displayed on the surface of yeast, and individual clones are selected based on their affinity toward the target protein. Using error-prone polymerase chain reaction to mutagenize the clones, further variation in affinity is introduced and the new clones are again sorted to identify those with more desirable properties. Yeast displaying the highest affinity scFv clones are first isolated using magnetic bead sorting, in which scFvs are complexed with antigen immobilized on the beads, which are separated by magnet. Once the library size has been reduced in this manner, fluorescence-activated cell sorting is used to sort clones that most strongly bind fluorescently-labeled antigen. After several successive rounds of this directed evolution procedure, the end result is an scFv binder that is highly specific to epitopes of the target antigen. [78] This method enables the creation of customized antibodies bearing desired affinity and specificity, and is instrumental in the discovery of monoclonal antibodies with novel anti-tumor properties.

A1.1.3 The Epidermal Growth Factor Receptor family

Four receptors comprise the members of the ErbB family of cell surface receptors. They are epidermal growth factor receptor (EGFR, ErbB1, HER1), ErbB2 (HER2), ErbB3 (HER3), and ErbB4 (HER4). These receptors are instrumental in directing the proliferation, migration, metabolism, and survival of a cell. Each receptor is capable of forming a homo- or heterodimer with any member of the family. EGFR, ErbB3, and ErbB4 can be bound by their ligands, after which the receptor will undergo a conformational change such that it can dimerize with another receptor. [79] Though HER2 has no known ligand, it is frequently involved with heterodimerization with any of the other three receptors. [80] With the receptors together, the juxtaposition of their tyrosine kinase domains leads to activation of the signal transduction pathway, allowing for the cascade to eventually alter the genetic expression of the cell. [81] Among the pathways initiated by these receptors are MAPK and PI3K/Akt, which are important modulators of cell growth. [82]

The manner in which these receptors are trafficked within the cell strongly contributes to their functions as initiators of signaling. In the case of EGFR, the receptor is involved in a cycle of endocytosis into the cell followed by quick recycling back to the surface of the cell. The mechanism by which EGFR is internalized is currently disputed, but it is generally believed that it occurs via clathrin-mediated endocytosis. EGFR can interact with clathrin adaptor protein complex (AP2) and growth factor receptor-bound protein 2 (Grb2), with the latter recruiting Cbl to carry out ubiquitination of EGFR. This allows interaction with the clathrin coat within which the receptors are internalized. [83] An alternate, clathrin-independent mechanism of endocytosis induced by high EGF has also been proposed as an additional phenomenon. [84] The mechanism by which EGFR is internalized following binding of ligand has been observed to depend on

which ligand is bound, with EGF following a clathrin-dependent route and HB-EGF showing less dependence on clathrin in knockout studies. [85]

While inactive, EGFR will be internalized with a half-life of approximately 30 minutes, followed by biphasic recycling back to the surface with half-lives of either 5 minutes or 20 minutes. A fraction of these receptors will head towards the lysosomal degradation pathway, such that a typical EGF receptor bears a half-life of 10-14 hours within the cell. [86] Receptor internalization via endocytosis serves as a means of attenuating the signal induced by ligand binding. EGFR signaling can continue while it resides in the endosome, and it has been suggested that endocytosis may be required for certain signaling pathways to proceed. [87] Upon ligand binding, EGFR is activated, and internalization occurs rapidly. [88]

The ErbB signaling network is extraordinarily complex, and given the sensitive nature of this receptor family's functions, proliferation and migration, it is to be expected that dysregulation within this network could lead to rampant growth and ultimately tumorigenesis. This is in fact the case for a variety of cancer types, where a significant percentage of tumors are observed to overexpress EGFR, and EGFR expression level in cancer has been correlated with poor prognosis. For example, in head and neck cancers, EGFR overexpression is observed in 80-100% of tumors, while in renal carcinomas, overexpression occurs in 50-90% of tumors. [89] This can occur via gene amplification, but overexpression can also occur solely at the protein level. [90] Enhanced transcription and elevated post-transcriptional recycling have been implicated as mechanisms for this effect. [91]

Though EGFR overexpression is common, there are other important mechanisms of oncogenic EGFR dysregulation. Increased signaling has been observed in tumors that express

elevated levels of EGFR ligands such as TGF-α or EGF. Such dysregulation leads to autocrine loops that result in aberrant cell growth due to overactive EGFR. [91]

EGFR can also bear a number of mutations that confer a constitutively active state. A common mutant is the EGFRvIII variant, which results from an in-frame deletion of exons 2-7, which includes the ligand binding domain. [91] This form of the receptor is also constitutively active, leading to constant stimulation of certain downstream pathways. Additionally, EGFRvIII fails to be ubiquitinated efficiently, leading to an extended half-life within the cell. [92]

Mutations in the intracellular domain also affect the activity of EGFR with oncogenic effects. In particular, a deletion of 6-7 residues in exon 19, the L858R substitution, and insertion or duplication of residues in exon 20 are particularly common in tumors. It is believed that these mutations stabilize the binding of ATP to the receptor, leading to prolonged EGFR signaling. [91]

Because of these functions, it follows logically that this receptor would be a highly attractive target for cancer therapy. In tumors with EGFR overexpression, the increased level of receptor provides a target to be utilized by therapies in distinguishing tumor tissue from normal tissue.

Cetuximab, the monoclonal antibody previously mentioned in Section A1.1.1, is a chimeric form of a mouse-derived antibody. Also known as C225 and marketed commercially as Erbitux, it is one of a large number of anti-EGFR monoclonal antibodies and the first to have been clinically approved. Its main function is to block the binding of EGF, the ligand for EGFR, which results in a decrease in signaling. ADCC has also been implicated as a possible mechanism of action through which cetuximab induces apoptosis of tumor cells. [93] However, the response rate to this drug has been poor, with some clinical trials with cetuximab showing a response rate of 0-10%. [94]

In addition to antibody therapies, tyrosine kinase inhibitors targeting EGFR kinases have also been developed such as gefitinib and erlotinib. [95] However, the response rate has been similarly poor, with many response rates falling between 0 and 17% in clinical trials. [94]

A1.1.4 Mechanisms of resistance to anti-EGFR therapy

Based on clinical data from cancer patients treated with anti-EGFR therapies, it is known that these drugs control only a fraction of cancers. Certain cancers exhibit primary resistance to EGFR-targeting treatments. One form of primary resistance arises in cancers where EGFR has been structurally mutated such that the treatments are unable to bind to it, or so that ligand binding is no longer necessary for the receptor to initiate the signal cascade. Another critical form of primary resistance occurs when a mutation in one of the downstream proteins of the ErbB effector cascade causes it to become constitutively active, rendering therapies altering elements upstream of that protein ineffective. Some proteins known to have such mutations include KRAS and BRAF; for certain types of cancers, the patient must have wild-type KRAS in order for cetuximab to be approved. [95]

Unfortunately, even in patients that are initially responsive, it is common for acquired resistance to develop. Subsets of the tumor cell population may contain additional mutations in EGFR that disrupt binding of treatments. The T790M mutation of EGFR has long been thought to sterically block the binding of TKIs such as erlotinib and gefitinib, but a recent study has suggested that the mutation increases the affinity of EGFR for ATP, conferring resistance to drugs. [96] Alternate redundant pathways in the signaling network may be upregulated to compensate for a blocked pathway, allowing these cells to survive anti-EGFR therapies. Recent studies have shown that ErbB2 or MET may be upregulated in this manner, and such signaling is

driven through ErbB3. [79] Notably, in certain cell lines that have been cultured to be resistant to anti-EGFR therapies, it is only when either the MET or the ErbB3 pathway is inhibited that the cell line is resensitized to the EGFR therapy. [97]

A1.1.5 Inhibition of KRAS and BRAF mutants

Spangler et. al. has established a successful format for an antibody-like cancer therapeutic targeting EGFR. This format takes a clinically-approved anti-EGFR antibody, cetuximab (C225), as its backbone and fuses additional binding domains to its heavy chain and light chain. These additional binding domains are derived from the tenth type 3 domain of human fibronectin (Fn3). Here, two variants of Fn3, clone A and clone D, have been designed to bind to epitopes of EGFR, forming the triepitopic antibody, HND+LCA. [103] When mice bearing xenografts of established cancer cell lines are treated with HND+LCA, tumor growth is significantly reduced, indicating that this compound could potentially be effective in the treatment of EGFR-driven cancers. [104] Surprisingly, although it is only expected to bind to surface EGFR with no direct interaction with intracellular components, the triepitopic HND+LCA showed therapeutic efficacy even in tumor cell lines harboring a BRAF mutation (HT-29) or a KRAS mutation (HCT-116). Mutations in the C225 CDRs, Y102A and D103A, decrease the affinity of C225 by 30-fold. When introduced into the triepitopic (called HND+LCAx), these mutations completely abrogate the therapeutic effect in all three of the tumor lines tested. [104]

In signaling experiments, it was demonstrated that ERK and AKT, effector proteins downstream of BRAF, KRAS, and EGFR, remained phosphorylated at ligand concentrations well below that which is required in order to achieve detectable phosphorylation of EGFR. [105] This recent evidence has inspired a hypothesis that rather than being constitutively active, cells

harboring these mutations may instead be hypersensitive to EGFR-based stimulation. One possible explanation is that rather than receptor downregulation being the critical component of this therapy, enhanced signal inhibition is what elicits an anti-proliferative effect. C225 binds competitively with EGF at the EGFR ligand binding site with an affinity of 5 nM. [106] With the additional binding domains tethering C225 to the surface of the cell, the effective affinity of C225 for EGFR, and thus its ability to block ligand binding and inhibit signaling, may be increased. This avidity effect may then be negated in the HND+LCAx mutant, which cannot effectively block EGF binding in this manner.

The correlation between affinity and therapeutic efficacy of antibodies, and C225 in particular, has been explored previously. In one study, antibodies of varying binding affinity to EGFR were produced and applied in cell proliferation and signaling assays. There was a positive correlation between antibody affinity and its ability to inhibit phosphorylation of AKT and ERK, effector proteins downstream of EGFR. The stronger binders also showed potency at lower concentrations in cell proliferation inhibition. [107]

Through protein engineering, antibodies can be generated to bind to targets with high affinity and specificity. Yeast display is an effective method of identifying novel antibodies by screening a large library of single chain antibody fragments (scFv) and isolating only those that bind to the target antigen. [78] Directed evolution via random mutagenesis can then be used to enhance the affinity of the discovered antibodies.

In this work, we identified a novel anti-EGFR antibody from an scFv library, then performed successive rounds of affinity maturation to enhance its binding properties. [108] This was done to leverage the relationship between antibody affinity and signal inhibition in order to develop a potent cancer therapy based on EGFR signaling antagonism. The antibody we

generated was then shown to inhibit ligand-based growth signaling in an affinity-dependent manner. Additionally, an *in vitro* cell assay demonstrates that this antibody reduced cell proliferation comparably to the clinically-approved anti-EGFR therapy, cetuximab (C225).

A1.2 Results and Discussion

A1.2.1 Isolation and affinity maturation of an EGFR-binding antibody

Using yeast surface display to perform a library screen on a naïve scFv library, potential EGFR-binding scFvs were isolated. Five clones were selected from this library at random to carry forth in affinity maturation via directed evolution. These clones were analyzed by titration with biotinylated EGFR to confirm binding (Figure A1.2). One clone in particular, E1v1, exhibited a 4-fold higher affinity to EGFR over the next highest affinity clone and was carried forward for additional rounds of affinity maturation. Successive rounds of error-prone PCR and FACS-based screening were conducted in order to generate binders to EGFR of increased affinity.

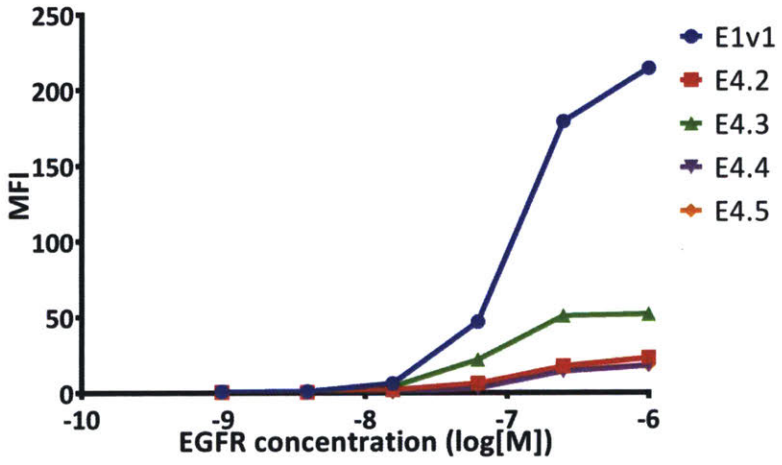

Figure A1.2. Titration of soluble EGFR demonstrating binding of 5 isolated scFv clones to EGFR. Yeast cultures of individual clones were incubated with biotinylated EGFR for 4 hours. Cells were washed and then incubated on ice with anti-human 488 antibody for 1 hour. Fluorescence was then measured.

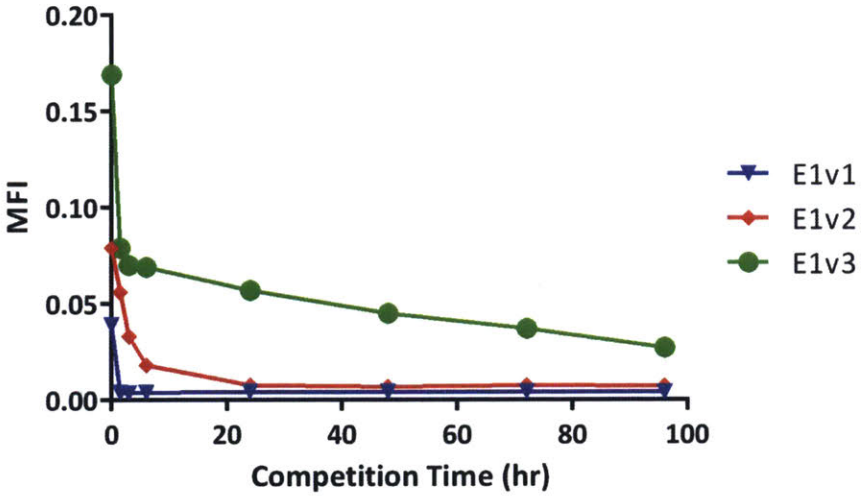

Figure A1.3. Kinetic competition for EGFR to demonstrate relative affinity of E1 clones. Successive rounds of directed evolution resulted in affinity maturation of the E1v1 antibody. To compare affinity, bound biotinylated EGFR was outcompeted with an excess of unbiotinylated EGFR, and the biotinylated protein that remained bound was measured by flow cytometry. E1v3 retained a higher signal even after 96 hours, indicating a greater k_{off} parameter.

The original clone, E1v1, was affinity matured, after which a derivative clone, E1v2, was isolated and sequenced. E1v2 was subjected to further affinity maturation, and another clone of higher apparent affinity, E1v3, was chosen for further characterization. These three clones were compared using kinetic competition assay (Figure A1.3). Yeast cultures of each clone were incubated with biotinylated EGFR for 1 hour, then washed and incubated with an excess of unbiotinylated EGFR for the indicated amounts of time. The amount of biotinylated EGFR that remained following the competition was measured with anti-biotin 488 antibody, with higher signal indicating a clone with higher affinity. From this, it was determined that E1v3 was in fact a higher affinity binder for EGFR than the previously engineered antibodies, E1v1 and E1v2. Affinity of E1v3 was quantified using BLItz (ForteBio) to give a value of 3.68 nM (Figure S2.1).

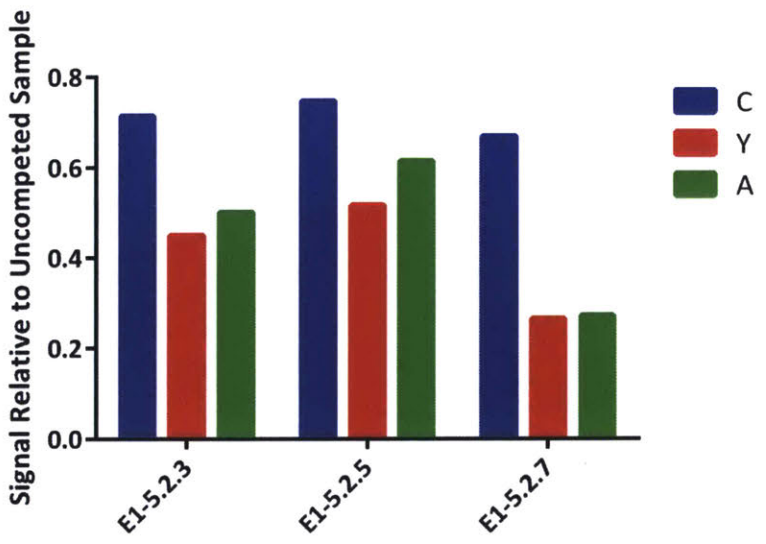

Figure A1.4. Kinetic competition comparing relative affinities of clones with mutated cysteine residue reveals that the cysteine residue is essential for the increased affinity of E1v3 variants. Isolated yeast clones with cysteine mutated to tyrosine and alanine were compared in kinetic competition assays. In all three cases, the cysteine variant possessed higher affinity than the mutants.

E1v3 was subjected to further mutagenesis to attempt to continue affinity maturation. However, sequencing of the clones generated revealed that a cysteine was consistently emerging at residue 53 preceding the light chain CDR 2 in clones of higher apparent affinity in FACS analysis. To determine if this free cysteine was necessary to retain the affinity of these clones for EGFR, the cysteine of three clones was mutated to either tyrosine or alanine and subjected to kinetic competition for 16 hours (Figure A1.4). The retained signal of the cysteine mutant was consistently higher than that of the tyrosine or alanine variant, with mutation away from cysteine resulting in reductions in affinity ranging from 19% to 60%. This indicates that the free cysteine, and potentially, disulfide chemistry, was vital for the activity of this antibody. Based on these results and a lack of increases in affinity for clones not bearing a free cysteine, affinity maturation of the E1 antibody was discontinued, and E1v3 was selected as the final product of the antibody engineering step.

A1.2.2 Characterization of the E1 antibody

To characterize the manner in which the E1 antibody interacts with EGFR, the DNA encoding E1v2's variable regions was grafted onto DNA for a full-length human IgG and expressed in HEK293f cells. A431 cells were incubated for 3 hours on ice with either E1v2, cetuximab (C225), the triepitopic antibody HND+LCA, or the variant HND+LCAx, a triple mutant of HND+LCA that has reduced binding affinity in the C225 domain. Cells were then washed with phosphate-buffered saline (PBS), then incubated for 1 hour on ice with human EGF labeled with Alexa Fluor 488. The amount of fluorescent EGF bound to the cells was measured by flow cytometry (Figure A1.5).

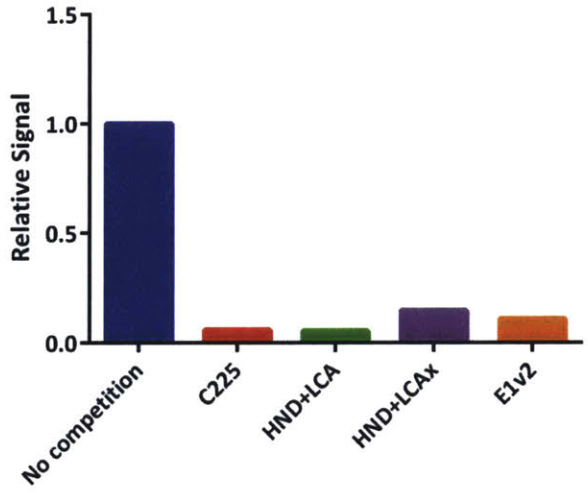

Figure A1.5. Fluorescence-based EGF competition assay shows E1v2 binds EGFR competitively with EGF. A431 cells were preincubated with EGFR antibodies, then labeled with fluorescent EGF. The signal for EGF was greatly diminished in all cases where an EGFR binder was present.

The results show that C225 and HND+LCA (which contains the C225 antibody) both block binding of EGF by over 95% as expected, since the known binding epitope of C225 is the same binding site for EGF. By comparison, HND+LCAx reduced binding by 85%, which could be because HND+LCAx still induces downregulation of EGFR available on the surface but does

not block the EGF binding site as efficiently. Additionally, E1v2 also blocked binding of EGF, reducing binding by 89% compared to unblocked cells. This suggests that E1v2 also binds to EGFR competitively with EGF, which could confer a signal inhibition property to this antibody.

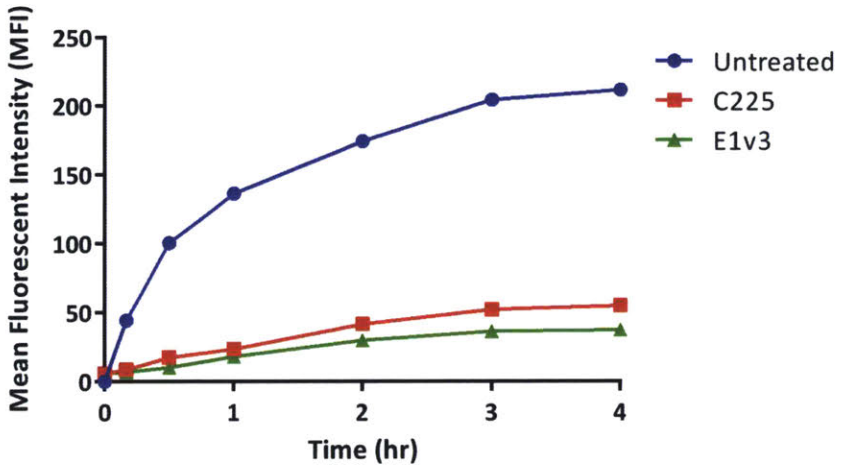

Figure A1.6. Internalization of EGF-pHrodo Red in A431 cells is inhibited by E1v3. Cells were cultured with or without antibody overnight, then incubated with EGF conjugated with pHrodo Red for various time points.

As part of the signal cascade initiated by EGF binding, EGFR is internalized into the cell via endocytosis. To determine if the E1 antibody influences internalization of EGFR, A431 cells were cultured overnight with C225 or E1v3 (Figure A1.6). Cells were then incubated with EGF conjugated to pHrodo Red for various amounts of time. pHrodo Red is a pH-sensitive fluorophore that only fluoresces at low pH, which allows it to be used to determine if proteins have been internalized into the acidic environment of the endosome. By measuring the fluorescence of cells treated with EGF, the degree of internalization can be determined. In this case, cells that were not treated with antibody internalized EGF at a high rate, while both C225 and E1v3 inhibited internalization of EGF, with E1v3-treated cells internalizing 32% less than C225-treated cells. This again points to the potential for E1v3 to exert a signal inhibition effect.

A1.2.3 E1v3 induces a biological response in cancer cell lines

Previous results demonstrated that E1v3 interacted with EGFR in a manner antagonistic to EGF. To determine if this affects processes downstream of EGFR, a signaling assay was performed (Figure A1.7). HT29 cells were cultured with C225, HND+LCA, E1v1, E1v2, or E1v3 overnight, after which EGF was spiked into the culture medium. C225 and HND+LCA have both been previously observed as inhibiting signaling downstream of EGFR. Cells were then lysed and analyzed by Western blot staining for phosphorylation of effector proteins AKT and ERK, which are normally activated by EGF-induced activation of EGFR. In the assay, E1v1, the lowest affinity antibody, did not inhibit signaling through AKT or ERK, but E1v2 and E1v3 both inhibited signaling to a degree similar to C225 and HND+LCA. This demonstrates that the affinity-matured antibodies are capable of altering the growth signaling pathway by blocking ligand-based signaling through EGFR.

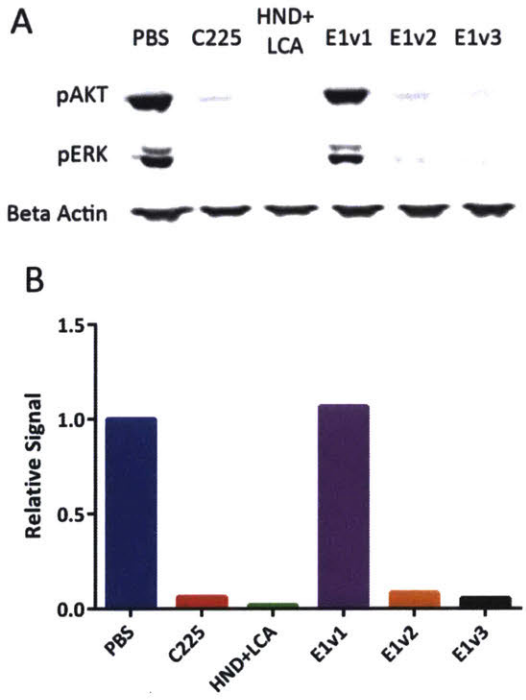

Figure A1.7. Inhibition of EGF-induced signaling through AKT and ERK by E1. (a) Western blot analysis showing HT29 lysates stained for phosphorylated AKT and ERK. E1v2 and E1v3 both were capable of inhibiting signaling caused by 10 minutes of EGF treatment. (b) Densitometry analysis of Western blot. The degree of signal inhibition is comparable to that of known EGFR antagonist C225.

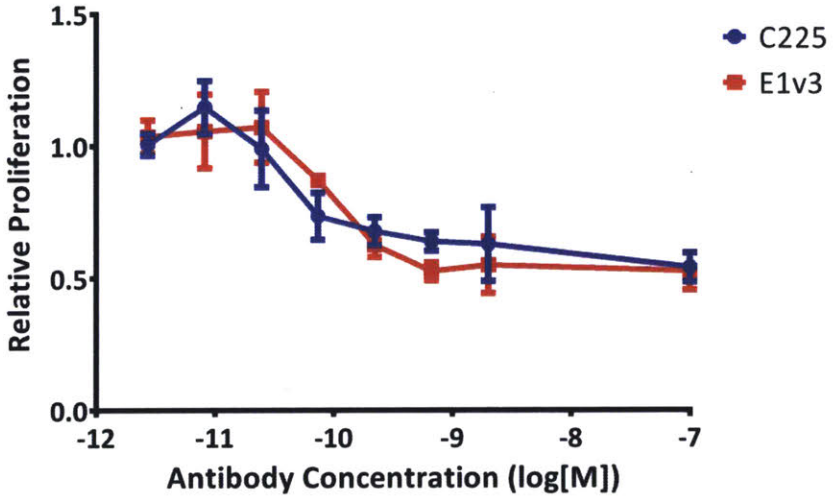

Figure A1.8. Inhibition of proliferation of NCI-H292 lung cancer cells. Cells were cultured in media containing varying concentrations of antibody for 72 hours. Cell viability was approximated using WST-1 reagent.

To assay the ability of E1v3 to induce a growth-inhibition phenotype, cell proliferation assays were performed (Figure A1.8). A lung cancer cell line, NCI-H292, was cultured in varying concentrations of C225 or E1v3. After 72 hours, WST-1 reagent was added to measure the viability of cells under these conditions. In a dose-dependent manner, E1v3 inhibited proliferation of NCI-H292 cells to a degree comparable to that caused by C225.

Based on the results of both the signaling assay and proliferation assay, there is strong evidence that the novel anti-EGFR antibody, E1v3, is capable of modulating the viability of EGFR-overexpressing cancer cell lines by antagonizing EGF-initiated growth signaling. In both signal inhibition assays and cell proliferation assays, the effect was comparable in potency to a clinically approved anti-EGFR antibody, cetuximab (C225). E1v3 also bears a potential advantage over the canonical EGFR antibody, cetuximab. The scFv library from which E1v3 was engineered was derived from human antibody sequences, while cetuximab was generated through immunization of a mouse. The murine sequence of cetuximab may generate immunogenicity issues with the human immune system that the native human sequence of E1v3

may not. Overall, E1v3 shows signs of promise as an anti-cancer therapeutic that warrants further investigation.

A1.3 Materials and Methods

A1.3.1 *Saccharomyces cerevisiae* yeast culture

EBY-100 yeast cells were cultured in SD-CAA media (20 g/L dextrose, 6.7 g/L yeast nitrogen base, 5 g/L casamino acids, 10.5 g/L sodium citrate, 7.4 g/L citric acid monohydrate, pH 4.5) at 30°C with shaking at 200 RPM. Induction of scFv expression was performed in SG-CAA media (2 g/L dextrose, 18 g/L galactose, 6.7 g/L yeast nitrogen base, 5 g/L casamino acids, 5.4 g/L Na_2HPO_4, 8.56 g/L $NaH_2PO_4 \cdot H_2O$, pH 6.0) at 20°C with shaking. [78]

A1.3.2 Transformation of yeast

To transform EBY-100 cells with scFv library DNA, yeast cultures were initially grown overnight in YPD buffer (10 g/L yeast extract, 20 g/L peptone, 20 g/L dextrose). Yeast were then diluted to OD = 0.1, then grown until cell density was $1.3\text{-}1.5 \times 10^7$ cells/mL. Cells were then resuspended in buffer (100 mM lithium acetate, 10 mM Tris, 1 mM EDTA, pH 7.5) at 30°C for 15 minutes. Tris pH 8.0 containing DTT was added to a final concentration of 10 mM, then the cells were cultured with shaking at 30°C for 30 minutes.

Cells were then pelleted, washed twice with buffer E (10 mM Tris, pH 7.5, 270 mM sucrose, 1 mM $MgCl_2$), and resuspended in 1 mL of buffer E. Cells were mixed with scFv library DNA and placed in a 2 mm electroporation cuvette, then pulsed at 25 uF, 0.57 kV. Electroporated cells were allowed to recover in YPD at 30°C for 1 hour, then cultured in SD-CAA. [78]

A1.3.3 Directed evolution via error-prone PCR

Yeast DNA was extracted using Zymoprep kit (Zymogen). For clone screening, DNA was then transformed into XL1-Blue *E. coli* and individual colonies picked and sequenced. Library DNA or individual clones were then subjected to mutagenesis for affinity maturation. DNA was amplified using Taq polymerase in a reaction containing additional nucleotide substitutes (2 μM 8-oxo-dGTP and dPTP). [78]

A1.3.4 Library screening of yeast binders

Biotinylated EGFR was immobilized on Dynabeads (Invitrogen). Induced yeast libraries expressing candidate scFvs were incubated with these beads. Beads bound with yeast were recovered using magnetic bead sorting and cultured in SD-CAA media. This process was repeated until biotinylated EGFR bound to beads could be detected by flow cytometry.

Induced libraries were incubated with anti-c-Myc antibody (Gallus Immunotech) and biotinylated EGFR. Anti-c-Myc signal was used to measure expression of full-length scFvs, while anti-biotin antibody was used to measure affinity of scFv clones toward EGFR. Cells were analyzed using FACS Aria (BD Biosciences) fluorescent cell sorter, and yeast showing a high binding signal relative to scFv expression were collected and cultured.

A1.3.5 Antibody expression

The heavy chain and light chain variable regions were amplified out of the scFv gene using PCR with the following primers for the heavy chain: HC forward primer 5'-TTGCTCTTCCTTGTCGCTGTTGCTACGCGTGAGGTTCAGCTGGTGGAGTC-3' and HC

reverse primer 5'-GGGGAAGACCGATGGGCCCTTGGTGCTAGCCGAGGAGACGGTG ACCAGGG-3'. The following primers were used for the light chain: LC forward primer 5'-CTGCTGCTCTGGCTCCCAGGTGCACGATGTGATATCCAGATGACCCAGTC-3' and LC reverse primer 5'-GATGAAGACAGATGGTGCAGCCACCGTACGTTTGATCTCCACC TTGGTAC-3'. These PCR products were then grafted onto the constant domains of human IgG to create a full-length antibody from the scFvs of interest. This DNA was then transiently transfected into HEK293f cells for protein expression. Supernatant was harvested after 7-10 days of culture and antibody was purified using affinity chromatography with Protein A resin (GenScript). Antibodies were further purified by size-exclusion chromatography using a Superdex 200 column (GE Healthcare).

A1.3.6 Flow cytometry assays

To measure affinity, A431 cells were incubated on ice with varying concentrations of EGFR-binding antibodies for 4 hours. Cells were then washed with PBSA and incubated with anti-human-488 fluorescent antibody for 1 hour (Life Technologies). Fluorescent signal was analyzed on Accuri C6 flow cytometer (BD Biosciences).

To perform kinetic competition assays to compare affinity of different antibodies, individual yeast clones were incubated with biotinylated EGFR for 1 hour, then washed and incubated with EGFR without biotin for various time points. Cells were then labeled with anti-biotin fluorescent antibody for 1 hour and fluorescence was measured on Accuri C6 flow cytometer.

To determine competition for binding with EGF, A431 cells were incubated with EGFR binders for 3 hours on ice. Cells were then washed with PBSA and then incubated for 1 hour on

ice with EGF conjugated to Alexa Fluor 488 (Life Technologies). Fluorescent signal was then analyzed on Accuri C6 flow cytometer.

To analyze effect of antibody binding on the rate of EGF internalization, A431 cells were cultured with EGFR antibodies overnight. Cells were washed with PBS and then cultured at various time points with EGF conjugated to pHrodo Red (Life Technologies), a pH-sensitive fluorophore. Cells were trypsinized and fluorescent signal was analyzed on Accuri C6 flow cytometer.

A1.3.7 Cell culture

A431, HT29, and NCI-H292 cells were obtained from American Type Culture Collection. A431 cells were maintained in a tissue culture incubator and grown in DMEM medium, HT29 cells were cultured in McCoy's 5A Medium, and NCI-H292 cells were cultured in RPMI-1640 medium. All media were supplemented with 10% fetal bovine serum, 100 units/mL penicillin, and 100 μg/mL streptomycin.

A1.3.8 Signaling assay

HT29 cells were grown in a 12-well tissue culture plate until 80% confluency. Cells were treated with media containing 20 nM antibody for 24 hours at 37°C. After this step, recombinant human EGF (R&D Systems) was spiked in at a concentration of 20 nM for 10 minutes. Cells were washed with PBS, then lysed using SDS buffer (50 mM Tris HCl, 2% SDS, 5% glycerol, 5 mM EDTA with protease and phosphatase inhibitors). The lysates were filtered using AcroPrep Filter Plates with Bio-Inert Membranes (Pall Life Sciences), then run on SDS PAGE gels and transferred to Western blot membranes. Western blots were sequentially

incubated with anti-pERK antibody or anti-pAKT antibody, and anti-beta-actin antibody (Cell Signaling Technologies), then incubated with anti-rabbit antibody labeled with IRDye and imaged on an Odyssey Imaging System (LI-COR Biosciences).

A1.3.9 Proliferation assay

NCI-H292 cells were seeded in a 96-well tissue culture plate at 10,000 cells per well and grown overnight. Cells were then treated with media containing varying concentrations of antibody. The plate was incubated at 37°C for three days.

Quantification of metabolic activity in cells was carried out using the WST-1 Cell Proliferation Reagent (Sigma Aldrich) according to manufacturer's protocols. 10 µL of WST-1 reagent was added to each well, then cells were cultured at 37°C for an additional 2 hours. Cells were shaken in order to mix the reagent, then absorbance was measured on a Tecan Infinite 200 PRO plate reader.

Appendix 2: Supplementary Figures

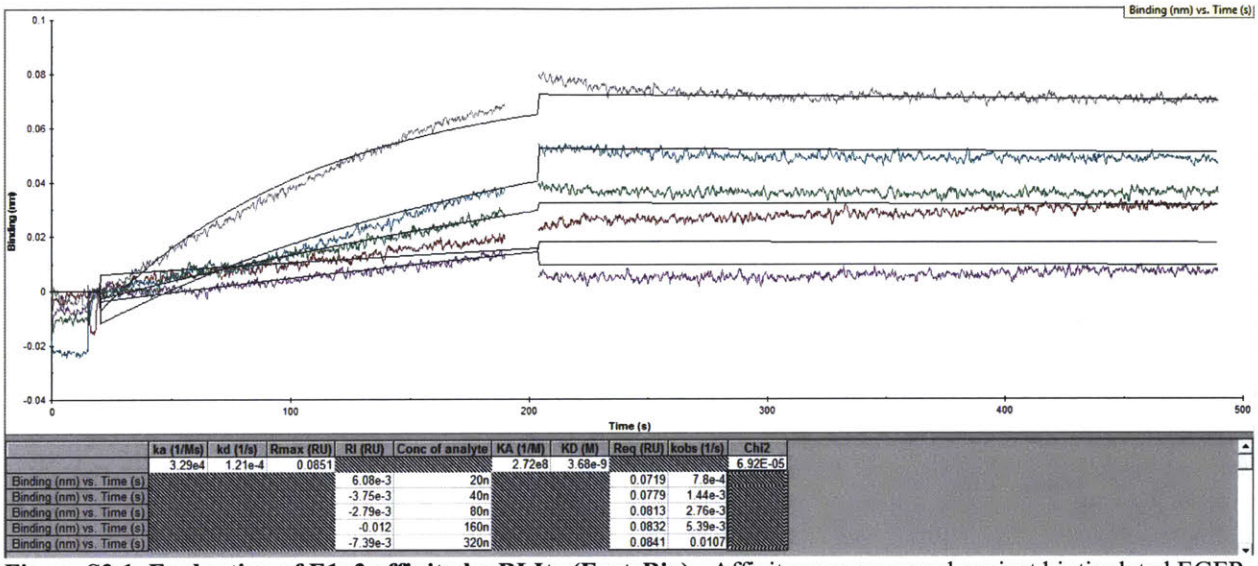

	ka (1/Ms)	kd (1/s)	Rmax (RU)	RI (RU)	Conc of analyte	KA (1/M)	KD (M)	Req (RU)	kobs (1/s)	Chi2
	3.29e4	1.21e-4	0.0851			2.72e8	3.68e-9			6.92E-05
Binding (nm) vs. Time (s)				6.08e-3	20n			0.0719	7.8e-4	
Binding (nm) vs. Time (s)				-3.75e-3	40n			0.0779	1.44e-3	
Binding (nm) vs. Time (s)				-2.79e-3	80n			0.0813	2.76e-3	
Binding (nm) vs. Time (s)				-0.012	160n			0.0832	5.39e-3	
Binding (nm) vs. Time (s)				-7.39e-3	320n			0.0841	0.0107	

Figure S2.1. Evaluation of E1v3 affinity by BLItz (ForteBio). Affinity was measured against biotinylated EGFR immobilized on streptavidin tips, giving an affinity of 3.68 nM.

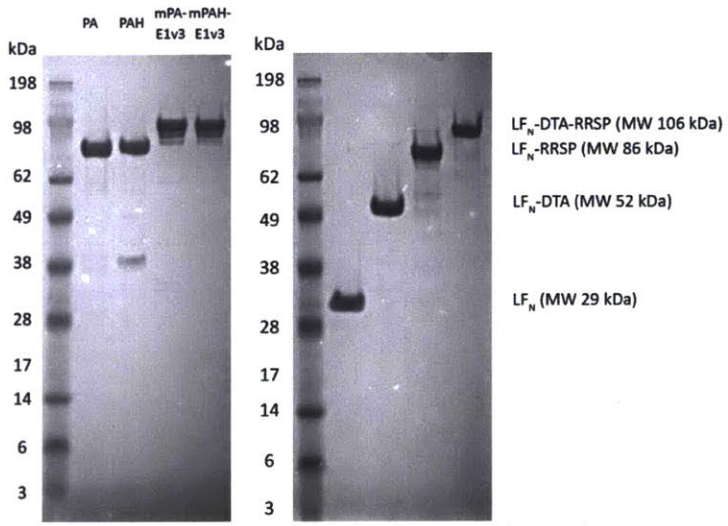

Figure S2.2. SDS-PAGE analysis of expressed proteins.

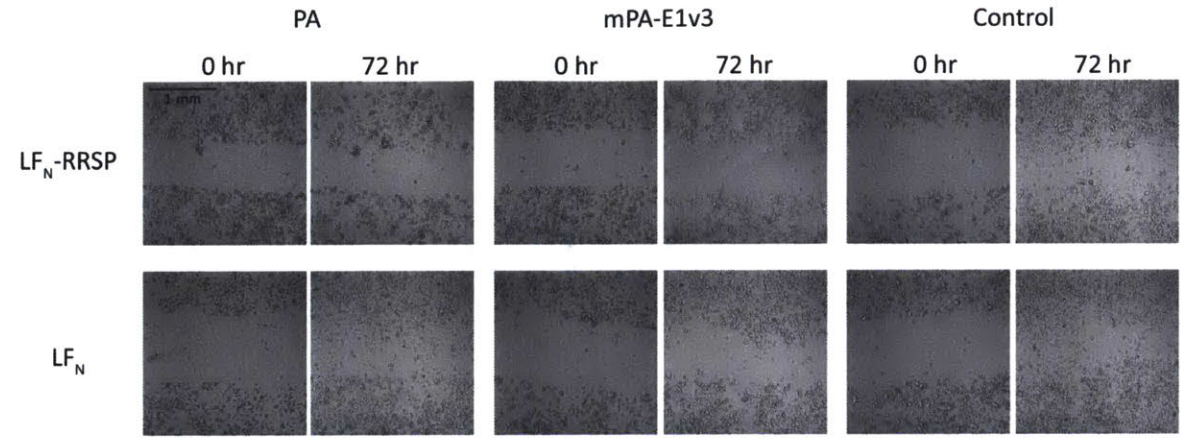

Figure S2.3. Raw image data for scratch test shown in Figure 2.6.

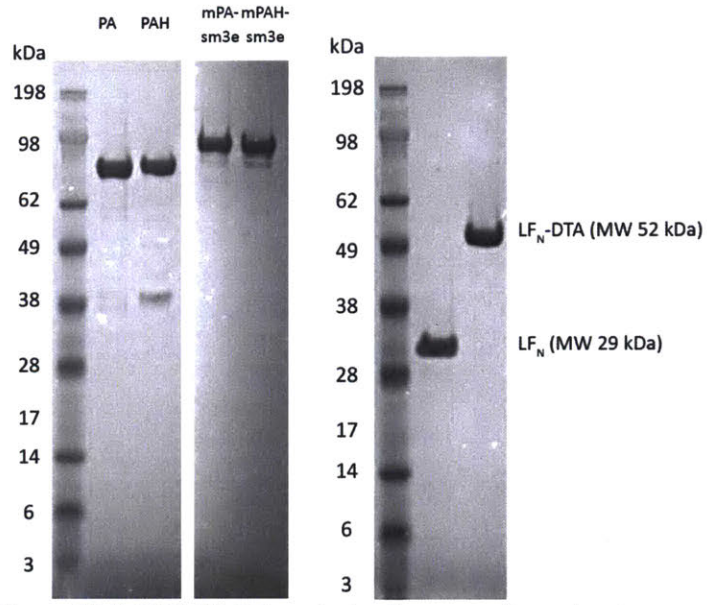

Figure S3.1. SDS-PAGE analysis of expressed constructs.

Table S2.1

Sequence of E1v3

scFV DNA sequence
GATATCCAGATGACCCAGTCCCCGAGCTCCCTGTCCGCCTCTGTGGGCGATAGGGTC
ACCATCACCTGCCGTGCCAGTCAGGGTTCTGATTCTTACAGTGTGGCCTGGTATCAA
CAGAAACCAGGAAAAGTTCCGAAGCTCCTGATTTACGGTGCATCCTACCTCTACTCT
GGAGTCCCTTCTCGCTTCTCTGGTAGCCGTTCCGAGACGGATTTCACTCTGACCATCA
GCAGTCTGCAGCCGGAAGACTTCGCAACTTATTACTGTCAGCAATCTTCTCCGTACC
CGTCTCTGATCACGTTCGGACAGGGTACCAAGGTGGAGATCAAAGGTACTACTGCC
GCTAGTGATAGTAGCGGTGGCAGTAGCAGTGGTGCCGAGGTTCAGCTGGTGGAGTC
TGGCGGTGGCCTGGTGCAGCCAGGGGGCTCACTCCGTTTATCCTGTGCAGCTTCTGG
CTTCAACATCTACTCTTACGGTATGCACTGGGTGCGCCAGGCCCCGAGTAAGGGCCC
GGAATGGGTTGCAGGTATTTACCCTGCTTACGGCTCTACTTACTATGCCGATAGCGT
CAGGGGCCGTTTCACTATAGGCGCAGACACATCCAAAAACACAGCCTACCTACAAA
TGAACAGCTTAAGAGCTGAGGACACTGCCGTCTATTATTGTGCTCGCCCGTACTCTT
ACACTGGTGCTATTGACTACTGGGGTCAGGGAACCCCGGTCACCGTCTCCTCGGGAT
TCGAACAAAAGCTTATTTCTGAAGAGGACTTGTAATAG

HC DNA sequence
GAGGTTCAGCTGGTGGAGTCTGGCGGTGGCCTGGTGCAGCCAGGGGGCTCACTCCG
TTTATCCTGTGCAGCTTCTGGCTTCAACATCTACTCTTACGGTATGCACTGGGTGCGC
CAGGCCCCGAGTAAGGGCCCGGAATGGGTTGCAGGTATTTACCCTGCTTACGGCTCT
ACTTACTATGCCGATAGCGTCAGGGGCCGTTTCACTATAGGCGCAGACACATCCAAA
AACACAGCCTACCTACAAATGAACAGCTTAAGAGCTGAGGACACTGCCGTCTATTAT
TGTGCTCGCCCGTACTCTTACACTGGTGCTATTGACTACTGGGGTCAGGGAACCCCG
GTCACCGTCTCCTCG

LC DNA sequence
GATATCCAGATGACCCAGTCCCCGAGCTCCCTGTCCGCCTCTGTGGGCGATAGGGTC
ACCATCACCTGCCGTGCCAGTCAGGGTTCTGATTCTTACAGTGTGGCCTGGTATCAA
CAGAAACCAGGAAAAGTTCCGAAGCTCCTGATTTACGGTGCATCCTACCTCTACTCT
GGAGTCCCTTCTCGCTTCTCTGGTAGCCGTTCCGAGACGGATTTCACTCTGACCATCA
GCAGTCTGCAGCCGGAAGACTTCGCAACTTATTACTGTCAGCAATCTTCTCCGTACC
CGTCTCTGATCACGTTCGGACAGGGTACCAAGGTGGAGATCAAA

References

1. Ribet, D. & Cossart, P. How bacterial pathogens colonize their hosts and invade deeper tissues. *Microbes and Infection* **17,** 173–183 (2015).
2. Kolstø, A.-B., Tourasse, N. J. & Økstad, O. A. What Sets *Bacillus anthracis* Apart from Other *Bacillus* Species? *Annual Review of Microbiology* **63,** 451–476 (2009).
3. Young, J. A. T. & Collier, R. J. Anthrax Toxin: Receptor Binding, Internalization, Pore Formation, and Translocation. *Annual Review of Biochemistry* **76,** 243–265 (2007).
4. Duesbery, N. S. Proteolytic Inactivation of MAP-Kinase-Kinase by Anthrax Lethal Factor. *Science* **280,** 734–737 (1998).
5. Leppla, S. H. Anthrax toxin edema factor: a bacterial adenylate cyclase that increases cyclic AMP concentrations of eukaryotic cells. *Proceedings of the National Academy of Sciences* **79,** 3162–3166 (1982).
6. Drum, C. L. *et al.* Structural basis for the activation of anthrax adenylyl cyclase exotoxin by calmodulin. *Nature* **415,** 396–402 (2002).
7. Liu, S. *et al.* Key tissue targets responsible for anthrax-toxin-induced lethality. *Nature* **501,** 63–68 (2013).
8. Milne, J. C., Furlong, D., Hanna, P. C., Wall, J. S. & Collier, R. J. Anthrax protective antigen forms oligomers during intoxication of mammalian cells. *Journal of Biological Chemistry* **269,** 20607–20612 (1994).
9. Petosa, C., Collier, R. J., Klimpel, K. R., Leppla, S. H. & Liddington, R. C. Crystal structure of the anthrax toxin protective antigen. *Nature* **385,** 833–838 (1997).
10. Santelli, E., Bankston, L. A., Leppla, S. H. & Liddington, R. C. Crystal structure of a complex between anthrax toxin and its host cell receptor. *Nature* **430,** 905–908 (2004).
11. Scobie, H. M., Rainey, G. J. A., Bradley, K. A. & Young, J. A. T. Human capillary morphogenesis protein 2 functions as an anthrax toxin receptor. *Proceedings of the National Academy of Sciences* **100,** 5170–5174 (2003).
12. Bonuccelli, G. ATR/TEM8 is highly expressed in epithelial cells lining Bacillus anthracis' three sites of entry: implications for the pathogenesis of anthrax infection. *AJP: Cell Physiology* **288,** C1402–C1410 (2005).
13. Reeves, C. V., Dufraine, J., Young, J. A. T. & Kitajewski, J. Anthrax toxin receptor 2 is expressed in murine and tumor vasculature and functions in endothelial proliferation and morphogenesis. *Oncogene* **29,** 789–801 (2010).
14. Wigelsworth, D. J. Binding Stoichiometry and Kinetics of the Interaction of a Human Anthrax Toxin Receptor, CMG2, with Protective Antigen. *Journal of Biological Chemistry* **279,** 23349–23356 (2004).
15. Scobie, H. M. & Young, J. A. Interactions between anthrax toxin receptors and protective antigen. *Current Opinion in Microbiology* **8,** 106–112 (2005).
16. Liu, S. *et al.* Capillary morphogenesis protein-2 is the major receptor mediating lethality of anthrax toxin in vivo. *Proceedings of the National Academy of Sciences* **106,** 12424–12429 (2009).
17. Christensen, K. A., Krantz, B. A., Melnyk, R. A. & Collier, R. J. Interaction of the 20 kDa and 63 kDa Fragments of Anthrax Protective Antigen: Kinetics and Thermodynamics†. *Biochemistry* **44,** 1047–1053 (2005).
18. Kintzer, A. F. *et al.* The Protective Antigen Component of Anthrax Toxin Forms Functional Octameric Complexes. *Journal of Molecular Biology* **392,** 614–629 (2009).

19. Abrami, L., Liu, S., Cosson, P., Leppla, S. H. & Goot, F. G. van der. Anthrax toxin triggers endocytosis of its receptor via a lipid raft–mediated clathrin-dependent process. *J Cell Biol* **160,** 321–328 (2003).
20. Abrami, L., Leppla, S. H. & van der Goot, F. G. Receptor palmitoylation and ubiquitination regulate anthrax toxin endocytosis. *The Journal of Cell Biology* **172,** 309–320 (2006).
21. Abrami, L., Bischofberger, M., Kunz, B., Groux, R. & van der Goot, F. G. Endocytosis of the Anthrax Toxin Is Mediated by Clathrin, Actin and Unconventional Adaptors. *PLoS Pathogens* **6,** e1000792 (2010).
22. Qa'dan, M., Christensen, K. A., Zhang, L., Roberts, T. M. & Collier, R. J. Membrane Insertion by Anthrax Protective Antigen in Cultured Cells. *Molecular and Cellular Biology* **25,** 5492–5498 (2005).
23. Krantz, B. A. A Phenylalanine Clamp Catalyzes Protein Translocation Through the Anthrax Toxin Pore. *Science* **309,** 777–781 (2005).
24. Jiang, J., Pentelute, B. L., Collier, R. J. & Zhou, Z. H. Atomic structure of anthrax protective antigen pore elucidates toxin translocation. *Nature* **521,** 545–549 (2015).
25. Krantz, B. A., Finkelstein, A. & Collier, R. J. Protein Translocation through the Anthrax Toxin Transmembrane Pore is Driven by a Proton Gradient. *Journal of Molecular Biology* **355,** 968–979 (2006).
26. Jernigan, J. Bioterrorism-Related Inhalational Anthrax: The First 10 Cases Reported in the United States. *Emerging Infectious Diseases* **7,** 933–944 (2001).
27. Patyar, S. *et al.* Bacteria in cancer therapy: a novel experimental strategy. *Journal of Biomedical Science* **17,** 21 (2010).
28. Pastan, I., Hassan, R., FitzGerald, D. J. & Kreitman, R. J. Immunotoxin therapy of cancer. *Nature Reviews Cancer* **6,** 559–565 (2006).
29. Hou, S.-C. *et al.* High throughput cytotoxicity screening of anti-HER2 immunotoxins conjugated with antibody fragments from phage-displayed synthetic antibody libraries. *Scientific Reports* **6,** 31878 (2016).
30. Simon, N. & FitzGerald, D. Immunotoxin Therapies for the Treatment of Epidermal Growth Factor Receptor-Dependent Cancers. *Toxins* **8,** 137 (2016).
31. Becker, N. & Benhar, I. Antibody-Based Immunotoxins for the Treatment of Cancer. *Antibodies* **1,** 39–69 (2012).
32. Foss, F. Clinical Experience With Denileukin Diftitox (ONTAK). *Seminars in Oncology* **33,** 11–16 (2006).
33. Alewine, C., Hassan, R. & Pastan, I. Advances in Anticancer Immunotoxin Therapy. *The Oncologist* **20,** 176–185 (2015).
34. Yang, N. J. *et al.* Antibody-Mediated Neutralization of Perfringolysin O for Intracellular Protein Delivery. *Molecular Pharmaceutics* **12,** 1992–2000 (2015).
35. Mechaly, A., McCluskey, A. J. & Collier, R. J. Changing the Receptor Specificity of Anthrax Toxin. *mBio* **3,** e00088-12-e00088-12 (2012).
36. Rosovitz, M. J. *et al.* Alanine-scanning Mutations in Domain 4 of Anthrax Toxin Protective Antigen Reveal Residues Important for Binding to the Cellular Receptor and to a Neutralizing Monoclonal Antibody. *Journal of Biological Chemistry* **278,** 30936–30944 (2003).
37. McCluskey, A. J., Olive, A. J., Starnbach, M. N. & Collier, R. J. Targeting HER2-positive cancer cells with receptor-redirected anthrax protective antigen. *Molecular Oncology* **7,** 440–451 (2013).

38. Löfblom, J. *et al.* Affibody molecules: Engineered proteins for therapeutic, diagnostic and biotechnological applications. *FEBS Letters* **584,** 2670–2680 (2010).
39. McCluskey, A. J. & Collier, R. J. Receptor-Directed Chimeric Toxins Created by Sortase-Mediated Protein Fusion. *Molecular Cancer Therapeutics* **12,** 2273–2281 (2013).
40. Chen, K.-H., Liu, S., Bankston, L. A., Liddington, R. C. & Leppla, S. H. Selection of Anthrax Toxin Protective Antigen Variants That Discriminate between the Cellular Receptors TEM8 and CMG2 and Achieve Targeting of Tumor Cells. *J. Biol. Chem.* **282,** 9834–9845 (2007).
41. Chen, K.-H. *et al.* Anthrax Toxin Protective Antigen Variants that selectively utilize either the CMG2 or TEM8 Receptors for Cellular Uptake and Tumor Targeting. *Journal of Biological Chemistry* jbc.M116.753301 (2016). doi:10.1074/jbc.M116.753301
42. Liu, S., Netzel-Arnett, S., Birkedal-Hansen, H. & Leppla, S. H. Tumor Cell-selective Cytotoxicity of Matrix Metalloproteinase-activated Anthrax Toxin. *Cancer Res* **60,** 6061 (2000).
43. Bachran, C. *et al.* Cytolethal distending toxin B as a cell-killing component of tumor-targeted anthrax toxin fusion proteins. *Cell Death and Disease* **5,** e1003 (2014).
44. Liu, S. *et al.* Matrix Metalloproteinase-activated Anthrax Lethal Toxin Demonstrates High Potency in Targeting Tumor Vasculature. *Journal of Biological Chemistry* **283,** 529–540 (2008).
45. Liu, S. Targeting of Tumor Cells by Cell Surface Urokinase Plasminogen Activator-dependent Anthrax Toxin. *Journal of Biological Chemistry* **276,** 17976–17984 (2001).
46. Phillips, D. D. *et al.* Engineering Anthrax Toxin Variants That Exclusively Form Octamers and Their Application to Targeting Tumors. *Journal of Biological Chemistry* **288,** 9058–9065 (2013).
47. Mogridge, J., Cunningham, K. & Collier, R. J. Stoichiometry of Anthrax Toxin Complexes. *Biochemistry* **41,** 1079–1082 (2002).
48. Arora, N. & Leppla, S. H. Residues 1-254 of anthrax toxin lethal factor are sufficient to cause cellular uptake of fused polypeptides. *Journal of Biological Chemistry* **268,** 3334–3341 (1993).
49. Feld, G. K. *et al.* Structural basis for the unfolding of anthrax lethal factor by protective antigen oligomers. *Nature Structural & Molecular Biology* **17,** 1383–1390 (2010).
50. Wesche, J., Elliott, J. L., Falnes, P. Ø., Olsnes, S. & Collier, R. J. Characterization of Membrane Translocation by Anthrax Protective Antigen †. *Biochemistry* **37,** 15737–15746 (1998).
51. Arora, N., Klimpel, K. R., Singh, Y. & Leppla, S. H. Fusions of anthrax toxin lethal factor to the ADP-ribosylation domain of Pseudomonas exotoxin A are potent cytotoxins which are translocated to the cytosol of mammalian cells. *Journal of Biological Chemistry* **267,** 15542–15548 (1992).
52. Arora, N. & Leppla, S. H. Fusions of anthrax toxin lethal factor with shiga toxin and diphtheria toxin enzymatic domains are toxic to mammalian cells. *Infection and Immunity* **62,** 4955–4961 (1994).
53. Collier, R. J. & Kandel, J. Structure and Activity of Diphtheria Toxin: I. THIOL-DEPENDENT DISSOCIATION OF A FRACTION OF TOXIN INTO ENZYMICALLY ACTIVE AND INACTIVE FRAGMENTS. *Journal of Biological Chemistry* **246,** 1496–1503 (1971).

54. Antic, I., Biancucci, M., Zhu, Y., Gius, D. R. & Satchell, K. J. F. Site-specific processing of Ras and Rap1 Switch I by a MARTX toxin effector domain. *Nature Communications* **6,** 7396 (2015).
55. Antic, I., Biancucci, M. & Satchell, K. J. F. Cytotoxicity of the Vibrio vulnificus MARTX toxin Effector DUF5 is linked to the C2A Subdomain. *Proteins* **82,** 2643–2656 (2014).
56. Hu, H. & Leppla, S. H. Anthrax Toxin Uptake by Primary Immune Cells as Determined with a Lethal Factor-β-Lactamase Fusion Protein. *PLoS ONE* **4,** e7946 (2009).
57. Liao, X., Rabideau, A. E. & Pentelute, B. L. Delivery of Antibody Mimics into Mammalian Cells via Anthrax Toxin Protective Antigen. *ChemBioChem* **15,** 2458–2466 (2014).
58. Rabideau, A. E., Liao, X., Akçay, G. & Pentelute, B. L. Translocation of Non-Canonical Polypeptides into Cells Using Protective Antigen. *Scientific Reports* **5,** 11944 (2015).
59. Rabideau, A. E., Liao, X. & Pentelute, B. L. Delivery of mirror image polypeptides into cells. *Chem. Sci.* **6,** 648–653 (2015).
60. Rabideau, A. E. & Pentelute, B. L. A d-Amino Acid at the N-Terminus of a Protein Abrogates Its Degradation by the N-End Rule Pathway. *ACS Central Science* **1,** 423–430 (2015).
61. Bachmair, A., Finley, D. & Varshavsky, A. In vivo half-life of a protein is a function of its amino-terminal residue. *Science* **234,** 179–186 (1986).
62. Shaw, C. A. & Starnbach, M. N. Both CD4+ and CD8+ T Cells Respond to Antigens Fused to Anthrax Lethal Toxin. *Infection and Immunity* **76,** 2603–2611 (2008).
63. Hanahan, D. & Weinberg, R. A. Hallmarks of Cancer: The Next Generation. *Cell* **144,** 646–674 (2011).
64. Chames, P., Van Regenmortel, M., Weiss, E. & Baty, D. Therapeutic antibodies: successes, limitations and hopes for the future. *Br J Pharmacol* **157,** 220–233 (2009).
65. Weiner, L. M., Surana, R. & Wang, S. Monoclonal antibodies: versatile platforms for cancer immunotherapy. *Nat Rev Immunol* **10,** 317–327 (2010).
66. Yeung, Y. A. *et al.* Engineering Human IgG1 Affinity to Human Neonatal Fc Receptor: Impact of Affinity Improvement on Pharmacokinetics in Primates. *J Immunol* **182,** 7663–7671 (2009).
67. Adams, G. P. & Weiner, L. M. Monoclonal antibody therapy of cancer. *Nat Biotech* **23,** 1147–1157 (2005).
68. Dunkelberger, J. R. & Song, W.-C. Complement and its role in innate and adaptive immune responses. *Cell Res* **20,** 34–50 (2009).
69. Gaetano, N. D. *et al.* Complement Activation Determines the Therapeutic Activity of Rituximab In Vivo. *J Immunol* **171,** 1581–1587 (2003).
70. Weber, J. Review: Anti–CTLA-4 Antibody Ipilimumab: Case Studies of Clinical Response and Immune-Related Adverse Events. *The Oncologist* **12,** 864–872 (2007).
71. Topalian, S. L. *et al.* Safety, Activity, and Immune Correlates of Anti–PD-1 Antibody in Cancer. *New England Journal of Medicine* **366,** 2443–2454 (2012).
72. Brahmer, J. R. *et al.* Safety and Activity of Anti–PD-L1 Antibody in Patients with Advanced Cancer. *New England Journal of Medicine* **366,** 2455–2465 (2012).
73. Ecker, D. M., Jones, S. D. & Levine, H. L. The therapeutic monoclonal antibody market. *mAbs* **7,** 9–14 (2015).
74. KöHler, G. & Milstein, C. Continuous cultures of fused cells secreting antibody of predefined specificity. *Nature* **256,** 495–497 (1975).

75. McCafferty, J., Griffiths, A. D., Winter, G. & Chiswell, D. J. Phage antibodies: filamentous phage displaying antibody variable domains. *Nature* **348,** 552–554 (1990).
76. Marks, J. D. *et al.* By-passing immunization: Human antibodies from V-gene libraries displayed on phage. *Journal of Molecular Biology* **222,** 581–597 (1991).
77. Ullman, C. G., Frigotto, L. & Cooley, R. N. In vitro methods for peptide display and their applications. *Briefings in Functional Genomics* **10,** 125–134 (2011).
78. Chao, G. *et al.* Isolating and engineering human antibodies using yeast surface display. *Nat. Protocols* **1,** 755–768 (2006).
79. Baselga, J. & Swain, S. M. Novel anticancer targets: revisiting ERBB2 and discovering ERBB3. *Nat Rev Cancer* **9,** 463–475 (2009).
80. Hynes, N. E. & Lane, H. A. ERBB receptors and cancer: the complexity of targeted inhibitors. *Nat Rev Cancer* **5,** 341–354 (2005).
81. Yarden, Y. & Sliwkowski, M. X. Untangling the ErbB signalling network. *Nat Rev Mol Cell Biol* **2,** 127–137 (2001).
82. Hynes, N. E. & MacDonald, G. ErbB receptors and signaling pathways in cancer. *Current Opinion in Cell Biology* **21,** 177–184 (2009).
83. Tomas, A., Futter, C. E. & Eden, E. R. EGF receptor trafficking: consequences for signaling and cancer. *Trends in Cell Biology* **24,** 26–34 (2014).
84. Sigismund, S. *et al.* Clathrin-independent endocytosis of ubiquitinated cargos. *PNAS* **102,** 2760–2765 (2005).
85. Henriksen, L., Grandal, M. V., Knudsen, S. L. J., van Deurs, B. & Grøvdal, L. M. Internalization Mechanisms of the Epidermal Growth Factor Receptor after Activation with Different Ligands. *PLoS ONE* **8,** e58148 (2013).
86. Wiley, H. S. Trafficking of the ErbB receptors and its influence on signaling. *Experimental Cell Research* **284,** 78–88 (2003).
87. Sigismund, S. *et al.* Clathrin-Mediated Internalization Is Essential for Sustained EGFR Signaling but Dispensable for Degradation. *Developmental Cell* **15,** 209–219 (2008).
88. Hofman, E. G. *et al.* Ligand-induced EGF Receptor Oligomerization Is Kinase-dependent and Enhances Internalization. *J. Biol. Chem.* **285,** 39481–39489 (2010).
89. Herbst, R. S. & Shin, D. M. Monoclonal antibodies to target epidermal growth factor receptor–positive tumors. *Cancer* **94,** 1593–1611 (2002).
90. Suzuki, S. *et al.* Protein overexpression and gene amplification of epidermal growth factor receptor in nonsmall cell lung carcinomas. *Cancer* **103,** 1265–1273 (2005).
91. Zandi, R., Larsen, A. B., Andersen, P., Stockhausen, M.-T. & Poulsen, H. S. Mechanisms for oncogenic activation of the epidermal growth factor receptor. *Cellular Signalling* **19,** 2013–2023 (2007).
92. Grandal, M. V. *et al.* EGFRvIII escapes down-regulation due to impaired internalization and sorting to lysosomes. *Carcinogenesis* **28,** 1408–1417 (2007).
93. Kimura, H. *et al.* Antibody-dependent cellular cytotoxicity of cetuximab against tumor cells with wild-type or mutant epidermal growth factor receptor. *Cancer Science* **98,** 1275–1280 (2007).
94. Rosell, R., Taron, M., Reguart, N., Isla, D. & Moran, T. Epidermal Growth Factor Receptor Activation: How Exon 19 and 21 Mutations Changed Our Understanding of the Pathway. *Clin Cancer Res* **12,** 7222–7231 (2006).

95. Mehra, R. *et al.* Protein-intrinsic and signaling network-based sources of resistance to EGFR- and ErbB family-targeted therapies in head and neck cancer. *Drug Resistance Updates* (2011). doi:10.1016/j.drup.2011.08.002
96. Yun, C.-H. *et al.* The T790M mutation in EGFR kinase causes drug resistance by increasing the affinity for ATP. *PNAS* **105,** 2070–2075 (2008).
97. Engelman, J. A. *et al.* MET Amplification Leads to Gefitinib Resistance in Lung Cancer by Activating ERBB3 Signaling. *Science* **316,** 1039–1043 (2007).
98. Citri, A. & Yarden, Y. EGF–ERBB signalling: towards the systems level. *Nat Rev Mol Cell Biol* **7,** 505–516 (2006).
99. Stewart, E. L., Tan, S. Z., Liu, G. & Tsao, M.-S. Known and putative mechanisms of resistance to EGFR targeted therapies in NSCLC patients with EGFR mutations—a review. *Translational Lung Cancer Research* **4,** 67–81 (2015).
100. Roock, W. D., Vriendt, V. D., Normanno, N., Ciardiello, F. & Tejpar, S. KRAS, BRAF, PIK3CA, and PTEN mutations: implications for targeted therapies in metastatic colorectal cancer. *The Lancet Oncology* **12,** 594–603 (2011).
101. Ostrem, J. M. L. & Shokat, K. M. Direct small-molecule inhibitors of KRAS: from structural insights to mechanism-based design. *Nature Reviews Drug Discovery* **15,** 771–785 (2016).
102. Tsao, M.-S. *et al.* Erlotinib in Lung Cancer — Molecular and Clinical Predictors of Outcome. *New England Journal of Medicine* **353,** 133–144 (2005).
103. Hackel, B. J. Fibronectin domain engineering. (Massachusetts Institute of Technology, 2009).
104. Spangler, J. B., Manzari, M. T., Rosalia, E. K., Chen, T. F. & Wittrup, K. D. Triepitopic Antibody Fusions Inhibit Cetuximab-Resistant BRAF and KRAS Mutant Tumors via EGFR Signal Repression. *Journal of Molecular Biology* **422,** 532–544 (2012).
105. Chen, W. W. *et al.* Input–output behavior of ErbB signaling pathways as revealed by a mass action model trained against dynamic data. *Molecular Systems Biology* **5,** (2009).
106. Patel, D. *et al.* Monoclonal Antibody Cetuximab Binds to and Down-regulates Constitutively Activated Epidermal Growth Factor Receptor vIII on the Cell Surface. *Anticancer Res* **27,** 3355–3366 (2007).
107. Zhou, Y. *et al.* Impact of Intrinsic Affinity on Functional Binding and Biological Activity of EGFR Antibodies. *Molecular Cancer Therapeutics* **11,** 1467–1476 (2012).
108. Van Deventer, J. A., Kelly, R. L., Rajan, S., Wittrup, K. D. & Sidhu, S. S. A switchable yeast display/secretion system. *Protein Engineering Design and Selection* **28,** 317–325 (2015).
109. Johannes, L. & Decaudin, D. Protein toxins: intracellular trafficking for targeted therapy. *Gene Therapy* **12,** 1360–1368 (2005).
110. Kalser, M. H., Barkin, J. & Macintyre, J. M. Pancreatic cancer. Assessment of prognosis by clinical presentation. *Cancer* **56,** 397–402 (1985).
111. Stathis, A. & Moore, M. J. Advanced pancreatic carcinoma: current treatment and future challenges. *Nature Reviews Clinical Oncology* **7,** 163–172 (2010).
112. Oberstein, P. E. & Olive, K. P. Pancreatic cancer: why is it so hard to treat? *Therapeutic Advances in Gastroenterology* **6,** 321–337 (2013).
113. Singh, Y., Klimpel, K. R., Goel, S., Swain, P. K. & Leppla, S. H. Oligomerization of anthrax toxin protective antigen and binding of lethal factor during endocytic uptake into mammalian cells. *Infect Immun* **67,** 1853–1859 (1999).

114. Liu, S. & Leppla, S. H. Cell Surface Tumor Endothelium Marker 8 Cytoplasmic Tail-independent Anthrax Toxin Binding, Proteolytic Processing, Oligomer Formation, and Internalization. *Journal of Biological Chemistry* **278,** 5227–5234 (2003).
115. Jorissen, R. N. *et al.* Epidermal growth factor receptor: mechanisms of activation and signalling. *Experimental Cell Research* **284,** 31–53 (2003).
116. Collins, M. A. *et al.* Oncogenic Kras is required for both the initiation and maintenance of pancreatic cancer in mice. *Journal of Clinical Investigation* **122,** 639–653 (2012).
117. Morton, J. P. *et al.* Mutant p53 drives metastasis and overcomes growth arrest/senescence in pancreatic cancer. *Proceedings of the National Academy of Sciences* **107,** 246–251 (2010).
118. Baeumer, S. *et al.* Antibody-mediated delivery of anti-KRAS-siRNA in vivo overcomes therapy resistance in colon cancer. *Clin Cancer Res* clincanres.2017.2013 (2015). doi:10.1158/1078-0432.CCR-13-2017
119. Collier, R. J. Effect of diphtheria toxin on protein synthesis: Inactivation of one of the transfer factors. *Journal of Molecular Biology* **25,** 83–98 (1967).
120. Collier, R. J. & Cole, H. A. Diphtheria Toxin Subunit Active in vitro. *Science* **164,** 1179–1182 (1969).
121. Cleeland, C. S. *et al.* Reducing the toxicity of cancer therapy: recognizing needs, taking action. *Nature Reviews Clinical Oncology* **9,** 471–478 (2012).
122. Hammarström, S. The carcinoembryonic antigen (CEA) family: structures, suggested functions and expression in normal and malignant tissues. *Seminars in Cancer Biology* **9,** 67–81 (1999).
123. Beauchemin, N. & Arabzadeh, A. Carcinoembryonic antigen-related cell adhesion molecules (CEACAMs) in cancer progression and metastasis. *Cancer Metastasis Rev* **32,** 643–671 (2013).
124. Hong, H., Sun, J. & Cai, W. Radionuclide-Based Cancer Imaging Targeting the Carcinoembryonic Antigen. *Biomarker Insights* **3,** 435–451 (2008).
125. Berinstein, N. L. Carcinoembryonic Antigen as a Target for Therapeutic Anticancer Vaccines: A Review. *JCO* **20,** 2197–2207 (2002).
126. Lesterhuis, W. J. Vaccination of colorectal cancer patients with CEA-loaded dendritic cells: antigen-specific T cell responses in DTH skin tests. *Annals of Oncology* **17,** 974–980 (2006).
127. Graff, C. P., Chester, K., Begent, R. & Wittrup, K. D. Directed evolution of an anti-carcinoembryonic antigen scFv with a 4-day monovalent dissociation half-time at 37 C. *Protein Engineering Design and Selection* **17,** 293–304 (2004).
128. Rainey, G. J. A. *et al.* Receptor-specific requirements for anthrax toxin delivery into cells. *Proceedings of the National Academy of Sciences* **102,** 13278–13283 (2005).
129. Lacy, D. B., Wigelsworth, D. J., Melnyk, R. A., Harrison, S. C. & Collier, R. J. Structure of heptameric protective antigen bound to an anthrax toxin receptor: A role for receptor in pH-dependent pore formation. *Proceedings of the National Academy of Sciences* **101,** 13147–13151 (2004).
130. Schmidt, M. M., Thurber, G. M. & Wittrup, K. D. Kinetics of anti-carcinoembryonic antigen antibody internalization: effects of affinity, bivalency, and stability. *Cancer Immunology, Immunotherapy* **57,** 1879–1890 (2008).
131. Taft, S. C. & Weiss, A. A. Toxicity of Anthrax Toxin Is Influenced by Receptor Expression. *Clin. Vaccine Immunol.* **15,** 1330–1336 (2008).

132. Akamatsu, Y. *et al.* A single-chain immunotoxin against carcinoembryonic antigen that suppresses growth of colorectal carcinoma cells. *Clin Cancer Res* **4,** 2825 (1998).
133. Shin, M. C. *et al.* Combination of antibody targeting and PTD-mediated intracellular toxin delivery for colorectal cancer therapy. *Journal of Controlled Release* doi:10.1016/j.jconrel.2014.08.030
134. Das, A. *et al.* A monoclonal antibody against neem leaf glycoprotein recognizes carcinoembryonic antigen (CEA) and restricts CEA expressing tumor growth. *J. Immunother.* **37,** 394–406 (2014).
135. Parkhurst, M. R. *et al.* T Cells Targeting Carcinoembryonic Antigen Can Mediate Regression of Metastatic Colorectal Cancer but Induce Severe Transient Colitis. *Mol Ther* **19,** 620–626 (2011).
136. Bornstein, G. G. Antibody Drug Conjugates: Preclinical Considerations. *The AAPS Journal* **17,** 525–534 (2015).
137. Voskoglou-Nomikos, T., Pater, J. L. & Seymour, L. Clinical Predictive Value of the *in Vitro* Cell Line, Human Xenograft, and Mouse Allograft Preclinical Cancer Models. *Clin Cancer Res* **9,** 4227 (2003).
138. Mestas, J. & Hughes, C. C. W. Of Mice and Not Men: Differences between Mouse and Human Immunology. *The Journal of Immunology* **172,** 2731–2738 (2004).
139. Dranoff, G. Experimental mouse tumour models: what can be learnt about human cancer immunology? *Nature Reviews Immunology* (2011). doi:10.1038/nri3129
140. Morton, C. L. & Houghton, P. J. Establishment of human tumor xenografts in immunodeficient mice. *Nature Protocols* **2,** 247–250 (2007).
141. Nehls, M., Pfeifer, D., Schorpp, M., Hedrich, H. & Boehm, T. New member of the winged-helix protein family disrupted in mouse and rat nude mutations. *Nature* **372,** 103–107 (1994).
142. Abboud, N. & Casadevall, A. Immunogenicity of Bacillus anthracis Protective Antigen Domains and Efficacy of Elicited Antibody Responses Depend on Host Genetic Background. *Clinical and Vaccine Immunology* **15,** 1115–1123 (2008).
143. Teicher, B. *et al.* The systemic administration of lethal toxin achieves a growth delay of human melanoma and neuroblastoma xenografts: Assessment of receptor contribution. *International Journal of Oncology* (2008). doi:10.3892/ijo.32.4.739
144. Koo, H.-M. *et al.* Apoptosis and melanogenesis in human melanoma cells induced by anthrax lethal factor inactivation of mitogen-activated protein kinase kinase. *Proceedings of the National Academy of Sciences* **99,** 3052–3057 (2002).
145. Ramirez, D., Leppla, S., Schneerson, R. & Shiloach, J. Production, recovery and immunogenicity of the protective antigen from a recombinant strain of Bacillus anthracis. *Journal of Industrial Microbiology & Biotechnology* **28,** 232–238 (2002).
146. Moayeri, M., Wiggins, J. F. & Leppla, S. H. Anthrax Protective Antigen Cleavage and Clearance from the Blood of Mice and Rats. *Infect Immun* **75,** 5175–5184 (2007).
147. Thurber, G. M., Schmidt, M. M. & Wittrup, K. D. Antibody tumor penetration: Transport opposed by systemic and antigen-mediated clearance. *Advanced Drug Delivery Reviews* **60,** 1421–1434 (2008).
148. Roberts, P. J. & Der, C. J. Targeting the Raf-MEK-ERK mitogen-activated protein kinase cascade for the treatment of cancer. *Oncogene* **26,** 3291–3310 (2007).